Characterization of a human renal organic anion transporter

Dissertation
zur Erlangung des Doktorgrades
der Mathematisch-Naturwissenschaftlichen Fakultäten
der Georg-August-Universität zu Göttingen

vorgelegt von
Glen Reid
aus Lower Hutt, Neuseeland

Göttingen 2000

D7

Referent:	Prof. Dr. R. Hardeland
Korreferent:	Prof. Dr. K. Jungermann
Tag der mündlichen Prüfung:	

For my Family

CONTENTS

List of Abbreviations

Å	Angstrom
ATP	adenosine triphosphate
bp	base pairs
C	Celsius
cAMP	cyclic adenosine monophosphate
C-terminus	carboxy-terminus
cDNA	complementary DNA
CKII	casein kinase II
cRNA	complementary RNA
Da	Dalton
dNTP	deoxyribonucleotide phosphate
EST	expressed sequence tag
(f)NaDC-3	(flounder) sodium/dicarboxylate cotransporter 3
fROAT	flounder renal organic anion transporter
GAPDH	glyceraldehyde phosphate dehydrogenase
GLC	glycolithocholate
GLC-S	sulfated glycolithocholate
h	hour
HEK293	human embryonic kidney cell line
hNLT	human novel liver transporter
hOAT1-1	human organic anion transporter isoform 1 (563aa)
hOAT2	human organic anion transporter 2
hPAHT	human PAH transporter
hROAT1	human renal organic anion transporter 1
k	kilo
K_m	Michaelis Menten constant
LB	Luria Bertani broth
M	molar (moles per litre)
µM	micromolar
MAPK	mitogen-associated protein kinase
ml	millilitre
mRNA	messenger RNA
MRP2	multiple drug resistance-associated protein 2
N-terminus	amino-terminus
NKT	novel kidney transporter
NLT	novel liver transporter
NPT1	sodium phosphate transporter 1
NSAIDs	non-steroidal anti-inflammatory drugs
OAT	organic anion transporter
OAT1	organic anion transporter 1
OAT3	organic anion transporter 3
OAT4	organic anion transporter 4
OCT1	organic cation transporter 1
OCT2	organic cation transporter 2
ORI	oocyte Ringer's solution
PAH	para-aminohippurate
PCR	polymerase chain reaction
PI3K	phosphatidyl inositol-3-kinase

PKA	cAMP-associated protein kinase
PKC	protein kinase C
pmol	picomole
RACE	rapid amplification of cDNA ends
(r)NaDC-1	rat sodium/dicarboxylate cotransporter
rOAT2	rat organic anion transporter 2
rOCT1A	rat organic cation transporter 1A, alternatively spliced from
rpm	revolutions per minute
RST	renal solute transporter
RT-PCR	reverse transcriptase PCR
TCA	tricarboxylic acid cycle
TK	tyrosine kinase
TLC	taurolithocholate
TLC-S	sulfated taurolithocholate
U	unit
UTR	untranslated region
UST1	unidentified solute transporter 1
VMAT1	vesicular monoamine transporter 1
VMAT2	vesicular monoamine transporter 2
V_{max}	maximum transport rate

ABSTRACT

The renal excretion of organic anions, including a variety of endogenous substances, xenobiotics and their metabolites, involves an organic anion transport system with multiple specificity. The well characterized basolateral uptake step of this process involves the organic anion transporter 1 (OAT1), recently cloned from the rat, mouse and flounder, which mediates the uptake of an organic anion in exchange for an intracellular dicarboxylate. This study represents the first reported cloning of a human OAT1 homologue, hROAT1, which was cloned via a degenerate PCR-based approach. The hROAT1 reading frame encodes a 550 amino acid protein with a calculated molecular mass of 60 kDa, and has significant homology to previously cloned OAT1 homologues. To enable heterologous expression in the *Xenopus laevis* oocyte system, an hROAT1 expression clone was constructed by subcloning the hROAT1 reading frame between the 5' and 3' UTRs of the flounder sodium dicarboxylate cotransporter, fNaDC-3. Expressed in *Xenopus laevis* oocytes, hROAT1 mediated the uptake of *p*-aminohippurate (PAH), the model substrate for this system. This uptake had an approximate K_m of 10 μM, and was inhibited by probenecid, dicarboxylates including the probable physiological exchange partner α-ketoglutarate, and the loop diuretics bumetanide and furosemide. Uptake also showed chloride dependence, characteristic of the basolateral organic anion/dicarboxylate exchange in renal systems. Mutation of two amino acids, Lys382 and Arg466, positions positively charged in all OATs and negatively charged or neutral in the related organic cation transporters (OCTs), abrogated transport function. Deletion of exons 9 and 10 also resulted in a non-functional transporter. Deletion of exon 10 alone, which contains a consensus site for phosphorylation by casein kinase II, increased transport by approximately two-fold. A second member of the OAT family, hOAT2, was also cloned from the human kidney. The hOAT2 cDNA encodes a protein of 541 amino acids, with high homology to the previously identified rat OAT2. The sequences of hOAT2 and hNLT, a second human OAT2 homologue cloned from the liver, are identical apart from exon 10, which is completely divergent and contains alternate protein kinase consensus sites. hOAT2 and hNLT appear to represent tissue-specific transcripts from the same gene. The observed effect on hROAT-mediated transport of deleting exon 10, and the apparent tissue-specific expression of the tenth exon of hOAT2 suggest an as yet unexplored role for exon 10 in the regulation of these transporters.

1 INTRODUCTION

A great number of the potentially toxic compounds in the human body are organic anions, including both endogenous compounds and xenobiotics such as industrial and environmental toxins, pharmaceutical agents, and plant and animal toxins. These compounds often exist in the ionized form at physiological pH, or are converted to more hydrophilic metabolites in the liver and kidney (Roch-Ramel and Diezi 1997). In the kidney, many substances are exchanged between the blood and the tubular lumen, enabling the excretion of potential toxins and the conservation of valuable metabolites. Renal excretion consists of a combination of filtration at the glomerulus and secretion in the proximal tubule, which possesses transport systems with multiple specificity that efficiently secrete a multitude of organic anions of varied structure.

1.1 THE MULTISPECIFIC ORGANIC ANION TRANSPORT SYSTEM (OAT)

Many organic anions secreted in the kidney are transported by the 'classical organic anion transport system', which consists of a well-defined active basolateral uptake step involving organic anion / α-ketoglutarate exchange, and a poorly characterized luminal efflux step (Roch-Ramel 1998). The importance of this process is shown by the observation that organic anion secretion has been found in the kidney of almost all vertebrates, as well the renal systems of some invertebrates (Dantzler 1989, Pritchard and Miller 1991). The original physiological role of the multispecific organic anion transport system is believed to be the secretion of endogenous anionic compounds, such as cyclic nucleotides, prostaglandins and uremic toxins (Gemba et al 1983, Podevin and Boumendil-Podevin 1975, Irish 1979, Prescott et al 1993).

The clinical relevance of the organic anion / α-ketoglutarate exchanger is that many anionic drugs and nephrotoxins are thought to be substrates for the system. Cephalosporin-based antibiotics such as cephaloridine, and mycotoxins such as ochratoxin A are both taken up by proximal tubule cells via this system, causing metabolic disorders (Endou 1998). In the case of ochratoxin A, nephrotoxicity is prevented by probenecid, the classical inhibitor of the multispecific organic anion system (Jung and Endou 1989). The model substrate for the organic anion transporting system is para-aminohippurate, or PAH, a product of 4-aminobenzoate metabolism.

This substance is efficiently secreted and is extracted to over 90% during the first pass through the kidney (Roch-Ramel and Diezi 1997) and is used diagnostically to determine renal plasma flow. Almost all studies of the renal organic anion transporting system have utilized PAH as a substrate. The chemical structures of PAH and probenecid are shown in Figure 1.1 below.

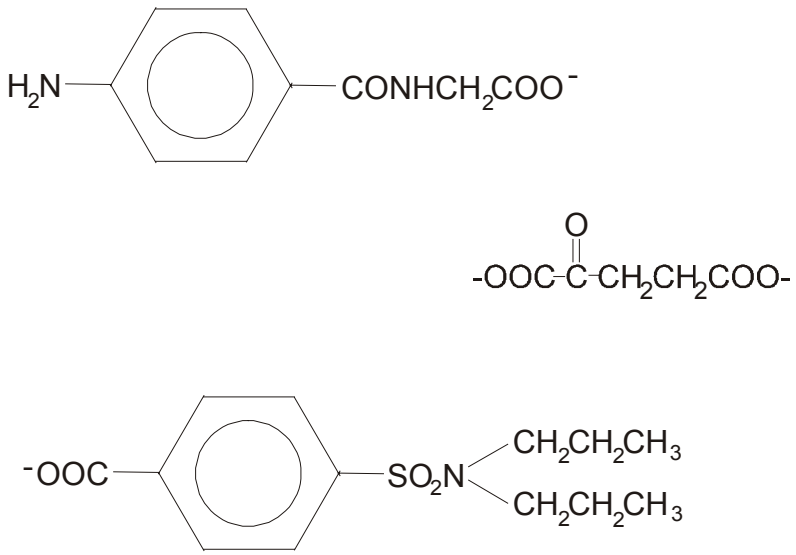

FIGURE 1.1: Compounds interacting with the organic anion transporting system. The compounds in this figure all interact with the multispecific organic anion transporting system of the kidney: PAH (top) is the model substrate, probenecid (bottom) is the classical inhibitor and α-ketoglutarate (middle) is an intracellular exchange partner for organic anion uptake. Properties common to most substances interacting with this system are a hydrophobic region and ionization at physiological pH.

Although the functional characteristics of the multispecific organic anion transport system have been known for many years, transport proteins mediating the active basolateral of organic anions have only recently been identified. These proteins, which have now been cloned from several different species, are termed OAT1 (for organic anion transporter 1), and all are functionally and structurally related (Lopez-Nieto et al 1997, Sekine et al 1997, Sweet el al 1997, Wolff et al 1997). In contrast, the protein(s) responsible for the less well-defined luminal efflux of organic anions have yet to be identified.

1.1.1 Specificity of basolateral organic anion uptake

The compounds classed as substrates of the renal organic anion transport system were identified by inhibition of their excretion, usually by PAH or probenecid (Møller and Sheikh 1983). These compounds belong to many chemical classes, as seen in Table 1.1. Subsequent studies carried out to determine the structural requirements of substrates of

the system relied on inhibition of PAH uptake by the test substance (Ullrich 1997). Although this approach undoubtedly identifies compounds that interact with the carrier, it provides no evidence as to whether they are actually translocated (Roch-Ramel 1998). Nevertheless, the affinity of the transporter for compounds identified as inhibitors, or potential substrates, is influenced by four factors: hydrophobicity, charge, charge distribution, and charge strength (Ullrich 1997). The classical organic anions, monovalent hydrophobic anions with a negative or partial negative charge, interact best with the transporter. These compounds require a hydrophobic moiety of at least 4 Å in length. The system also interacts with divalent anions, including some zwitterions, for which optimal interaction with the transporter requires a charge separation of 6-7 Å. In addition, these compounds may contain a hydrophobic moiety of up to 10 Å in length. The affinity of the transporter for both mono- and divalent anions increases with hydrophobicity and charge strength. Finally, non-ionizable hydrophobic compounds also interact with the transporter.

Chemical class	*Examples*	*Properties*
Conjugated compounds	*p*-Aminohippurate	Classical substrate, diagnostic agent
Benzoate derivatives	Probenecid	Classical inhibitor
	Salicylate	Analgesic
	Bumetanide	Loop diuretic
Acetate and proprionate derivatives	Diodrast	Contrast agent
	Indomethacin	Analgesic
	Ethacrynic Acid	Loop diuretic
Heterocyclic carboxylates	Benzylpenicillin	β-lactam antibiotic
	Cephaloridin	β-lactam antibiotic
Sulfonamides	Acetazolamide	Carbonic anhydrase inhibitor
Other heterocyclic compounds	Urate	End product of purine degradation
Sulfonates	Phenol red	Diagnostic dye
Amino acid derivatives	Methotrexate	Antitumor drug, folic acid derivative
Miscellaneous	Prostaglandin E2	Local hormone
	cAMP	Second messenger molecule

TABLE 1.1: Examples of substrates of the classical organic anion transport system of the kidney. The substances in this table are excreted by the kidney via a process that can be inhibited by PAH, probenecid, or another representative substrate of the classical organic anion transport system (Møller and Sheikh 1983).

1.1.2 Site of organic anion secretion in the kidney

The site of organic anion transport was first demonstrated by studies of the secretion of the organic anion phenol red in aglomerular marine teleosts (Marshall and Grafflin 1928, Shannon 1938). This was not only the first demonstration of the existence of renal secretion, but because the kidney of these fish consists almost entirely of proximal tubule, this also proved that organic anion secretion occurs in the proximal tubules (Marshall and Grafflin 1928, Shannon 1938). Later studies in the chicken, flounder and mammals confirmed the proximal tubule to be the site of organic anion secretion (Chambers and Kempton 1933, Cortney et al 1965, Forster 1948, Malvin et al 1958). In fact, secretion takes place in the proximal tubule of representative species from all five vertebrate classes (Dantzler and Wright 1997).

1.1.3 Basolateral uptake by the organic anion transporting system

Early studies demonstrated that secreted anions are concentrated in proximal tubule cells and the tubular lumen, suggesting distinct basolateral and luminal steps. In addition, the inside-negative potential of the proximal tubule cell requires uphill transport supported by the finding that inhibiting energy production reduces uptake. However, no direct coupling to ATP hydrolysis could be demonstrated (Maxild 1978, Podevin and Boumendil-Podevin 1975, Ross and weiner 1972, Sheikh et al 1981). For many years it was also known that the sodium gradient is essential to the functioning of the organic anion transporting system. Although sodium-organic anion cotransport was initially suggested as the mechanism for the basolateral uptake of organic anions, such a process was never demonstrated (Berner and Kinne 1976, Kasher et al 1983, Kinsella et al 1979).

Almost 20 years elapsed before the link between metabolic energy production and organic anion uptake was elucidated. An important finding was that an outwardly directed gradient of unlabelled PAH with an inwardly directed sodium gradient stimulated the uptake of labelled PAH (Kasher et al 1983, Eveloff 1987), which lead to the suggestion that PAH uptake might occur via exchange for an anionic metabolite (Pritchard and Miller 1993). Furthermore, anionic metabolites such as dicarboxylates, which are taken up across the basolateral membrane by direct coupling to the sodium gradient, could stimulate PAH uptake (Kippen and Klinenberg 1978, Ullrich et al 1987). The current model for basolateral PAH uptake was first proposed by Burckhardt and co-

workers (Shimada et al 1987) and Pritchard (Pritchard 1987). In this model, the ATP-dependent step involved in generation of the sodium gradient by the Na^+-K^+-ATPase drives sodium-dicarboxylate cotransport into the cell, which, by creation of an outwardly directed dicarboxylate gradient, drives organic anion uptake via dicarboxylate-organic anion exchange. The net effect predicted by this model is that of uptake of sodium with the organic anion and recycling of the anionic exchange partner, at the cost of one molecule of ATP per organic anion imported. This process is termed tertiary active transport, as the uptake of the organic anion is driven by ATP hydrolysis two steps removed. The model was verified by subsequent vesicle studies and also by new and reevaluated studies with intact tissue, all of which demonstrated that certain dicarboxylates were able to stimulate the uptake of PAH (Pritchard 1987, Shimada et al 1987, Sullivan and Grantham 1992).

In the currently accepted model, α-ketoglutarate is believed to act as the physiological exchange partner for basolateral PAH uptake. Of the dicarboxylates capable of exchanging with organic anions, α-ketoglutarate is the most abundant in proximal tubule cells (Terlouw et al 2000). In addition, the physiological concentrations of α-ketoglutarate and its ability to stimulate PAH uptake in vesicles and intact tubules support this assumption (Shimada et al 1987, Chadsudthipong and Dantzler 1991 and 1992). Intracellular concentrations of around 100 to 200 μM combined with plasma concentrations of 5-12 μM provide the gradient required to drive organic anion uptake (Boyd and Goldstein 1979, Lemieux et al 1980, Martin et al 1989, Rocchiccioli et al 1984); concentrations similar to the plasma concentration also maximally stimulate PAH uptake into vesicles or tissue slices (Pritchard 1988, Pritchard 1990). In addition to its metabolic production, α-ketoglutarate is also taken into proximal tubule cells via sodium-dependent cotransport at the basolateral and luminal membranes, maintaining the necessary outwardly directed gradient (Dantzler and Wright 1997). This uptake has been calculated to contribute approximately half of the exchangeable α-ketoglutarate for organic anion exchange (Welborn et al 1998).

1.1.4 Cellular model of the basolateral uptake of organic anions

In recent years the proposed model for basolateral organic anion uptake has been strengthened by the cloning and characterization of the transporters responsible for this functionally coupled system. The organic anion / dicarboxylate exchanger and the

sodium-dicarboxylate cotransporter from several species have now been cloned and characterized (Sweet et al 1997, Wolff et al 1997, Sekine et al 1997, Steffgen et al 1999). The model is shown in Figure 1.2. Organic anion (PAH) uptake in exchange for an intracellular dicarboxylate (α-ketoglutarate) is mediated by the organic anion transporter 1, OAT1. Recycling of α-ketoglutarate back into the cell, together with three sodium ions, occurs via the sodium-dicarboxylate cotransporter, NaDC-3, and the sodium ions are pumped out of the cell by the Na^+-K^+-ATPase, at the cost of one molecule of ATP.

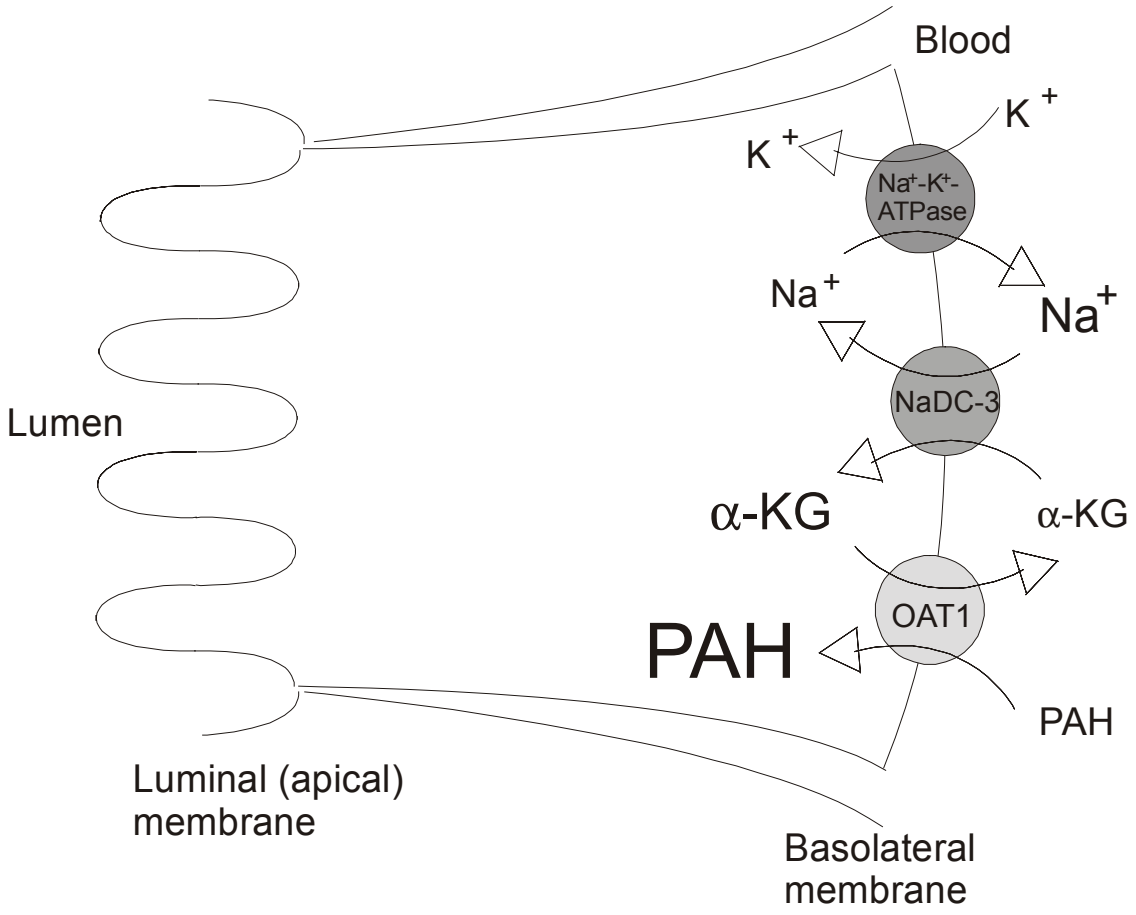

Figure 1.2: Model of basolateral organic anion transport in proximal tubule cells. The current model for basolateral organic anion uptake involves import of an organic anion, represented here by PAH, in exchange for an intracellular dicarboxylate (α-ketoglutarate), by OAT1. The intracellular pool of α-ketoglutarate is maintained by metabolism and import by NaDC-3, which returns α-ketoglutarate to the cell together with three sodium ions, in a process driven by the inwardly directed sodium gradient. The Na^+-K^+-ATPase pumps the sodium ions from the cell and is the energy consuming step of the system.

1.1.5 Cytoplasmic transport of organic anions

Following basolateral uptake, organic anions must arrive at the luminal membrane to enable secretion to be completed. From the few studies to have addressed this process, it appears that organic anions are not uniformly distributed within the cell. Fluorescein, a fluorescent substrate of the organic anion transporting system, was shown to be compartmentalized in renal cells after uptake, possibly within vesicles (Miller et al 1993). It has also been shown that fluorescein is taken up into the mitochondria of proximal tubule cells, via a process involving at least three metabolite carriers (Terlouw et al 2000). Although there is insufficient evidence to allow conclusions to be drawn, it has been suggested that intracellular binding or sequestration may protect the cell from the nephrotoxic effects of many of the substrates of the organic anion transporting system (Crawford 1991).

1.1.6 Luminal exit

In comparison with the well-defined process of uptake of organic anions into the cell across the basolateral membrane, events at the luminal membrane are less clear. Vesicle studies have shown that this process is both saturable and probenecid sensitive, and that this transport is not driven by the sodium gradient (Berner and Kinne 1976, Dantzler 1974). Early results were complicated by the differences observed in species that reabsorb urate, the end product of purine metabolism, compared with urate-secreting species (Aronson 1989, Martinez et al 1990). The presence of an anion exchange system capable of transporting PAH has been shown, although the characteristics of this system would be more likely to mediate reabsorption of organic anions rather than their efflux, and it is thought that this system probably mediates urate reabsorption (Aronson 1989). Other studies have demonstrated a probenecid-sensitive potential-dependent system in luminal membrane vesicles, which could mediate the transport of organic anions down an electrochemical gradient into the lumen (Kinsella et al 1979, Eveloff et al 1979). Despite the characterization of these systems in brush-border membrane vesicles, they have yet to be demonstrated in situ (Roch-Ramel 1998). Figure 1.3 shows the model of organic anion transport at the luminal membrane.

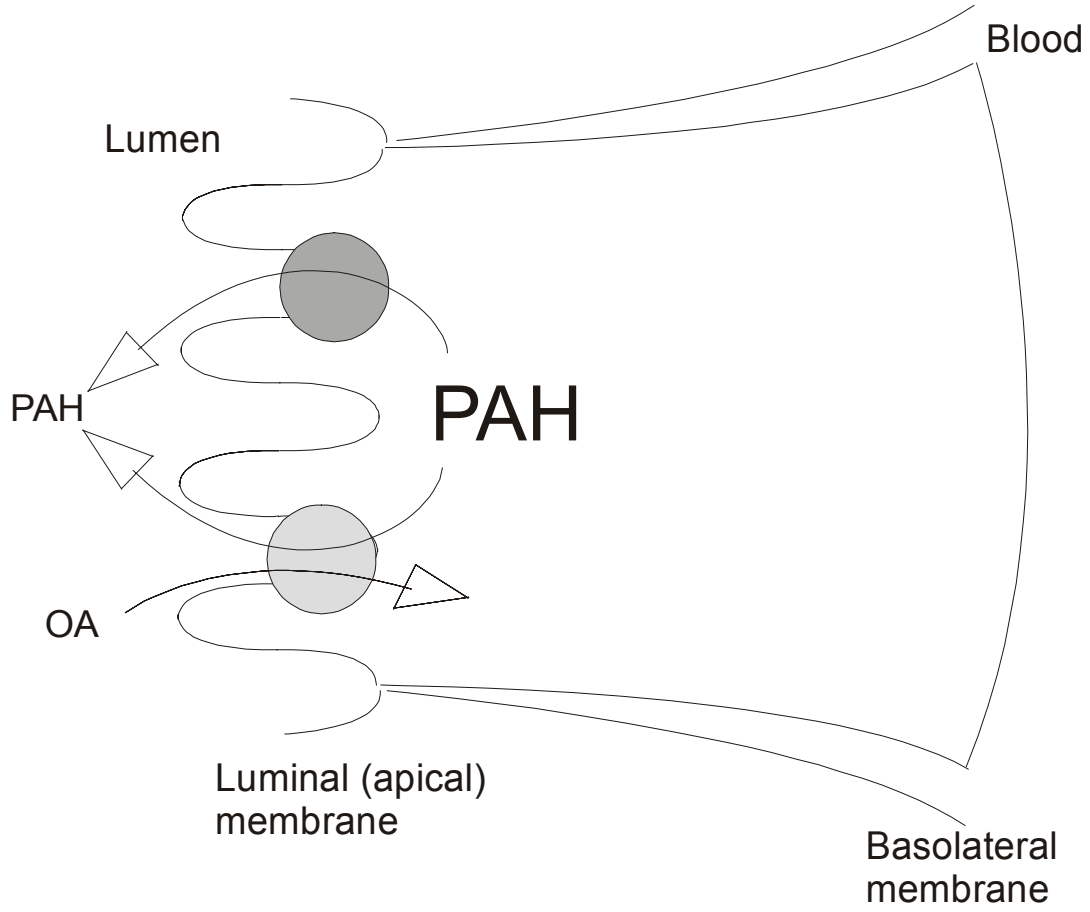

Figure 1.3: Model of the luminal efflux of organic anions in proximal tubule cells. This model shows two functionally characterized systems for luminal efflux of organic anions (PAH), for which the proteins responsible have yet to be identified. As discussed in the text, the organic anion exchanger (bottom) would probably mediate organic anion reabsorption. The facilitated transporter (top) would be driven by the electrochemical gradient.

1.2 STUDIES OF ORGANIC ANION TRANSPORT IN THE HUMAN KIDNEY

It is well known that the human kidney efficiently excretes PAH, however, physiological studies with human tissue have been limited by the availability of source material. In one of the few studies of PAH uptake by basolateral vesicles derived from human proximal tubules (Guisan and Roch-Ramel 1995), it was shown that PAH uptake was stimulated by external oxoglutarate only when combined with an inward sodium gradient, consistent with the proposed model for basolateral PAH uptake. At the luminal membrane, the presence of a system similar to that found at the basolateral membrane has been demonstrated (Roch-Ramel et al 1996). In brush-border (luminal)

membrane vesicles, PAH uptake was cis-stimulated by α-ketoglutarate only in the presence of an inwardly directed sodium gradient. However, as mentioned in the previous section, such a system would favour the reabsorption of PAH from the tubular lumen, rather than excretion.

1.3 PREVIOUSLY CLONED OAT1 HOMOLOGUES

At the beginning of this study, proteins with the properties of the basolateral multispecific organic anion transport system had been cloned and characterized from the rat and flounder kidney. The rat homologue was cloned independently by two groups and named OAT1 (Sekine et al 1997) and ROAT1 (Sweet et al 1997), respectively. A flounder homologue, fROAT, appeared a short time later (Wolff et al 1997). In addition, a homologous protein previously cloned from the mouse kidney, named NKT (for novel kidney transporter), had been isolated, but no function had been demonstrated (Lopez-Nieto et al 1997).

The rat OAT1/ROAT1 clones were isolated by functional expression in *Xenopus laevis* oocytes. When injected into oocytes, the protein mediates the uptake of PAH with an estimated K_m of approximately 15 μM (Sekine et al 1997) or 70 μM (Sweet et al 1997). Preincubation of the OAT1-injected oocytes with glutarate lead to a two to three-fold increase in PAH uptake (Sekine et al 1997, Sweet et al 1997), and a ten-fold increase was observed in oocytes co-injected with rNaDC-1, a rat sodium-dicarboxylate cotransporter (Sekine et al 1997). Transport of PAH was also cis-inhibited by diverse endogenous and exogenous organic anions, and furthermore, OAT1 mediated uptake of among others, labelled α-ketoglutarate, methotrexate and urate (Sekine et al 1997). In situ hybridization patterns suggested that OAT1 is most strongly expressed in the S2 portion of the proximal tubule (Sekine et al 1997). These observations lead the authors to conclude that OAT1 represents the protein mediating the multispecific organic anion-dicarboxylate exchange at the basolateral membrane of the proximal tubule.

The flounder OAT1, fROAT, was also cloned by functional expression in *Xenopus laevis* oocytes (Wolff et al 1997). The PAH uptake mediated by fROAT showed an apparent K_m of 20 μM, and was probenecid sensitive. In cis-inhibition studies the dicarboxylates α-ketoglutarate, glutarate, and suberate, as well as urate and the loop

diuretic bumetanide inhibited PAH uptake. The functional characteristics suggest that fROAT is the basolateral organic anion-dicarboxylate exchanger of the flounder kidney.

In addition to the functional similarities detailed above, the OAT1 homologues also exhibit similarities on the sequence level; the rat OAT1 and mouse NKT are 93 % identical, and both are 46 % identical to the flounder fROAT. Furthermore, a sequence database search reveals homology to another organic anion transporter isolated from the rat liver, NLT (Simonson et al 1994) subsequently renamed rOAT2 based on its functional properties (Sekine et al 1998), and homology to members of a family of proteins mediating the renal transport of organic cations, OCT1 (Gründemann et al 1994) and OCT2 (Okuda et al 1996), as seen in Table 1.2 below.

	OAT1/ROAT	NKT	fROAT	NLT	OCT1	OCT2
OAT1/ROAT	-	95	68	56	49	49
NKT	**93**	-	67	57	49	49
fROAT	**46**	**46**	-	55	49	47
NLT	**37**	**37**	**37**	-	48	49
OCT1	**31**	**33**	**32**	**31**	-	83
OCT2	**31**	**32**	**31**	**31**	**69**	-

Table 1.2: Sequence homologies of OAT1 and related proteins. The table shows sequence identities and homologies for six related proteins known at the beginning of the study. Values in bold represent sequence identity and those in normal type represent the similarity, calculated using the NCBI Blast server, www.ncbi.nlm.nih.gov/BLAST/.

The rat OAT1, fROAT and NKT cDNAs encode proteins of 551, 562 and 546 amino acids, respectively, and hydropathy analysis predicts twelve putative transmembrane domains with internal N- and C-termini; a model of the membrane topology of the rat OAT1 is shown in Figure 1.4.

Further shared structural features are shown in Table 1.3. These include conserved cysteine residues and consensus sites for N-linked glycosylation within the large extracellular loop between the first and second transmembrane domains, consensus sites

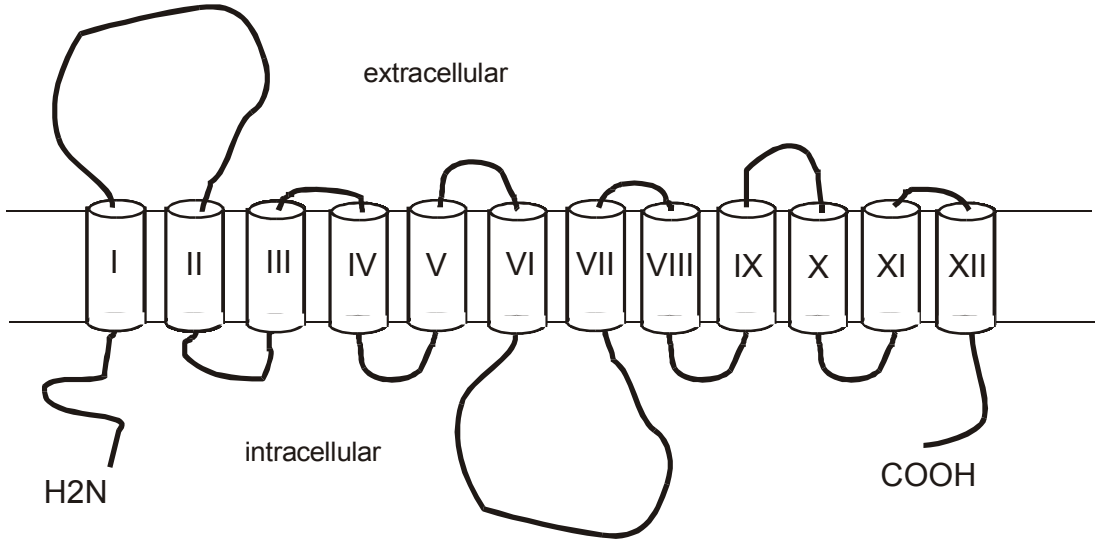

Figure 1.4: Membrane topology model of the rat OAT1. This model shows the putative model for membrane organization of the rat OAT1, as predicted by TopPred 2 (von Heijne 1992), consisting of twelve transmembrane domains (I-XII), a large extracellular loop between transmembrane domains 1 and 2, a large intacellular loop between transmembrane domains 6 and 7, and intracellular N- and C-termini.

for phosphorylation by various protein kinases within the large intracellular loop between transmembrane domains six and seven, and further protein kinase consensus sites in the C-terminus.

	OAT1/ROAT	NKT	fROAT
GenBank accession number	AB004559/AAC18772	NP_032792	Z97028
Length of ORF (amino acids)	551	546	562
Number of transmembrane domains	12	12	12
Conserved cysteines	4	4	4
N-glycosylation sites	5	5	3
Protein kinase consensus sites PKC	4	4	7
PKA	-	-	2
CKII	3	3	4

Table 1.3: Sequence features shared by the cloned OAT1 homologues. The GenBank accession numbers are those from the original publications. The number of transmembrane domains was predicted with the TopPred 2 server (von Heijne 1992). Conserved cysteines are those present within the large extracellular loop of all OATs and OCTs. The presence and location of N-glycosylation and protein kinase consensus sites was determined with the Prosite database . PKC = protein kinase C, PKA = cAMP-associated protein kinase, CKII = casein kinase II.

1.4 AIMS OF THE PRESENT STUDY

The major aim of this study was to isolate and characterize a human homologue of the basolateral organic anion-dicarboxylate exchanger, OAT1. The human kidney is known to efficiently excrete organic anions such as PAH, and this process has been shown to share the functional characteristics of the previously cloned OAT1 homologues. Using sequence data available from rat, flounder and mouse OAT1 homologues, an organic anion transporter isolated from the rat liver, as well as cloned members of the organic cation transporter (OCT) family, it was hoped to identify suitable regions from which primers could be designed to PCR-amplify a human OAT1 homologue. If successful this would present a rapid means of isolating a clone, thus abrogating the need for the time-consuming construction and screening of a cDNA library. A secondary aim was to investigate the renal expression of OAT2 in the human kidney. The characteristics of the rat OAT2, low PAH affinity and function as a facilitatory transporter, are similar to those demonstrated for luminal PAH transport in vesicle studies. The presence of OAT2 in the kidney would therefore make it a candidate for the luminal efflux of organic anions.

2 MATERIAL

2.1 Bacteria

Bacterial strains used for cloning and maintenance of plasmid constructs are listed in Table 2.1.

strain	company	genotype
INVaF'	Invitrogen	F′, *endA1*, *recA1*, *hsdR17* (r_k^-, m_k^+), *supE44*, *thi-1*, *gyrA96*, *relA1*, *Φ80lacZΔM15Δ(lacZYA-argF)U169*
TOP10F	Invitrogen	F′ {*lacI*^{q} Tn10(Tet^R)}, *mcrA*, *Δ(mrr-hsdRMS-mcrBC)*, *Φ80lacZΔM15 ΔlacX74*, *deoR*, *recA1*, *araD139*, *Δ(ara-leu)7697*, *galU*, *galK*, *rpsL* (Str^R), *endA1*, *nupG*
XL10 Gold	Stratagene	Tet^{r}Δ *(mcrA)183*, *Δ(mcrCB-hsdSMR-mrr)173*, *endA1*, *supE44*, *thi-1 recA1*, *gyrA96*, *relA1*, *lac* Hte [F' *proABlacI*^{q}*ZΔM15* Tn10 (Tet^r) Amy Cam^r]
XL10-Gold Km^r	Stratagene	Tet^{r}Δ *(mcrA)183*, *Δ(mcrCB-hsdSMR-mrr)173*, *endA1*, *supE44*, *thi-1*, *recA1*, *gyrA96, relA1 lac* Hte [F' *proABlacI*^{q}*ZΔM15* Tn10 (Tet*r*) Tn5 (Kan^r) Amy]
XL1-Blue	Stratagene	*recA1*, *endA1*, *gyrA96*, *thi-1*, *hsdR17*, *supE44*, *relA1*, *lac* [F' *proAB lacI*^{q}*ZΔM15* Tn10 (Tet^r)]

Table 2.1. Bacterial (*E. coli*) strains used in this study.

2.2 Plasmid vectors

The plasmid vectors used for cloning and maintenance of PCR amplicons, cell transfection and cRNA synthesis are listed in Table 2.2.

plasmid	properties	source
pPCR-script	ColE1 origin, ampicillin resistance, *lacZ* reporter, T7 and T3 RNA polymerase promoters.	Stratagene
pCRII.1	ColE1 origin, ampicillin and kanamycin resistance, *lacZ* reporter, TA-cloning site, T7 RNA polymerase promoter.	Invitrogen
pSPORT	pUC origin, ampicillin resistance, *lacZ* reporter and *lacI* repressor, T7 and SP6 RNA polymerase promoters.	Gibco
pCR-Blunt II-TOPO	pMB1 origin, *ccdB* lethal gene, *kan* gene, *lacZα* reporter, kanamycin resistance, T7and SP6 RNA polymerase promoters, TOPO-cloning site.	Invitrogen
pGEMHE	X origin, *X. laevis* β-globin gene 5' and 3'UTRs, ampicillin resistance, T7 RNA polymerase promoter	Liman et al 1992

Table 2.2: Vector plasmids used in this study.

2.3 Oligonucleotide Primers

General PCR reactions for the screening and sequencing of clones, and incorporation of restriction sites, were carried out with sequence-specific primers from NAPS or Interactiva. Sequence specific primers for 5' and 3' RACE, sequence analysis, amplification of full-length clones and mutagenesis were obtained from NAPS or Interactiva.

Oligonucleotides used for RT-PCR, PCR-based cloning, PCR screening of clones, sequencing, generation of mutants, and cRNA synthesis are listed in Table 2.3.

A. Primers used in the cloning characterization and mutational analysis of hROAT1

name	sequence	use
5.1[a]	TIATGGCNWSNCAYAAY	degenerate primer for hROAT1 cloning; specific to the 5'end ('forward')
5.2[a]	GGIACITGYGCNGCNTWY	degenerate primer for hROAT1 cloning specific to the 5'end ('forward')
3.1[a]	ARNCCRTARTANGCRAA	degenerate primer for hROAT1 cloning specific to the 3'end ('reverse')
3.2[a]	NCCRAADATNACYTGDAT	degenerate primer for hROAT1 cloning specific to the 3'end ('reverse')
3.3[a]	GCNARRCANCCYTTNCC	degenerate primer for hROAT1 cloning specific to the 3'end ('reverse')
Si	GTTCTTGCTGAGGTTGGCATCGGCAG	hROAT1-specific 5' RACE primer
So	GAGGTGAAGCGGAGGCAGGACTCAG	hROAT1-specific 5' RACE primer
GSP1	TTCCTCTGCCTCTCCATGCTGTG	hROAT1-specific 3' RACE primer
GSP2	AGGGCTTTGGAGTCAGCATCTAC	hROAT1-specific 3' RACE primer
QoQi-dT	CGCAGATGTACGTCCTACCATCGCCTCT--AGACCAGCCTACGAGC(T)17	universal RACE primer
Qo:	CGCAGATGTACGTCCTACCATCGCC	universal RACE primer
Qi:	ATCGCCTCTAGACCAGCCTACGAGC	universal RACE primer
hR5[b] specific	TCTAGATGGCCTTTAATGACCTCCTGCARC	amplification of the hROAT1 ORF, 5'-
hR3[b]	TCAAAATCCATTCTTCTCTTGTGCT	amplification of the hROAT1 ORF, 3'-specific
hR 5' +Bam[b]	GGATCCATGGCCTTTAATGACCTCCTGCARC	as for hR5, with BamHI recognition sequence
hR 3' +Xba[b]	TCTAGACCTCAAAATCCATTCTTCTCTTGTGC	as for hR3, with XbaI recognition sequence
hR578f	TCCTCTCGGGCATGGCTCTGGC	sequencing primer
hR599r	GCCAGAGCCATGCCCGAGAGG	sequencing primer
hR1153f	GGGCTTCCTTGTCATCAACTCCC	sequencing primer
hR1174r	GGGAGTTGATGACAAGGAAGCCC	sequencing primer
R5UTR 5'UTR	GAGCTGTCCAGACCCCCG	5'UTR cloning, specific for the rOAT1
M5UTR 5'UTR	AAGGAGGGGCAGCCCACCAG	5'UTR cloning, specific for the NKT
hR5' UTR[b]	AAGTGAGGAGAAGCTGCAAGG	Specific for the hROAT1 5'UTR sequence
K382A-f	GGACCTGCCTGCCGCGCTTGTGGGCTTCC	Forward primer for the generation of the hROAT1 K382A point mutation
K382A-r	GGAAGCCCACAAGCGCGGCAGGCAGGTC	Reverse primer for the generation of the hROAT1 K382A point mutation
R466D-f	GCAGCACCATGGCCGACGTGGGCAGCATCG	Forward primer for the generation of the

		hROAT1 R466D point mutation
R466D-r	CGATGCTGCCCACGTCGGCCATGGTGCTGC	Reverse primer for the generation of the hROAT1 R466D point mutation
hROAT1A	AACTTCGGATCCATGTGCGCCTTCCGGCT--CCTCTC	Forward primer for generation of an hROAT1 N-terminal deletion; with BamHI site and artificial start codon
hR-5'deletion	ATTAAAGGCCATGGATCCCCAGAGGAAA	Reverse primer for the above reaction; with BamHI site
hR-exon 10	GCTATCTAGACTCACCTGCTCTCCAGG--TCCTG	Forward primer for generation of hROAT1 mutant lacking exon 10; with XbaI site
hR-exons 9&10	GCTATCTAGACTCACCGGATCATTGTG--GGATAC	Forward primer for generation of hROAT1 mutant lacking exons 9 and 10; with XbaI site
hR-3' deletion	AATGGATTTTGAGGTCTAGACCC	Reverse primer for the reaction above with XbaI site and artificial stop codon
B. Primers used in the cloning of hOAT2		
h2-hEST1	ATGGGCTTTGAGGAGCTGCTG	Specific to the hEST containing the putative start codon of hOAT2
h2-hEST3	CTTTCTCTCCACGTCCTGGCTG	Specific to the last NLT-homologous 3'end sequence of hEST3
h2-3'RACE	CAGACAGACAGGGATGGGGC	hOAT2-specific 3'RACE primer
h2-5'end + Bam	GGATCCATGGGCTTTGAGGAGCTGCTG	Specific to the 5'end of hOAT2; includes BamHI site
h2-3'end + Xba	TAATTCTAGATATCACACGTACACAGA--CACAG	Specific to the 3'end of hOAT2; includes XbaI site
h2-513f[b]	CTGCTGCTGGTAGCCTAC	hOAT2-specific sequencing primer
h2-531r[b]	GTAGGCTACCAGCAGCAG	hOAT2-specific sequencing primer
h2-1072f[b]	CTATTACGGCCTGAGTCTG	hOAT2-specific sequencing primer
h2-1090r[b]	AGACTCAGGCGGTAATAGG	hOAT2-specific sequencing primer
hNLT-3´end	TTAGTTCTGGACCTGCTTCATGGG	Specific to the 3'end of the liver-specific hOAT2 isoform (hNLT)
C. Primers used to construct the hOAT2:hROAT1 chimera		
hR2-5´+Bam	ATGCGGATCCATGGGCTTTGAGGAGCT--GCT	hOAT2 5'end-specific primer with BamHI site
hR1-3´+Xba	TAGCTCTAGACTCAAAATCCATTCTTC--TCTTGTGC	hROAT1 3'end-specific primer with XbaI site
chimera(2:1)-f	GCCTCTGGTGGGTGCCTTCGGCCCGCT--GGCACTCC	Bipartite primer for creation of the hOAT2:hROAT1 chimera via overlapping PCR
chimera(2:1)-r	GGAGTGCCAGCGGGCCGAAGGCACCCA--CCAGAGGC	Bipartite primer for creation of the hOAT2:hROAT1 chimera via overlapping PCR
D. Primers specific to sequence of vectors used in this study		
T7[c]	GTAATACGACTCACTATAGGGC	Specific for T7 RNA polymerase promoter
T3[c]	AATTAACCCTCACTAAAGGG	Specific for T3 RNA polymerase promoter
SP6[c]	ATTTAGGTGACACTATAG	Specific for SP6 RNA polymerase promoter
M13forward[c]	GTAAAACGACGGCCAGT	vector specific
M13reverse[c]	GGAAACAGCTATGACCATG	vector specific

Table 2.3 Oligonucleotide primers used in this study. Primers were ordered from Interactiva, except a = Eurogentec, b = NAPS, c = MWG. Sequence details: A= adenosine, G= guanosine, C= cytosine, T= thymine, R= A or G, S= G or C, W=, Y= C or T, N= A,G, C or T, I= inosine.

2.4 Enzymes

All restriction enzymes were purchased from New England Biolabs Inc (Beverly, MA, USA) or MBI Fermentas (Vilnius, Lithuania). Various DNA polymerases were used according to the application (the polymerase used for each application is detailed in Methods) and were purchased from Stratagene (La Jolla, CA, USA), Invitrogen (Carlsbad, CA, USA), or PAN Systems (Aidenbach, Germany). T4 DNA ligase was purchased from Boehringer Mannheim (Mannheim, Germany), and calf intestinal alkaline phosphatase was purchased from New England Biolabs (Beverly, MA, USA).

2.5 Kits

All kits used are listed in Table 2.4 below

A. Nucleic acid purification	
QIAquick™ Gel Extraction Kit QIAprep Spin Miniprep Kit Oligotex mRNA minikit PCR purification kit	QIAgen (Hilden, Germany)
Nucleotrap™ Extraction Kit NucleoSpin™ Extract 2 in 1	Macherey-Nagel (Düren, Germany)
B. PCR cloning kits	
TA™ Cloning Kit TOPO™ TA Cloning Kit TOPO™ XL PCR Cloning Kit ZeroBlunt™ TOPO™ Cloning Kit	Invitrogen (Carlsbad, CA, USA)
PCR-Script™ Amp Cloning Kit	Stratagene (La Jolla, CA, USA)
C. Mutagenesis	
QuikChange Site-directed Mutagenesis Kit	Stratagene (La Jolla, CA, USA)
D. cRNA synthesis	
T7 mMessage mMachine™ Kit	Ambion (Austin, TX, USA)
E. RT-PCR	
Omniscript RT-PCR	QIAgen (Hilden, Germany)

Table 2.4: Kits used in this study.

2.6 Chemicals

All chemicals used in this study were obtained from Sigma, Merck, Applichem, Serva, Roth or Boehringer, unless otherwise stated in the text. Radioactively labelled chemicals were obtained from NEN.

2.7 Sequence analysis software

Table 2.5 lists the software and online servers used to analyse raw sequence data, perform sequence alignments, identify putative secondary structures of protein sequences and consensus sequences for enzyme recognition sites, and primer design.

A. Software		
Program	Use	Reference
Wisconsin Pack	various sequence analyses	Genetics Computer Group Inc
Generunner	primer design	Hastings Software Inc
Chromas	sequence reading program	Technelysium Pty Ltd
EZ-fit	enzyme kinetic	Perella Scientific Inc
Quattro Pro	evaluation of uptake experiments	Borland international Inc
SigmaPlot	statistical analyses	Jandel Corporation

B. Online sequence analysis servers		
Program	Use	Reference
MAP	multiple sequence alignments	http://genome.cs.mtu.edu/map.html
Genebee	multiple sequence alignments	http://www.genebee.msu.su/
Translation tool	N sequence to aa sequence	http://www.expasy.ch/tools/dna.html
Webcutter	restriction maps	http://www.medkem.gu.se/cutter/
TopPred 2	secondary structure prediction	http://www.biokemi.su.se/~server/toppred2/
Blast	finds similar database sequences	http://www.ncbi.nlm.nih.gov/BLAST/
Prosite	consensus sites in a sequence	http://www.ebi.ac.uk/searches/prosite
Entrez Browser	sequence retrieval	http://www.ncbi.nlm.nih.gov/Entrez/

Table 2.5: Software used in this study. Manufacturer or website is given. N = nucleotide, aa = amino acid.

2.8 Equipment

Appliance	Model	Manufacturer
Thermocycler	2400	Perkin Elmer (Norwalk CT, USA)
	Omn-E HBTRE	Hybaid Ltd (Teddington, England)
	PTC-200	MJ Research (Watertown MI, USA)
Vortexer	REAX 1	Heidolph Elektro (Kelheim, Germany)
	REAX Top	Heidolph Elektro (Kelheim, Germany)
	MS1	IKA (Staufen, Germany)
Dissection microscope	Stemi1000	Zeiss (Jena, Germany)
Nanoliter injector		World Precision Instruments (Sarasota FL, USA)
Scintillation counter	1500 Tri-Carb	Packard Instrument Co (Meriden CT,USA)
	2100 TR	Packard Instrument Co (Meriden CT,USA)

Centrifuges	Biofuge fresco	Heraeus (Osterode, Germany)
	5417R	Eppendorf (Hamburg, Germany)
	1394	Hettich (Stockholm, Sweden)
	C-1200	National Labnet Co (Woodbridge NJ, USA)
	RC-5B	Sorvall (Newtown, CT, USA)
Spectrophotometer	Novaspec II	Pharmacia (Uppsala, Sweden)
	GeneQuant II	Pharmacia (Uppsala, Sweden)
Power pack	P24	Biometra (Göttingen, Germany)
	LKB Bromma 2297	Pharmacia (Uppsala, Sweden)
	LKB Bromma 2303	Pharmacia (Uppsala, Sweden)
Gel chambers	Midi	MWG-Biotech (Ebersberg, Germany)
	VEU 2001	Pharmacia (Uppsala, Sweden)
Shaking incubator	3031	GFL (Burgwedel, Germany)
Circulating water baths	D8	Haake (Karlsruhe, Germany)
Speed vac concentrator	SVC 100E	Savant (Holbrook NY, USA)
Refrigerated aspirator	Unijet II	UniEquip (Martinsried, Germany)
Gel documentation	Gel Print 2000 I	Biophotonics (Ann Arbor, MI, USA)
UV transilluminator	TM40	UVP Inc (Upland, CA, USA)
pH meter	pH-Meter 611	Orion Research Inc (Beverly MA, USA)
Balance	1474	Sartorius (Göttingen, Germany)
Automated DNA sequencer	ABI Prism	Applied Biosystems (Laguna Beach CA, USA)
Heated magnetic stirrer	RCT B	IKA (Staufen, Germany)
Microwave	Privileg 8017, 8521	Quelle Schikedenz (Fürth, Germany)
Electroporator	Easyject	Equibio (Monchelsea, England)

3 METHODS

3.1 MOLECULAR

3.1.1 cDNA Synthesis

The first step in cloning hROAT1 and hOAT2 was the synthesis of cDNA. To clone hROAT1, cDNA was synthesized from human kidney total mRNA using the Superscript system (Life Technologies).

Reagents:

NotI primer	1 µg
Superscript II RT	200 units/µg mRNA
mRNA in DEPC water	1-5 µg
5x first strand buffer	250 mM Tris-HCl (pH 8.3), 375 mM KCl, 15 mM $MgCl_2$
DTT	0.1 mM
dNTP	500 µM each dATP, dCTP, dGTP, dTTP
DEPC water	to 20 µl

Synthesis was carried out as per the manufacturers instructions (37 °C 1 hour), with the following exceptions: 40 U RNasin (Promega) was added to each reaction; random 9-mers and QoQidT17 were substituted for the *Not*I primer to generate template for 5' RACE and 3' RACE, respectively. First strand cDNA was then used as the template for subsequent PCR reactions.

For hOAT2, human liver and kidney cDNA were synthesized from poly(A) RNA. The poly(A) fraction was first isolated from total RNA using a poly(dT) column (Qiagen). This was then reverse-transcribed into cDNA using the Omniscript reverse transcription kit (Qiagen).

Reagents:

10x RT buffer	composition not provided by manufacturer
dNTPs	500 µM each dATP, dCTP, dGTP, dTTP
Oligo-dT primer	1 µM
RNase inhibitor	10 units
Omniscript RT	4 units
template RNA	50 ng
RNase-free water	to 20 µl

After thorough mixing the reaction was incubated at 37 °C for 1 hour. For subsequent PCR reactions 2 µl aliquots were used as the template. The remainder of the reaction was stored at –20 °C for future use.

3.1.2 Polymerase Chain Reaction

The polymerase chain reaction, or PCR, is a powerful technique with many applications in basic research. Devised by Kary Mullis (Mullis 1990), PCR enables the specific exponential amplification of DNA regions for which flanking sequence information is available. Based on the known flanking sequence, a pair of oligonucleotides primers, usually 20-25 nucleotides in length, are designed with homology to the 5' and 3' ends of the target sequence (outlined in Figure 3.1). These are then added in molar excess to a DNA sample containing the sequence of interest, together with a thermostable DNA polymerase and dNTPs, and the mix is then subjected to a regimen of temperature cycling. Initial heating leads to disassociation (denaturation) of the complementary strands of the target sequence (or template) and is followed by rapid cooling to a temperature permissive for the hybridisation (annealing) of the oligonuleotide primers to the template. The temperature is then raised to a temperature optimal for the function of the thermostable DNA polymerase, allowing extension of the DNA sequence of interest from the site of primer annealing (polymerisation). From this process of denaturation, annealing and polymerisation, one copy of the target sequence is synthesized from each template molecule to which the primers annealed; with each successive cycle, the number of copies doubles, yielding an exponential increase in copies of the target sequence.

Of the great number of applications of PCR, many were used in this work. Synthesis of the template cDNA from poly(A)-RNA (reverse transcriptase (RT) PCR), amplification of the initial PCR product of hROAT1 (degenerate PCR), construction of expression clones, mutational analysis, and generation of the hOAT2:hROAT1 chimera all relied on methods derived from the classical PCR.

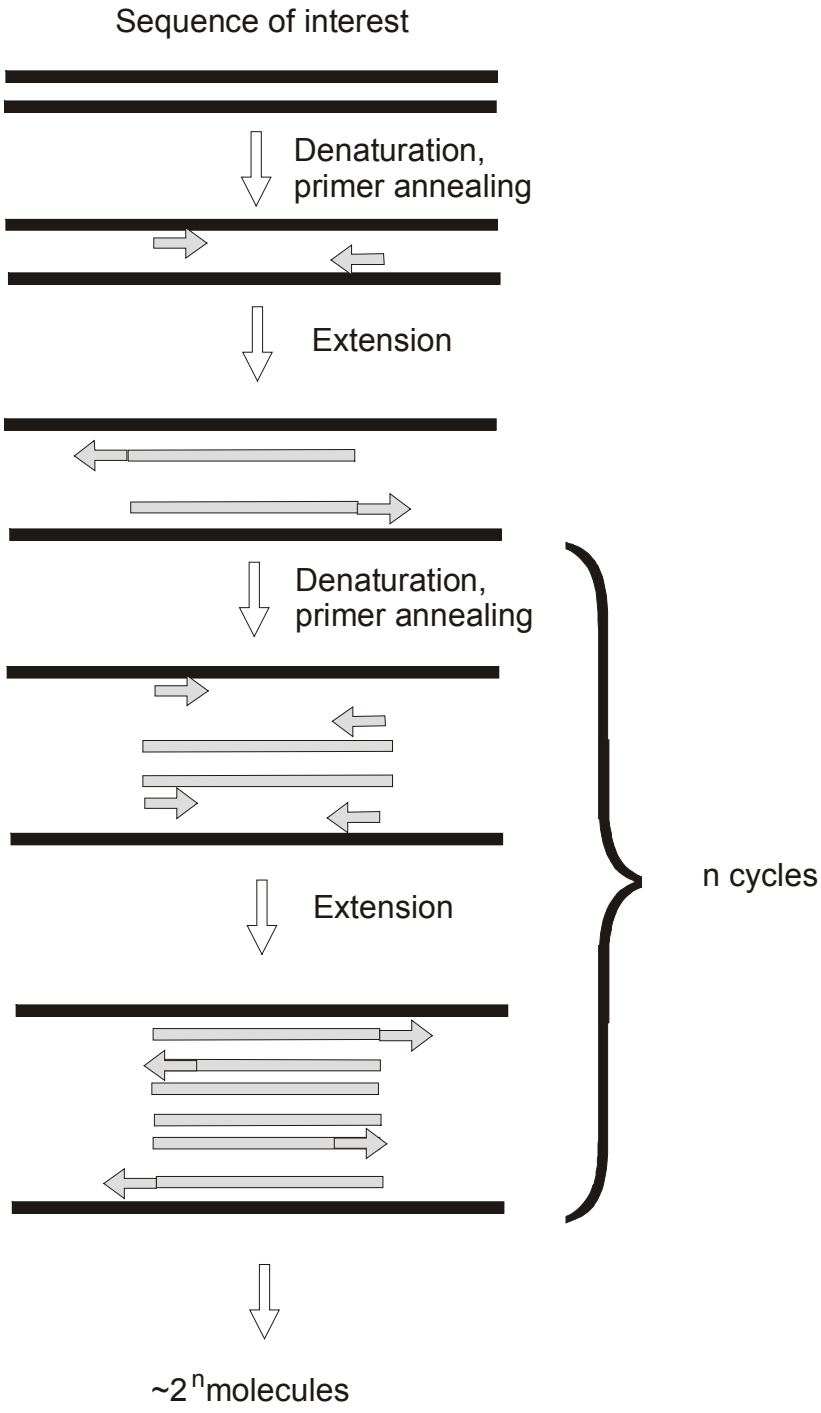

Figure 3.1: The PCR principle. The basis of the polymerase chain reaction is outlined here. Following denaturation of the target DNA sequence (double black line) at 94-95 °C, primers flanking this region (grey arrows) are allowed to bind at the permissive temperature. Raising the temperature to that optimal for polymerase function leads to extension (extended grey arrows) from the primer sequence, and a doubling in copies of the target sequence. Repeating this process yields an exponential increase in copy number.

3.1.2.1 Standard PCR

A standard PCR was used to screen all transformed bacterial clones to minimize plasmid isolation from false positives. Suspected positive clones were first transferred with a sterile toothpick to a standard 20 µl PCR reactions, and the same toothpick was then used to inoculate 50 µl LB media. The PCR contained one primer specific for the vector and one primer specific for the insert (Table 2.3), and consisted of 25 cycles of 94 °C for 20 s, 50-55 °C for 15 s (depending on primers used), and 72 °C for 30-90 s (depending on length of expected product; 1 minute / kb). Clones yielding a positive PCR result were then used to inoculate a 2-5 ml overnight culture.

3.1.2.2 Degenerate PCR

PCR can be applied to the cloning of a cDNA based on the amino acid sequence of a protein of interest. Moreover, where the sequences of a family of proteins are known, these can be used to clone a homologue from a novel species. To do this, degenerate primers representing all possible nucleotide sequences encoding a stretch of conserved amino acids are used in a PCR. In addition, inosine can be incorporated at highly degenerate positions to reduce overall numbers in the primer pool. To amplify hROAT1 from a human renal cDNA template, a PCR-based homology cloning strategy incorporating degenerate primers was used. The degenerate primers were designed based on a amino acid sequence alignment of previously cloned members of the related OAT (fROAT, OAT1/ROAT1, NKT and NLT) and OCT (rOCT1, rOCT2) families (Figure 4.1). From this alignment, regions were chosen that indicated both greatest homology between the organic anion transporters whilst at the same time maximal divergence from the organic cation transporters. The regions selected for primer synthesis are highlighted and the primer sequences are presented in Table 4.1 with the degeneracy factor of each primer shown. The degenerate primers were synthesized by Eurogentec. The composition and parameters for PCR using degenerate primers were determined empirically. The degenerate PCR consisted of the following components: 5x PCR buffer, 200 µM of each dNTP, 1.5 mM MgCl, 200 ng of each primer, 2 units Taq polymerase, with nanopure water to a volume of 50 µl. The successful PCR was carried out with primers 5.1 and 3.2 (Table 2.3). A 35 cycle PCR comprised: 94°C for 30s, 40°C for 1 min, 50°C for 1 min, and 72°C for 1.5 min. PCR products were cloned into pCR2.1 (Invitrogen) and sequenced.

3.1.2.3 Rapid amplification of cDNA ends (RACE)

Following the amplification of an initial PCR product from the gene or cDNA of interest, the clone can be extended in both the 5' and 3' directions using a technique known as rapid amplification of cDNA ends (RACE), using either a cDNA or RNA template (Frohman et al 1988), outlined in Figure 3.2. From the cloned sequence, primers are designed which are oriented in the direction of the missing sequence. For 3' RACE, PCR is carried out with a gene-specific primer in combination with a second primer consisting of a stretch of poly(dT) fused to a unique sequence which serves as the anchor sequence. The product resulting from this PCR is then used as the template for a second, nested, PCR with a second gene-specific primer and a primer specific to the unique anchor sequence. In 5' RACE, a similar process is carried out, preceeded by the generation of an synthetic poly-(A) tail using a terminal deoxynucleotidyltransferase (TdT). The same anchor primer can then be used with primers specific to the 5' region of the known sequence in subsequent PCR.

5' RACE

Reagents:

Tailing reaction	
Terminal Transferase	15 U
Template	50 ng
dATP	200 µM
RNase-free H_2O	to 20 µl

	initial PCR	second (nested) PCR
template	first strand cDNA (tailed)	1 µl initial PCR reaction
anchor primer	QoQidT17, 20 ng	-
RACE primer	Qo, 200ng	Qi, 200 ng
gene-specific primer	So, 200ng	Si, 200 ng
DNA polymerase	Takara Taq, 1 U	Takara Taq, 1 U

The tailing reaction was incubated at 37 °C for 10 minutes, after which the reaction was stopped and the enzyme inactivated by incubation at 65 °C for 15 minutes. The first stage PCR of the 5' RACE extension of the hROAT1 clone was performed with 20 ng of QoQidT17, plus 200 ng each of Qo (anchor-specific outer primer) and So (gene-specific outer primer) and 1 U of Takara Taq-Polymerase. PCR conditions were as follows: 3 cycles of 94°C for 20 sec, 42°C for 2 min, 72°C for 3 min, followed by 35 cycles of 94°C for 20 sec, 65°C for 20 sec and 72°C for 1 min. Second stage PCR was

performed with 1µl of the first stage products with 200 ng each of Qi (anchor-specific inner primer) and Si (sequence-specific inner primer) plus 1U Takara Taq-Polymerase.

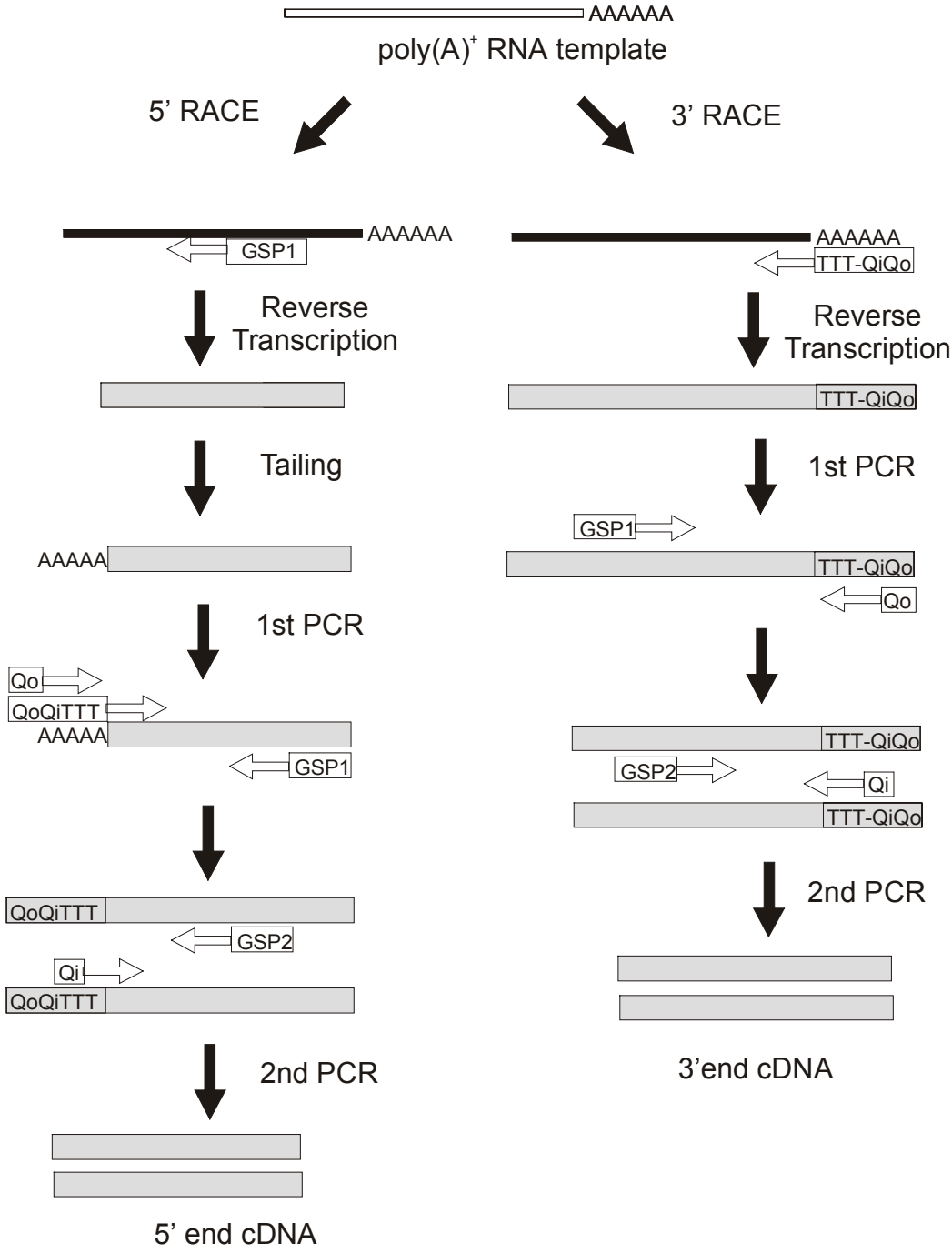

Figure 3.2: Rapid amplification of cDNA ends – RACE. 5' and 3' RACE are shown, starting with a poly(A)-RNA template. In 5' RACE, first strand reverse transcription cDNA synthesis, from a gene-specific primer GSP1, is followed by a tailing reaction. For 3' RACE, reverse transcription proceeds from the poly-A tail of the RNA template. In 5' and 3' RACE, the first nest PCR reaction contains the QoQidT anchor primer together with the QoQidT-specific Qo primer, and a gene-specific primer GSP1, with the first strand cDNA as template. The second PCR involves internal primers and cDNA generated by the first PCR reaction

Amplifications were for 35 cycles of 94°C for 20 sec, 65°C for 20 sec and 72°C for 1 min. PCR products (200 to 300 nucleotides) were cloned into pCR2.1 and sequenced.

3’ RACE

Reagents:

	initial PCR	second (nested) PCR
template	first strand cDNA, generated with QoQidT17 primer	1 µl initial PCR reaction
RACE primer	Qo, 200ng	Qi, 200 ng
gene-specific primer	GSP1, 200ng	GSP2, 200 ng
buffer	composition not provided by manufacturer	
dNTPs	200 µM	200 µM
DNA polymerase	Takara Taq, 1 U	Takara Taq, 1 U

For 3' RACE extension of hROAT1, the first stage PCR contained 200 ng each of primers Qo and GSP1 (gene-specific primer 1). PCR conditions were as follows: 94°C for 20 sec, 65°C for 30 sec and 72°C for 1.5 min for 35 cycles. The second, nested, PCR was carried out with the Qi and GSP2 (a second template-specific primer), and 1 µl of the first stage PCR product, with 30 cycles of the conditions used in the first stage. PCR products of approximately 800 base pairs, were cloned into pCR2.1 and sequenced.

The 3’ RACE for hOAT2 consisted of a half-nested PCR. The initial PCR contained the reagents listed above, with the exception that the GSP1 primer was replaced with an hOAT2-specific primer, hOAT2-3’RACE. Following amplification as above, the first round products were reamplified with the internal RACE primer, Qo, and the hOAT2-3’RACE primer.

3.1.2.4 Generation of high-fidelity cDNA clones:

In order to generate cDNA clones corresponding as closely as possible to the expressed mRNA sequence, PCR was carried out with proof-reading DNA polymerases to maximize polymerization fidelity. Of the many proof-reading polymerase commercially available, the PowerScript polymerase mix was used. The advantages of this product are that it has high polymerase fidelity and is less sensitive to changes in the concentration of cations, template and primers in the PCR mix.

Based on the sequence contig of hROAT1 constructed from the initial degenerate PCR product and 5’ and 3’ RACE reactions, sequence-specific primers with restriction sites incorporated where required, were designed to PCR-amplify full-length clones from

human kidney cDNA. In the case of hOAT2, sequence-specific primers derived from the sequence of the expressed sequence tags (ESTs) retrieved from the human dbEST database were used to amplify an initial product comprising almost the entire reading frame. The complete sequence was then amplified with a forward primer derived from this initial product, and a reverse primer derived from subsequent 3' RACE data.

Reagents:

template	cDNA
sequence-specific 5' primer	20 pmol
sequence-specific 3' primer	20 pmol
Powerscript DNA polymerase	1 U
dNTPS	200 µM each
10x PCR buffer	composition not provided by manufacturer
5x Optizyme enhancer	composition not provided by manufacturer
$MgCl_2$	2 mM

The amplification with Powerscript polymerase was carried out as per the manufacturer's instructions (PAN Systems), with 30 cycles of the following amplification parameters: 94°C for 20 sec, 55-60°C for 20 sec and 68-72°C for 4 min; followed by a final extension period of 10 min at 72°C. The full-length cDNAs were cloned into pPCR-Script (Stratagene) or pCR-TOPO (Invitrogen), and polymerase fidelity was confirmed by sequencing.

3.1.2.5 Deletion mutant construction

To introduce large deletions into the hROAT1 reading frame and to remove the reading frame of fNaDC-3 during the construction of the expression clone, PCR with a proof-reading polymerase was carried out. The deletions were in essence a long PCR directed away from the region to be deleted, with primers incorporating appropriate 5'-terminal restriction sites. This process is detailed in Figure 3.3.

Reagents:

template	50 ng plasmid DNA
forward primer (Table 2.3)	20 pmol
reverse primer (Table 2.3)	20 pmol
Powerscript DNA polymerase	1 U
dNTPS	200 µM each
10x PCR buffer	composition not provided by manufacturer
5x Optizyme enhancer	composition not provided by manufacturer
$MgCl_2$	2 mM

The amplification was carried with 30 cycles of the following amplification parameters: 94°C for 20 sec, 55-60°C for 20 sec and 68-72°C for 4 min, followed by a final extension period of 10 min at 72°C. For the removal of the fNaDC-3 reading frame, detailed in 4.7, unique restriction sites were incorporated at each end of the amplification product to enable the directional ligation of the hROAT1 between the 5' and 3' UTRs of fNaDC-3. To delete N- and C-terminal parts of the hROAT1 reading

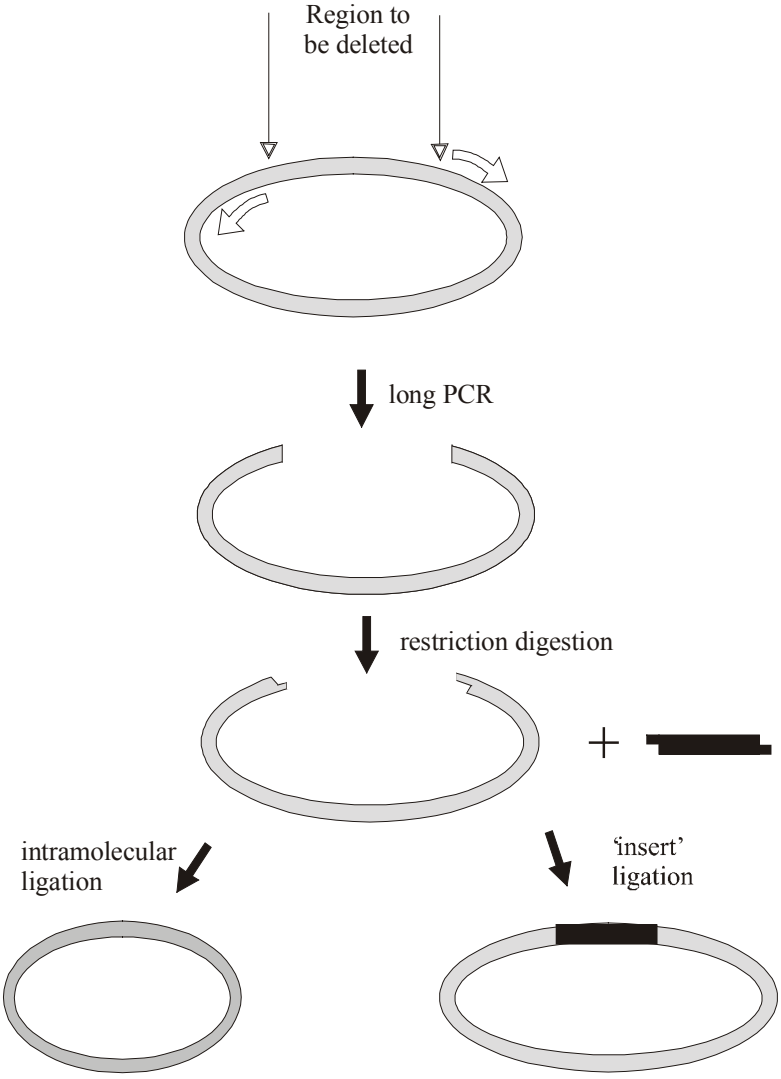

Figure 3.3: 'Deletion' PCR. The method used to construct deletion mutants and the hROAT1 expression clone is outlined schematically. Primers are designed which flank, and are directed away from the region within a plasmid clone to be deleted (grey circle, top), and a long PCR is carried out. By incorporating the appropriate restriction sites in the primers, the amplification product (incomplete grey circle) can then be restricted and ligated either intramolecularly as in the construction of deletion mutants (bottom left) or to a second, similarly restricted DNA molecule (black line) as in the construction of the hROAT1 expression clone (bottom right).

frame, the same unique restriction site was incorporated at both ends, and following restriction, this allowed intramolecular ligation of the amplification product to take

place. To maintain translation competence in subsequent cRNA syntheses, a start or stop codon was incorporated immediately after the restriction site within the primer. After ligation, products were transformed as described in 3.2.1.1.

3.1.2.6 Overlapping PCR

The construction of chimeric proteins is often carried out by making use of compatible restriction sites present in the DNA sequence of the proteins of interest. However, this method is limited in that it depends on the occurrence of two compatible sites at the location desired for the junction point between the two protein fragments. In contrast, the overlap PCR is ideally suited to the creation of a chimeric protein at any position required (Ishii et al 1998). This PCR application is carried out with two plasmids, each containing one of the donor sequences from which the chimera is to be constructed, and bipartite primers which contain sequence specific to both donors and form the junction of the chimera (Figure 3.4). By way of explanation, a chimera to be constructed from donor sequences A and B, can be represented by 5'-AB-3', where A is the 5'- terminal half of sequence the first donor, linked to B, the 3'-terminal part of the second donor. To achieve this chimeric sequence, two rounds of PCR are required. First, donors A and B are separately amplified in the first round using a specific primer and a bipartite primer, and in the second round the resulting amplification products are mixed with the two specific primers from the first round leading to amplification of a chimeric sequence. The bipartite primers consist of a sequence at the 3' end specific for of the donors in the first round, fused to a sequence at the 5' end specific for the other donor. Thus, when the two initial amplification products are mixed, they can hybridize at the site of incorporation of the bipartite primer. Such a duplex can be extended to create a double stranded chimeric sequence, which then acts as the template for the second round of PCR.

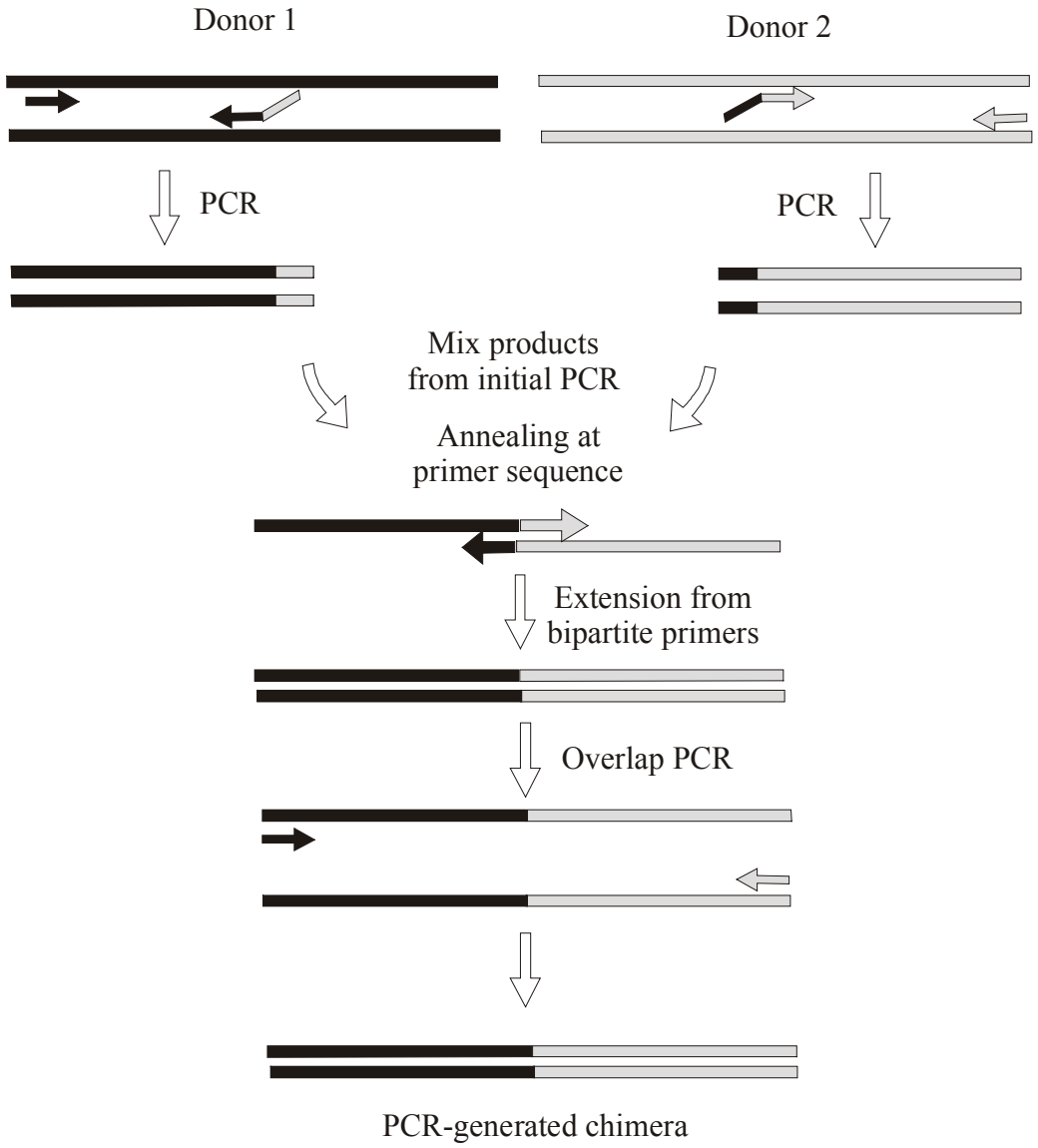

Figure 3.4: Overlapping PCR. Schematic representation of the overlapping PCR method. In two separate PCRs, donor sequences 1 (black) and 2 (grey) are amplified. Each reaction contains a donor-specific primer (black and grey arrows) and a bipartite primer (arrow with oppositely coloured tail) containing a 5' end complementary to the other donor sequence. This yields two PCR products (grey and black double lines) each with a terminus homologous to the other donor. Mixing the two products allows annealing at the bipartite primer sequence (attached arrows) and extension, yielding a duplex chimeric sequence (black-gray double line) which acts as the template in a subsequent PCR.

Reagents:

	initial PCR – donor 1	initial PCR – donor 2
template	50 ng hOAT2	50 ng hROAT1
forward primer (Table 2.3)	20 pmol hR2-5´+Bam	20 pmol chimera(2:1)-f
reverse primer (Table 2.3)	20 pmol chimera(2:1)-r	20 pmol hR1-3´+Xba
buffer	(composition not supplied by manufacturer)	
optizyme enhancer	20 % v/v	20 % v/v
dNTPs	200 µM each	200 µM each
MgCl2	2 mM	2 mM
DNA polymerase	Power Script, 1 U	Power Script, 1 U

	Overlap PCR
template	products of initial PCR, 40 ng each
forward primer (Table 2.3)	20 pmol hR2-5´+Bam
reverse primer (Table 2.3)	20 pmol hR1-3´+Xba
buffer	(composition not supplied by manufacturer)
optizyme enhancer	20 % v/v
dNTPs	200 µM each
MgCl2	2 mM
DNA polymerase	Power Script, 1 U

The initial PCR comprised 30 cycles of: 94° for 10 s, 55° for 15 s, and 72° for 2 min, followed by a final extension period of 10 min at 72°. The products were visualized by agarose gel electrophoresis and bands of the expected size were excised and purified using the Nucleo©Trap gel extraction kit (Macherey and Nagel). After determining the concentration, 40 ng of each amplified donor were used as the template in an overlap PCR, comprising 30 cycles of: 94° for 10 s, 65° for 15 s, and 72° for 4 min, followed by a final extension period of 10 min at 72°. Following amplification, a band of predicted size was purified as above and cloned into the pCR©-Blunt II-TOPO vector using the ZeroBlunt TOPO cloning kit, described in section 3.1.7.2.2. Plasmid DNA from several positive transformants was isolated and sequenced to determine polymerase fidelity, and one chimera was subcloned into pSport between the fNaDC 5' and 3' UTRs as described for construction of the expression clone detailed in section 4.1.2.

3.1.3 Site-directed Mutagenesis

In vitro mutation of targeted nucleotides, site-directed mutagenesis, allows controlled changes to be introduced into DNA molecules. The QuikChange™ Site-Directed Mutagenesis Kit (Stratagene) was the method of choice for the generation and disruption of restriction enzyme recognition sites, correction of errors introduced by PCR amplification, and amino acid exchanges. Unlike the difficult labour-intensive methods involving M13-based bacteriophage vectors and ssDNA rescue, the QuikChange kit enables mutagenesis to be carried out with most plasmids. The basic principle of the method is the repeated extension, by *Pfu* polymerase, of the entire plasmid clone from two complementary primers, both of which contain the desired mutation. This generates a mutant plasmid with staggered nicks, and the template can be removed by digestion with a methylation-dependent endonuclease, *Dpn*I, which reacts only with the methylated template plasmid isolated from bacteria (with the target

sequence 5'-G^{m6}ATC-3"), and not the methyl-free polymerase-extended mutant. The mutant plasmid can then be transformed into *E. coli*, where the nicks are repaired.

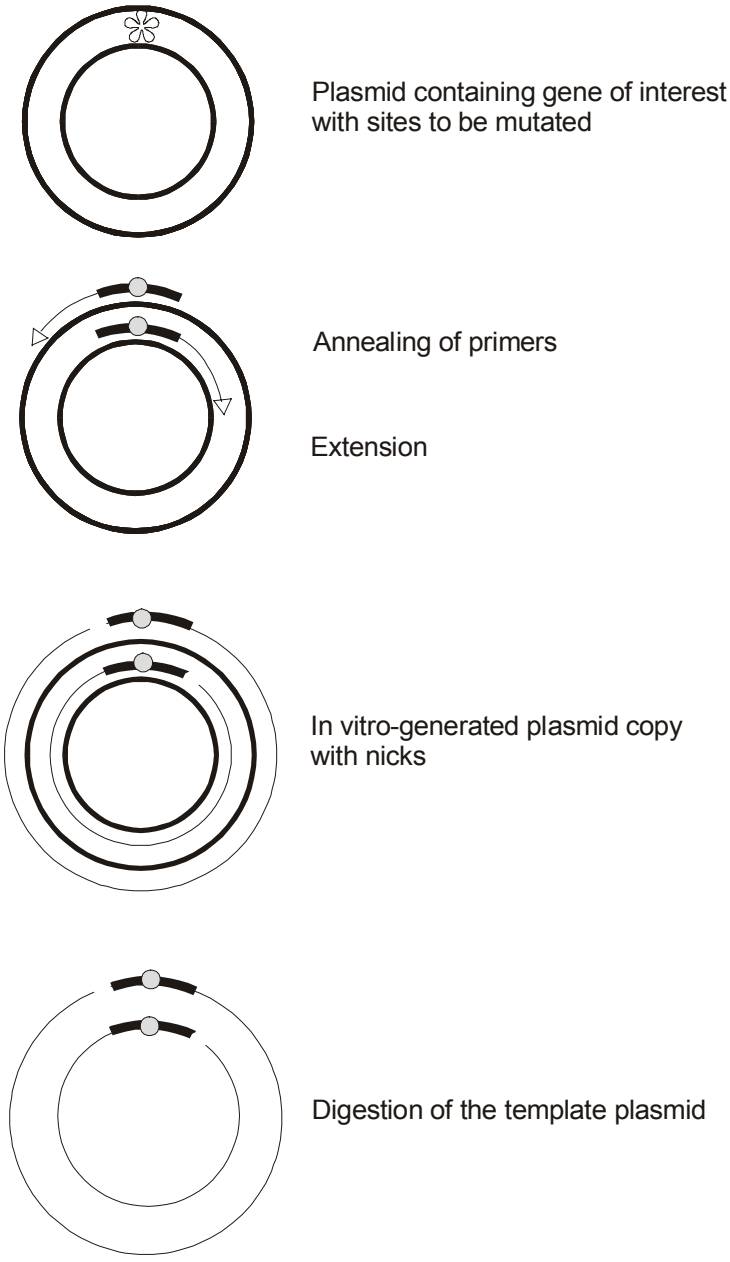

Figure 3.5: Site-directed mutagenesis. A schematic representation of site-directed mutagenesis using the QuickChange mutagenesis kit. A plasmid (bold circles) containing the gene of interest with site targeted for mutation (asterisk), is extended (arrows) from complementary primers (bold arcs) containing the desired mutation (closed circles). The extension process continues until the site of primer annealing is reached, yielding an in vitro generated copy of the plasmid with staggered nicks (thin circles). The parent plasmid template, originally isolated from a methylation-competent bacterial host, is methylated; the in vitro-extended copy is not. The addition of *Dpn*I leads to the digestion of the parent plasmid leaving the nicked copy, which is repaired in the bacterium following transformation

Reagents:	
Pfu DNA Polymerase	2.5 U/µl
10x Reaction Buffer	100 mM KCl, 100 mM $(NH_4)_2SO_4$, 200 mM Tris-HCl (pH8.8), 20 mM $MgSO_4$, 1 % Triton® X-100, 1 mg/ml nuclease-free bovine serum albumin (BSA)
dNTP mix	composition not supplied by manufacturer
Oligonucletide primers	Specific forward and reverse primers for each mutation: 125 ng (Table 2.3)
*Dpn*I restriction enzyme	10 U/µl
Competent cells	Epicurian Coli® XL1-Blue super-chemically competent cells
SOC medium	2 % Tryptone, 0.5 % Yeast Extract, 10 mM NaCl, 2.5mM KCl, 10 mM MgCl2, 10 mM MgSO4, 20 mM glucose (dextrose).

To generate desired nucleotide base substitutions, sequence-specific primers with the appropriate mismatches were designed; these are listed in Table 2.3. All primers used satisfied the following criteria: both primers contained the desired mismatch and annealed to the same sequence on opposite strands of the template plasmid; all were 25 - 45 nucleotides in length with an annealing temperature of approximately 75 - 80 °C; the mutation was situated as close as possible to the middle of the primer, with at least 12 bases of perfectly annealing sequence on either side; each primer had a GC content of at least 40 %, and terminated in at least 2 G or C bases. The extension reaction consisted of 125 ng of each primer, 5, 15 or 50 ng of template plasmid (to empirically determine the optimal conditions), 5 µl of 10x reaction buffer, 1 µl of the dNTP mix, ddH_20 to 49 µl, and 1 µl (2.5 U) *Pfu* DNA polymerase. Cycling parameters were: 95 °C for 30 seconds, followed by 12 (for point mutations) or 16 (for two or more point mutations) cycles of: 95 °C for 30 seconds, 55 °C for 1 minute, and 68 °C for 2 minutes/kb of plasmid length. Following temperature cycling, the reaction was cooled to 37 °C and after the addition of 1 µl *Dpn*I was incubated for at least 2 hours at 37 °C. Once *Dpn*I-digestion was complete, 1 µl of the extension mix was added to pre.thawed Epicurian Coli XL1-Blue competent cells in a pre-chilled Falcon® 2059 polypropylene tube, mixed by swirling and incubated on ice for 30 minutes. The cells were then exposed to a 45 second heat shock at 42 °C, and after 2 minutes on ice, 500 µl SOC medium was added. Antibiotic resistance was elaborated by incubation for at least 1 hour at 37 °C at 220rpm in a shaking incubator, after which a 250 µl aliquot was plated on an LB agar plate, supplemented with antibiotics specific for the plasmid used, and incubated at 37 °C overnight. On the following day, transformants were used to

innoculate a LB culture from which plasmid DNA was isolated and sequenced to confirm that only the desired mutation(s) had taken place.

3.1.4 cDNA Sequencing and Analysis

Both strands of the cDNAs generated in this study were sequenced by dye terminator cycle sequencing (Applied Biosystems) with M13/pUC sequencing primers (Fermentas) or insert-specific primers, respectively (automatic sequencer: ABI Prism, Applied Biosystems).

Reagents	
Linear template, OR	100 ng
Plasmid template	200-500 ng
Primer	4 pmol
Sequencing premix	4 µl (Ready Reaction BigDye Terminator Kit: AmpliTaq® DNA polymerase FS, thermostable pyrophosphate, dNTPs dITP, BigDye labelled ddNTPs, buffer (PE Biosystems))
dH_2O	to 20 µl

Each PCR comprised 25 cycles of: 96 °C for 10 s, 50 °C for 15 s, and 60 °C for 4 min. Amplification products were precipitated by the addition of 80 µl water, 10 µl 3M NaAcetate and 250 µl 100 % ethanol (room temperature) followed by centrifugation for 15 min at 10 000 x g. After washing with 70 % ethanol (also room temperature) and centrifugation for 5 minutes at 10 000 x g the products were dried in the vacuum dessicator (Speedy Vac) and finally resuspended in sequence loading buffer (5:1 formamide:EDTA (25 mM, pH 8)). The sequence was assembled and analyzed with various software packages, as listed in Table 2.5. Sequence homology searches were performed at the National Centre for Biotechnology Information using the BLAST network service. Sequence analyses were performed with various software packages and online providers (Table 2.5).

3.1.5 Modification of nucleic acids

3.1.5.1 Restriction digestion

Restriction digestion was an integral part of many of the methods used. Subcloning, generation of deletion mutants, and site-directed mutagenesis all required involved a restriction digestion stage.

Reagents:

DNA to be cut	100 ng – 5 µg
Restriction enzyme	1-5 U/µg DNA, <10 % of the final reaction volume
Enzyme buffer	10 % v/v; composition varies with enzyme

After mixing, the reaction was incubated at 37 °C for 1-3 hours, depending on degree of digestion required. In standard digestions, such as excision of open reading frames during subcloning, complete digestion was not required, so enzyme used and incubation time were minimized. Where complete digestion was necessary, such as in the preparation of template for cRNA synthesis, a 3 hour digestion in combination with a higher ratio of enzyme to template was used.

3.1.5.2 Ligation

Ligation of two restricted DNA fragments with compatible ends was carried out using T4 DNA ligase. Standard ligation reactions consisted of a 4:1 insert to vector ratio, with 1 unit ligase/µg DNA incubated in 10 or 20 µl 1x ligation buffer (66 mM Tris-HCl, 5 mM $MgCl_2$, 1 mM dithioerythritol, 1 mM ATP, pH 7.5) for at least 16 hours at 4 °C. Following incubation a 2 µl aliquot was used to transform the appropriate host strain (section 3.2.1.1).

3.1.5.3 Vector dephosphorylation

The ligation of a vector and insert restricted with the same enzyme is limited by intramolecular ligation of the vector. To overcome this the vector can be treated with calf intestinal alkaline phosphatase (CIP), which prevents ligation of the two ends of the vector by removal of the 5' phosphate group. This was used in an attempt to clone hROAT1 into the pGEMHE vector. Following restriction 1 µg of linear pGEMHE was suspended in the buffer supplied, and 0.5 units of CIP were added (1 unit per pmol DNA ends). After 1 hour incubation at 37 °C, EDTA was added to a final concentration of 5 mM and the reaction was then incubated at 75 °C for 10 minutes. The DNA was extracted using the PCR purification kit following the manufacturer's protocol, and eluted in 5 mM Tris buffer (pH 8). The dephosphorylated vector was then used in a standard ligation reaction.

3.1.6 Isolation of nucleic acids

3.1.6.1 Agarose gel electrophoresis

Agarose gel electrophoresis was used to isolate DNA molecules following PCR amplification or restriction digestion. Gels were 0.7 – 2 %, depending on the size of the DNA molecule to be isolated, and consisted of agarose in TBE buffer (45 mM Tris, 45 mM borate, 1 mM EDTA). This solution was heated in a microwave to dissolve the agarose. After cooling, 2 µl of a 10 mg/ml ethidium bromide solution was added per 100 ml gel, the solution was mixed thoroughly, and the gel was poured. Gels were routinely run at 70-100 V for 1-2 hours, depending on the degree of band separation required.

3.1.6.2 Isolation of linear DNA molecules

Linear DNA molecules generated by the various PCR methods detailed above, as well as those resulting from restriction digestion, were isolated either directly using a nucleic acid purification kit, or after agarose gel electrophoresis using a gel extraction kit from QIAgen or Machery-Nagel. Fragments to be used as blunt-end inserts DNA were always eluted with water pH 8, to allow further concentration if required.

3.1.6.3 Plasmid isolation

Plasmid DNA was routinely isolated by alkaline lysis. Cells from 1.5 ml to 100 ml of an overnight culture grown in LB medium were harvested by centrifugation. The pellet was resuspended in 0.1 volumes of solution I by mechanical agitation using an auto vortex mixer. Solution II was added at 0.2 volumes of the original culture volume and mixed gently by rolling of the centrifuge tube. Once lysis had occurred (solution became clear and viscous), 0.15 volumes of solution III were added and mixed until a white precipitate formed and the solution was no longer viscous. The precipitate was then collected by centrifugation (14 800 x g, 10 minutes at room temperature) and the supernatant transferred to a new tube. DNA was precipitated with 2 volumes of ice cold 100% ethanol, collected by centrifugation, washed with 1 mL of 70% ethanol and air dried before being dissolved in 20 µl of dH_2O. For sensitive applications such as sequencing, plasmid DNA was purified over columns obtained from QIAgen or Machery-Nagel, as per the manufacturers instructions.

3.1.7 Cloning of amplified products

Depending on the polymerase used for amplification, different methods were used to clone PCR products. For products generated by *Taq* polymerase, which are characterized by 3' deoxyadenosine overhangs, TA cloning was the method of choice. To clone blunt-end PCR products generated by polymerases with proof-reading exonucleolytic activity, such as *Pfu* polymerase or the Powerscript polymerase mixture, a range of methods specific for cloning blunt-end products were used. Bacteria transformanted with vectors containing the *lacZ* reporter gene were screened with blue-white selection followed by PCR screening (section 3.1.2.1). Blue-white selection is based on the properties of the *lacZ* reporter gene, which cleaves a chromogenic substrate, X-gal, yielding blue bacterial colonies grown on LB agar (1 % tryptone, 1 % NaCl, 1% yeast extract, 1.5 % agar, pH 7.6) plates containing this substrate. Insertion of DNA within the cloning site disrupts *lacZ* and the galactosidase gene product is not synthesized. Thus, colonies arising from transformants with inserts cannot cleave X-gal and are white. If the host bacterial strain encodes *lac*I^q, a repressor of the *lac* promoter, IPTG is added to the LB agar plates to induce expression from the *lac* promoter.

3.1.7.1 TA Cloning

Degenerate PCR- and RACE-amplified products were cloned into pCR2.1 (Table 2.2) using the TA-cloning kit (Invitrogen). This cloning method allows direct cloning of PCR products amplified by the *Taq* polymerase, obviating the need for enzymatic modification of the PCR products or amplification with primers containing restriction enzyme recognition sequences. The TA Cloning method relies on a template-independent activity of the Taq polymerase that leads to an addition of a single deoxyadenosine to the 3' ends of PCR products. As the linearized pCR2.1 vector supplied with the kit has 3' deoxythymidine overhangs, ligation of insert and vector proceeds very efficiently.

Reagents:

linearized pCR2.1 vector	25 ng/µl in 10 mM Tris-HCl, 1 mM EDTA, pH8
T4 DNA Ligase	4.0 Weiss units/µl
10x Ligation Buffer	60 mM Tris-HCl pH7.5, 60 mM MgCl2, 50 mM NaCl, 1 mg/ml bovine serum albumin, 70 mM β-mercaptoethanol, 1 mM ATP, 20 mM dithiothreitol, 10 mM spermidine.
SOC medium	2 % Tryptone, 0.5 % Yeast Extract, 10 mM NaCl, 2.5mM

	KCl, 10 mM MgCl2, 10 mM MgSO4, 20 mM glucose (dextrose).
Competent cells	*E. coli* INVαF'

After PCR amplification, products were visualized by agarose gel electrophoresis, excised from the gel using a clean scalpel and then extracted from the gel using a column- or activated silica-based gel extraction kit (QIAgen, Macherey Nagel, respectively). Following purification and quantification of the PCR product, the following formula was used to calculate the amount of insert required for a 1:1 molar ratio of insert to vector:

$$\text{Xng PCR product} = \frac{(\text{Ybp PCR product})(50 \text{ ng pCR}^{\circledR}2.1)}{(\text{size of pCR}^{\circledR}2.1 \text{ vector: 3900bp})}$$

Based on this equation, two ligation reactions were set up for each insert - a 1:1 and 4:1 insert to vector ratio. Each ligation reaction was carried out in a 10 µl volume with 1 µl 10 x ligation buffer, 2 µl pCR®2.1 vector (50 ng), X µl PCR product (usually 2-3 µl as excess salt from larger volumes reduces efficiency), sterile water to 9 µl, and 1µl T4 DNA Ligase (4 Weiss units), and incubated overnight at 14° C. Following incubation, an aliquot from the ligation reaction was used to transform *E. coli* INVαF' cells. To a 50 µl vial of chemically-competent *E. coli* INVαF' cells, 2 µl of β-mercaptoethanol was added and gently stirred, after which 2 µl of the ligation reaction was added and mixed by stirring with the pipette tip, and the remaining ligation reaction was stored at -20° C. The vial was incubated for 30 minutes on ice and then the cells were subjected to a 30 second heat shock at 42° C, and immediately placed on ice, before the addition of 250 µl of room temperature SOC medium. In order to allow elaboration of antibiotic resistance, the vial was incubated at 37° C for at least 1 hour at 220 rpm in a shaking incubator. After this recovery period, aliquots of 50-200 µl were plated on LB agar (section 3.1.7) plates supplemented with 0.4 % X-gal and 50 µg/ml ampicillin, and incubated at 37° C overnight. Following 2-3 hours colour development at 4 °C, single isolated white colonies were chosen for PCR screening.

3.1.7.2 Blunt-end Cloning

To clone Blunt-end cloning of products generated by proof-reading polymerases (Powerscript, *Pfu* Polymerase), PCR-Script cloning (Stratagene), Zero Blunt TOPO cloning (Invitrogen) were the methods of choice.

3.1.7.2.1 PCR-Script cloning

Using the PCR-Script cloning kit, blunt-end PCR products generated by proof-reading polymerases can be ligated into the pPCR-Script vector. The basis of the PCR-Script cloning kit is the use of the linearized pPCR-Script vector, the ends of which, in the case of intramolecular vector ligation, form the recognition site for the *Srf*I restriction enzyme. By inclusion of the *Srf*I during the ligation step, and hence restriction of ligated vector molecules, the efficiency of ligation of blunt-end PCR products is increased. The *lacZ* gene contained in the pPCR-Script vector allows blue-white selection of transformants.

Reagents:

linear pPCR Script vector	10 ng/µl
PCR-Script reaction buffer	composition not provided by manufacturer
rATP	10 mM
*Srf*I restriction enzyme	5 U/µl
T4 DNA Ligase	4 U/µl
β-mercaptoethanol	concentration not provided by manufacturer
Competent cells	Epicurian Coli® XL10-Gold™ Kan ultracompetent cells
SOC Medium	2 % Tryptone, 0.5 % Yeast Extract, 10 mM NaCl, 2.5mM KCl, 10 mM MgCl2, 10 mM MgSO4, 20 mM glucose (dextrose).

Following amplication by *Pfu* polymerase, purification using a gel extraction kit, and quantification of the purified insert, the molar ratio of insert to vector was calculated using the following formula:

$$\text{Xng of PCR product} = \frac{(\text{size of PCR product in bp})(10 \text{ ng of pPCR Script vector})}{\text{size of pPCR Script: 2961 bp}}$$

The equation above provides the amount of insert required for a 1:1 insert-to-vector ratio, however, the manufacturers recommend a insert-to-vector ratio of between 40:1 and 100:1. For this reason, the elution of the PCR products during the purification step was always carried out with dH_2O, pH 8. Thereafter, the concentration of the insert could be increased by evaporation in the Speedy-Vac, enabling the ligation to take place with a insert-to-vector ratio of at least 50:1. The prescribed ligation reaction consisted of the following components, added in order: 1 µl linear pPCR-Script Amp SK (+) vector (10 ng), 1 µl PCR-Script 10x reaction buffer, 0.5 µl rATP, 2-4 µl blunt-end PCR product, 1 µl *Srf*I restriction enzyme (5 U), 1 µl T4 DNA Ligase (4 U), and finally dH_2O to 10 µl. However, as the required insert-to-vector ratio was so high, and the

concentration of insert frequently remained low even after evaporation in the Speedy-Vac, the ligation reaction was prepared as above with the following exceptions: 0.5 µl vector, 0.8 µl *Srf*I, 0.8 µl T4 DNA ligase, 4 - 6.4 µl insert. After gentle mixing, the ligation reaction was incubated for 1 hour at room temperature, and was then heated for 10 minutes at 65° C, and stored on ice. For transformation, XL 10-Gold Kan ultracompetemt cells were thawed on ice and transferred to a pre-chilled 15 ml Falcon 2059 polypropylene tube, after which 1.6 µl of the β-mercaptoethanol mix provided was added to the cells, gently mixed and incubated on ice for 10 minutes with occassional swirling. After this incubation period, 2 µl of the ligation mix was added to the cells, which were then incubated on ice for a further 30 minutes. Following this incubation period, the cells were exposed to a heat shock of 30 seconds at 42° C and then returned to ice for two minutes. Finally, 450 µl of SOC medium was added and the cells were incubated at 37° C for at least 1 hour at 220 rpm in a shaking incubator. Aliquots of 250 - 500 µl were then plated on LB agar (section 3.1.7) plates supplemented with 50 µg/ml ampicillin, X-gal and IPTG, and incubated at 37° C overnight, after which white colonies were selected for screening.

3.1.7.2.2 Zero Blunt™ TOPO™ Cloning

The cloning of blunt-end products with the Zero Blunt™ TOPO™ cloning kit relies on the same principle as that for the TOPO-XL™ kit detailed above - the activation of the linear vector with topoisomerase. In addition, the pCR©-Blunt II-TOPO vector contains the lethal E. coli ccdB gene fused to the C-terminus of the *lacZ* gene, so that only transformants containing inserts are able to grow.

Reagents:

pCR©-Blunt II-TOPO	10 ng/µl plasmid DNA in: 50 % glycerol, 50 mM Tris-HCl pH 7.4, 1 mM EDTA, 2 mM DTT, 0.1 % Triton X-100, 100µg/ml BSA, bromophenol blue.
6x TOPO™ stop solution	0.3 M NaCl, 0.06 M $MgCl_2$
SOC Medium	2 % Tryptone, 0.5 % Yeast Extract, 10 mM NaCl, 2.5mM KCl, 10 mM MgCl2, 10 mM MgSO4, 20 mM glucose (dextrose).
Competent cells	*E. coli* TOP10F' One Shot™ cells

The blunt-end PCR product was purified by gel extraction using a column- or activated silica-based kit (QIAgen or Macherey Nagel, respectively) and quantified using the GeneQuant photometer (Pharmacia Biotech, Uppsala, Sweden). As the Zero Blunt™ TOPO™ Cloning Kit proved to be highly efficient it was not necessary to further

concentrate the insert. The ligation mix suggested by the manufacturers (0.5 - 4 µl PCR product, sterile water to 4 µl and 1µl pCR©-Blunt II-TOPO vector) was altered, and consisted of mixing 4.5 µl of the PCR product with 0.5 µl of the pCR©-Blunt II-TOPO vector. The ligation mix was incubated for 5 minutes at room temperature, after which 1 µl of 6x TOPO™ Stop Solution was added, mixed for 10 seconds and placed on ice. From this ligation mix, 2 µl were added to a vial of pre-thawed One Shot™ competent cells, gently mixed, and incubated on ice for 30 minutes. Following this incubation period, the cells were exposed to a heat shock of 30 seconds at 42° C, returned to ice for 2 minutes, and finally 250 µl of room temperature SOC medium was added. The cells were then incubated for at 37° C for at least 1 hour at 220 rpm in a shaking incubator. After elaboration of antibiotic resistance, 100 and 200 µl aliquots were plated on LB agar (section 3.1.7) plates supplemented with 50 µg/ml kanamycin and incubated at 37° C overnight. On the following day, colonies were PCR-screened to isolate positive clones with an insert of the appropriate size.

3.1.8 cRNA synthesis

The synthesis of cRNA was carried out using the T7 mMESSAGE mMACHINE kit (Ambion). This kit enables the synthesis of large amounts of capped cRNA from a linear cDNA template, by incorporation of a 7-methyl guanosine cap analogue (m7G(5')ppp(5')G) during polymerisation. Capped cDNAs can then be used for microinjection of oocytes.

Reagents:

10 x Enzyme mix	bacteriophage T7 RNA polymerase, ribonuclease inhibitor and other unlisted components
10 x Transcription Buffer	composition not provided by manufacturer
2 x Ribonucleotide mix	buffered solution containing 10 mM ATP, CTP, UTP, 2 mM GTP and 8 mM Cap analogue
DNaseI	RNase-free in 50 % glycerol buffer.
Precipitation solution	7.5 M LiCl, 75 mM EDTA
Nuclease-free H2O	to 20 µl
Template DNA	*Not*I-cut, at a concentration of at least 160 ng/µl

Template cDNA was digested with *Not*I (5U / µg DNA) for 3 h at 37 °C, and column-purified using the PCR-purification kit from QIAgen. The linearized product was eluted in 30 µl elution buffer and the concentration was determined. For cRNA synthesis, the following reagents were added in order, to a 1.5 ml microfuge tube: 2 µl

10x transcription buffer, 10 µl 2x ribonuceotide mix, 6 µl linearized template, and 2 µl enzyme mix. The reaction was incubated at 37 °C for 2 - 3 hours, after which template DNA was removed by the addition of 1 µl RNase-free DNaseI and further incubation at 37 °C for 15 minutes. The reaction was terminated by adding 30 µl of nuclease-free dH_2O and 25 µl LiCl precipitation solution, and after thorough mixing the sample was incubated at -20 °C for 1 hour. Following incubation, the cRNA was collected by centrifugation for 15 minutes at 4 °C, washed with one volume 70 % ethanol, and centrifuged once more for 5 minutes. After careful removal of the ethanol, the cRNA was resuspended in nuclease-free dH_2O and the concentration was determined. Samples were diluted to either 1 or 2 µg/µl and were stored at –80°C.

3.2 CELLULAR

3.2.1 Bacteriological

All strains used were grown routinely at 37 °C. Overnight cultures were inoculated from single colonies present on selective plates and were grown under the appropriate antibiotic selection. For long term storage, strains were stored in a mixture of LB plus 5% glycerol at -80°.

3.2.1.1 Transformation

Heat shock

To transform E. coli with plasmid DNA other than that generated with kits detailed above, a standard heat shock protocol was used. Competent cells (Stratagene, Invitrogen) in 40 or 50 µl aliqouts were thawed on ice to maintain competence, and in the case of cells from Stratgene were transferred to Falcon 2059™ polypropylene tubes. Once thawed, Stratagene cells were further treated by the addition of 1.6 µl β-mercapto-ethanol (concentration not provided by manufacturer) and the cells were incubated on ice for a further 5 min. After the addition of the desired DNA sample, corresponding to between 10 and 100 ng of DNA, and a further 30 minute incubation on ice, cells were exposed to heat shock at a 42°C water bath for 30 seconds (for Invitrogen cells) or 45 seconds (Stratagene cells) and then transferred immediately to ice for 2 min. Following addition of SOC, transformants were elaborated for at least 1 h at 37°C at 220 rpm in a shaking incubator. Aliquots were then spread on LB agar (1 % tryptone, 1 % NaCl, 1% yeast extract, 1.5 % agar, pH 7.6) plates supplemented with the appropriate antibiotic, and with X-gal and IPTG if blue-white seletion was required.

Electroporation

Electrocompetent cells were prepared as described by the manufacturer and stored at -80°C. Electroporation was carried out using an Easyject™ (Equibio) electroporator set with capacitance at 25 µF, pulse-controlled resistance at 200 Ω, and voltage at 1.8 kV using a cuvette with a 0.1cm gap. Following electroporation, cells were placed on ice for 1 minute, after which 500 µl SOC was added. These cultures were incubated at 37 °C with shaking at 200 rpm for at least 1 hour to allow expression of the antibiotic

resistance. Transformants were selected by plating on LB agar plates (section 3.1.7) supplemented with the appropriate antibiotic.

3.2.2 Xenopus laevis oocytes

The determine the function of the hROAT1 and hOAT2 clones generated in this study, *Xenopus laevis* oocytes were injected with cRNA derived from wild-type, mutant or chimera cDNAs, and uptake assays were carried out as outlined below.

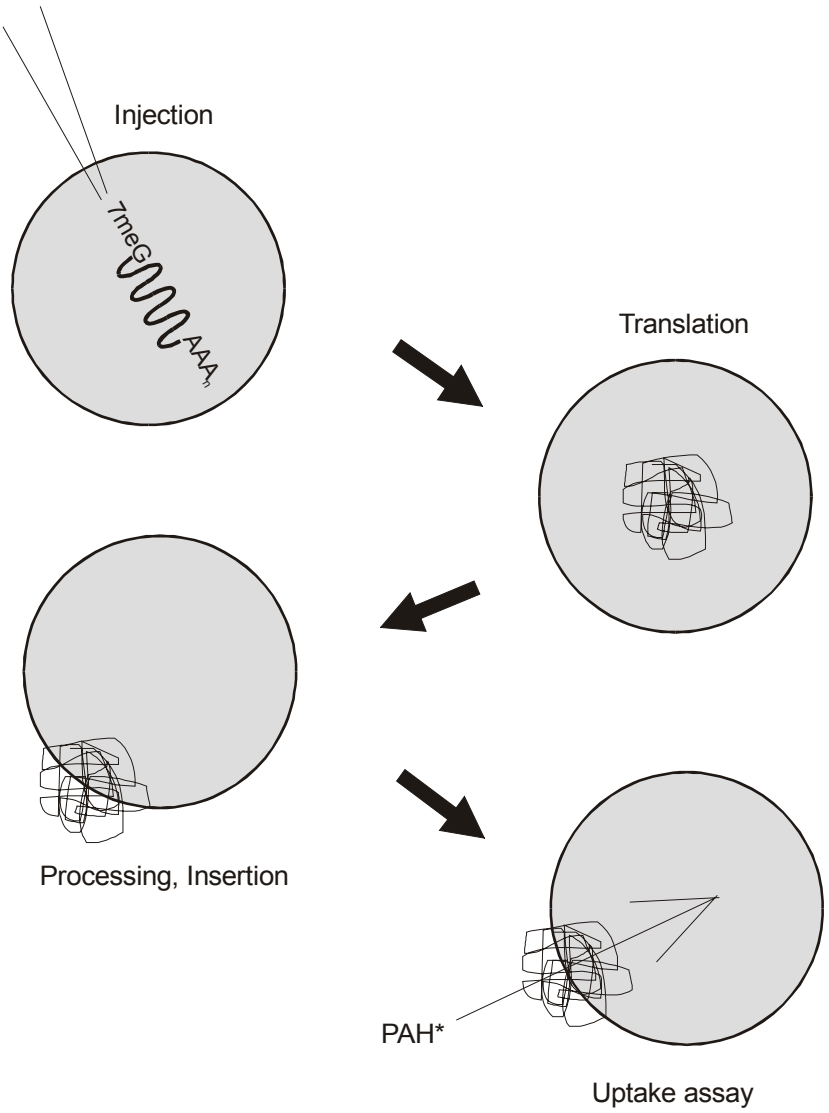

Figure 3.6: The oocyte assay system. Isolated or in vitro synthesized poly(A)$^+$-RNA, with cap and poly-A tail, is injected into the vegetal pole of the oocyte. After translation of the polypeptide encoded by the RNA, and its processing and insertion, uptake assays can be carried out in which uptake of a radioactively labelled substance can be measured.

3.2.2.1 Preparation of oocytes.

Reagents

Barth's	88 mM NaCl, 1 mM KCl, 0.3 mM $Ca(NO_3)_2$, 0.41 mM $CaCl_2$, 0.82 mM $MgSO_4$, 15 mM HEPES, 10 mg/l Steptomycin or Gentamicin pH set at 7.6 with NaOH

Individual oocytes were separated from ovarian lobes manually or by collagenase treatment. Manual dissection was carried out with pincers and surgical scissors; oocytes were cut away from the lobe and then as much ovarian tissue as possible was removed without damaging the oocyte. Suitable oocytes were incubated in Barth's solution at 18 °C overnight prior to injection. Collagenase treatment involved overnight incubation of several ovarian lobes in 20 ml Barth's solution containing 5 mg/ml collagenase. The oocytes were washed several times with Barth's on the following day, and after sorting were then incubated for 10 min in Ca^{2+} free medium. Oocytes were then returned to Barth's solution and maintained at 18 °C until required for injection.

3.2.2.2 Injection of cRNA

Oocytes were routinely injected with 25-50 ng of cRNA in a 23-46 nl volume, or the equivalent volume of nanopure water as a control, using a Nanolitre injector. Glass capillaries (World Precision Instruments) were loaded with the cRNA to be tested, or with water as a control. Oocytes were arranged on a specially designed plastic receptacle with grooves to facilitate the injection process. Injection took place in the vegetal pole, and consisted of one or two injections of 25 nl separated by a 5 s pause.

3.2.2.3 Transport assays.

Reagents

ORI	90 mM NaCl, 3 mM KCl, 2 mM $CaCl_2$, 1 mM $MgCl_2$, 5 mM HEPES, pH set at 7.6 with 1 mM Tris

Prior to transport assays, on either the second or third day after injection, surviving oocytes were sorted to remove unhealthy or matured oocytes. The selected oocytes were divided into groups of 8-14 and transferred to 2 ml of ORI per well of a 24-well plate. After equilibration in ORI, oocytes were transferred to ORI uptake medium containing radioactively labelled-PAH, with or without desired test substrates at the appropriate concentrations, in a 10 ml vial. For the ion dependence studies, the uptake

medium was of altered ion composition, as detailed in results. For cis-inhibition studies, stock solutions of each potential inhibitor were made in ORI. Final concentrations in uptake experiments were 1 mM in all cases except for bile acids, were only 100 μM was used. The concentration of radioactivity in a standard assay was 5 μCi/ml. The PAH concentration in a standard transport assay consisted of 5 μCi ^{3}H-PAH (specific activity 1.28-4.08 μCi/nmol) and the final concentration was set at 10 μM by the addition of unlabelled PAH. For determination of K_m, total radioactivity was 1-5 μCi, with the final PAH concentration achieved by the addition of the appropriate quantity of unlabelled PAH. Uptake took place from 10 minutes to 1 hour, as required, with agitation at room temperature. Upon completion of the incubation period, uptake was stopped by the addition of ice-cold ORI. The uptake medium was aspirated, and the oocytes were washed three times with ice-cold ORI. Following the final washing step, individual oocytes were transferred to 5 ml scintillation vials, to which 100 μl 1N NaOH was added. After incubation overnight, the dissolved oocytes were neutralized by addition of 100 μl 1 N HCl, and finally 4.5 ml Lumasafe scintillation fluid (Lumac-LSC) was added. This mixture was shaken thoroughly and after 1 hour ^{3}H-PAH content was determined over 10 minutes in a scintillation counter.

4 RESULTS

4.1 CLONING AND FUNCTIONAL CHARACTERIZATION OF hROAT1, A HUMAN ORGANIC ANION TRANSPORTER

The human kidney efficiently secretes organic anions such as PAH via a multispecific organic anion transporting system. As a number of previously cloned proteins from other species, known collectively as OAT1, satisfy the physiological characteristics of the basolateral system involved (Sekine et al, 1997, Sweet et al, 1997, Wolff et al, 1997), a homology cloning approach was adopted to clone a human OAT1 homologue.

4.1.1 Cloning hROAT1

4.1.1.1 Degenerate PCR

In order to isolate a human PAH transporter by homology cloning, a degenerate PCR strategy was used. The first step of this process involved the design of degenerate primers based on the amino acid sequence of previously cloned organic anion and organic cation transporters. Six transporters, three organic anion transporters from flounder (fROAT), rat (OAT1) and mouse (NKT), a related transporter isolated from rat liver (NLT) and two rat organic anion transporters (rOCT1 and rOCT2), were aligned as shown in Figure 4.1. The rationale was to choose regions of greatest homology between the anion transporters that simultaneously provided divergence from the cation transporters, thus increasing the probability of amplifying an organic anion transporter. The regions chosen are shown in Figure 4.1 and are detailed in Table 4.1.

The thermocycling parameters for the PCR used were empirically determined, as an appropriate annealing temperature could not be calculated from the degenerate sequence of the primers. Initially, a PCR was carried out using the fROAT clone as a positive control with all possible primer pairs and a product of approximately 1 kb was successfully amplified from fROAT using primers 13 and 16, enabling an approximate annealing temperature range to be determined. Although the homology of the primers to the human sequence was unknown, these PCRs suggested an annealing temperature of around 40 °C. However, applying these parameters to a human kidney cDNA

Primer	amino acid sequence	nucleotide sequence	primers in pool	degeneracy factor
5.1	M/L M A S H N	$^{5'}$TIATGGCNWSNCAYAAY$^{3'}$	256	1024
5.2	G T C A A F/Y	$^{5'}$GGIACITGYGCNGCNTWY$^{3'}$	128	2048
3.1	L G Y Y A F	$^{5'}$ARNCCRTARTANGCRAA$^{3'}$	256	256
3.2	G F I V Q I	$^{5'}$NCCRAADATNACYTGDAT$^{3'}$	576	576
3.3	A L C G K G	$^{5'}$GCNARRCANCCYTTNCC$^{3'}$	512	512

Table 4.1: Degenerate primers used to amplify hROAT1. The five degenerate primers designed to PCR-amplify hROAT1. The amino acid sequence corresponds to the shaded regions in figure 4.1; the nucleotide sequence represents the degenrate sequence of the primer. I = inosine, N = A/C/G/T, W = A/T, S = C/G, Y = C/T, R = A/G, D = A/G/T. The number of primers in each pool equals the total number of different primers; degeneracy factor represents the total number of sequences with which each primer might theoretically bind.

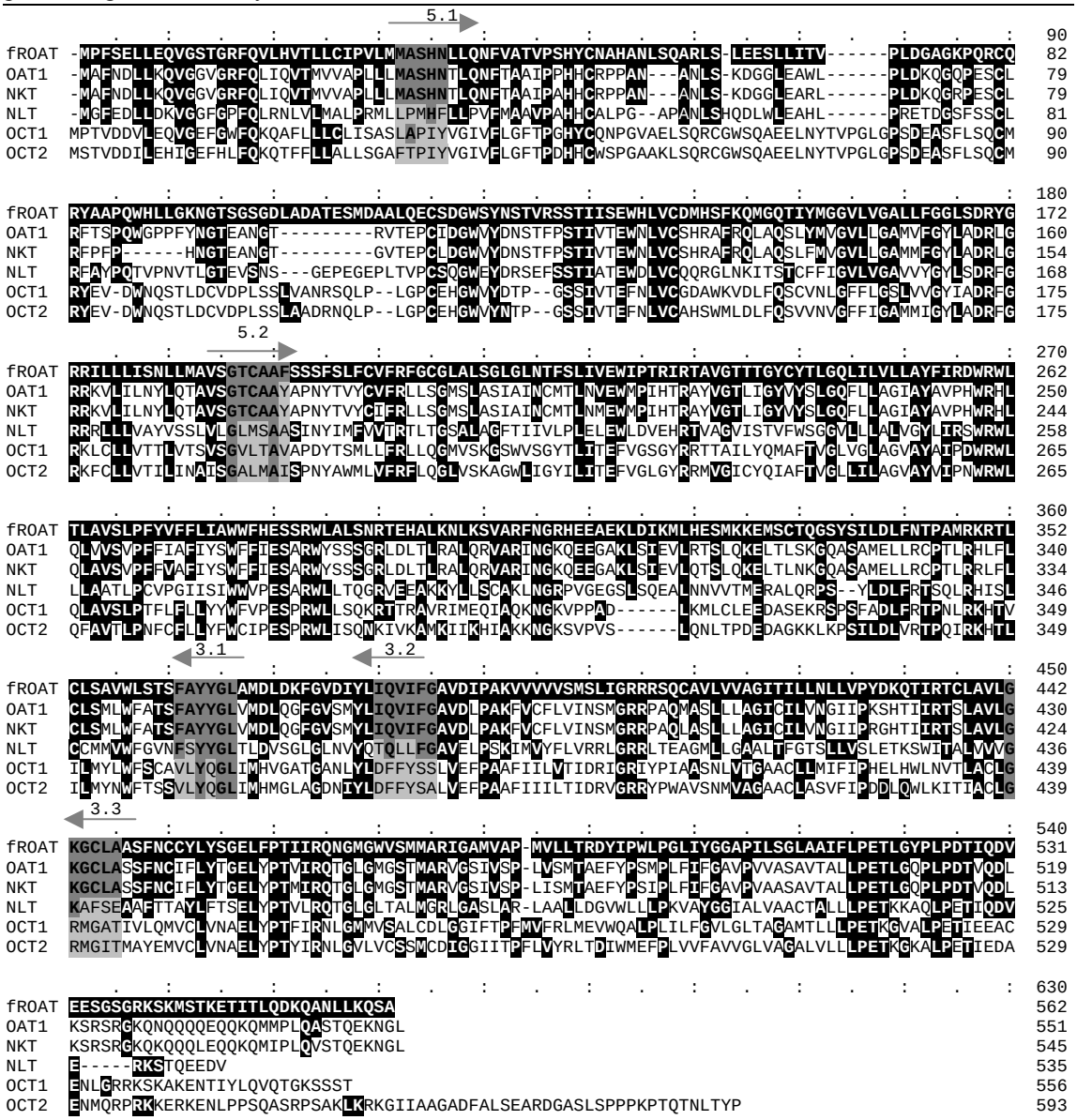

Figure 4.1: Degenerate primer design. An alignment of three organic anion transporters (fROAT, OAT1, NKT), a related liver transporter (NLT) and two organic cation transporters (OCT1 and OCT2) is shown. Amino acid residues shaded black are identical to those in fROAT. Grey residues signify the regions used for degenerate primer design. Arrows designate primer directionality - forward (→) and reverse (←) – and numbers are primer names. 5.1 and 3.2 represent the primer pair with which the initial PCR product of approximately 1 kb was amplified. The numbers in the right column represent amino acid number.

template, did not yield any specific amplification. In order to increase the potential for amplification from poorly annealed primers, an additional pre-extension step of 50 °C was added. A successful amplification, the faint band in Figure 4.2, was eventually obtained using these PCR cycling parameters. After reamplification, the 1 kb amplicon was cloned into pCR2.1 and sequenced (Figure 4.2). The sequence data yielded was used to search the GenBank sequence databank, and the product was found to have high identity to the OAT1 and NKT sequences (85-88 %) and significant homology to the fROAT clone.

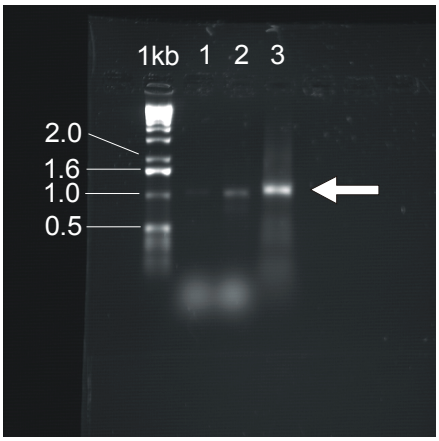

Figure 4.2: Amplification of a human OAT1 homologue by degenerate PCR. The arrow denotes the successful amplification of a 1 kb product (lane 2), which was then reamplified (lane 3) to facilitate cloning. Sizes of relevant bands from the 1 kb standard are shown in kb. Lane 1 is a negative control.

4.1.1.2 5' and 3' RACE

Using the sequence obtained from the initial PCR product, sequence-specific primers were designed with which to carry out 5'- and 3'-RACE reactions. The 3'-RACE reaction yielded a product of 850 bp, which was sequenced and also found to have similar levels of homology to the clones listed above. The sequence contained the remainder of the 3'-coding sequence and the 3'-untranslated region (UTR), including a polyadenylation signal. With the 5'-RACE reaction, a product of around 300 bp was amplified. The sequence from this clone yielded an additional 89 bp of new sequence, including the 2nd and 3rd nucleotides of what was assumed to be the start codon. Although no direct comparison with the Kozak consensus sequence for transcriptional start sites could be carried out, a multiple alignment of these related carriers strongly

suggested that the assumed start codon obtained from 5' RACE would be the favored site for transcription in vivo (see Figure 4.4).

4.1.1.3 PCR-amplification of the complete hROAT1 open reading frame

A sequence contig was generated using the PCR products and was analyzed using the GCG Wisconsin Package (Table 2.7). A Blast search of the GenBank database revealed the contig sequence to be 88% identical to the rat organic anion transporter (OAT1/ROAT), and 85% identical to the then functionally uncharacterized mouse homologue (NKT). Thus, the contig, named hROAT1, represents the first reported cloning of a human homologue of the renal organic anion transporter (Reid et al, 1998). Based on the sequence contig, specific primers were designed to amplify the entire known sequence – the full coding sequence as well as the 3'UTR. The successfully amplified product was cloned into pPCR-Script, confirmed by sequencing and deposited in the GenBank database where it was assigned the accession number AF057039.

4.1.1.4 Sequence characteristics of hROAT1

Further analysis of the sequence was performed to identify features of the primary amino acid sequence and the predicted secondary structure. In addition to the high homology to the rat and mouse OAT1 homologues (88 and 85 %, respectively), there was significant homology – 48% identity - to the flounder homologue (fROAT). hROAT1 also showed 36% identity to a related liver transporter from the rat (NLT/rOAT2) and the organic cation transporter family; a sequence alignment is shown in Figure 4.4. The open reading frame of 550 amino acids predicts a calculated molecular mass of 60 kDa. Hydropathy analysis with the TopPred2 program (window setting of 11-21, upper cut-off 1.0, lower cut-off 0.6; von Heijne 1992) predicted twelve transmembrane domains with intracellular N- and C- termini; a model of the predicted secondary structure is shown in Figure 4.5. hROAT1 was also found to contain: consensus sites for N-glycosylation in the large extracellular loop between transmembrane domains 2 and 3 ($Asn^{39,56,92,97,113}$), four conserved cysteine residues ($C^{49,78,105,128}$) that could be involved in disulfide bond formation, and consensus sites for phosphorylation by protein kinase C ($Ser^{271,278}$, $Thr^{284,334}$, Ser^{521}), protein kinase A (Ser^{276}, $Thr^{318,334}$, Ser^{469}), tyrosine kinases (Tyr^{536}) and casein kinase II ($Thr^{325,515}$) in the large intracellular loop between transmembrane domains 6 and 7 and also in the C-terminal region (Figure 4.5).

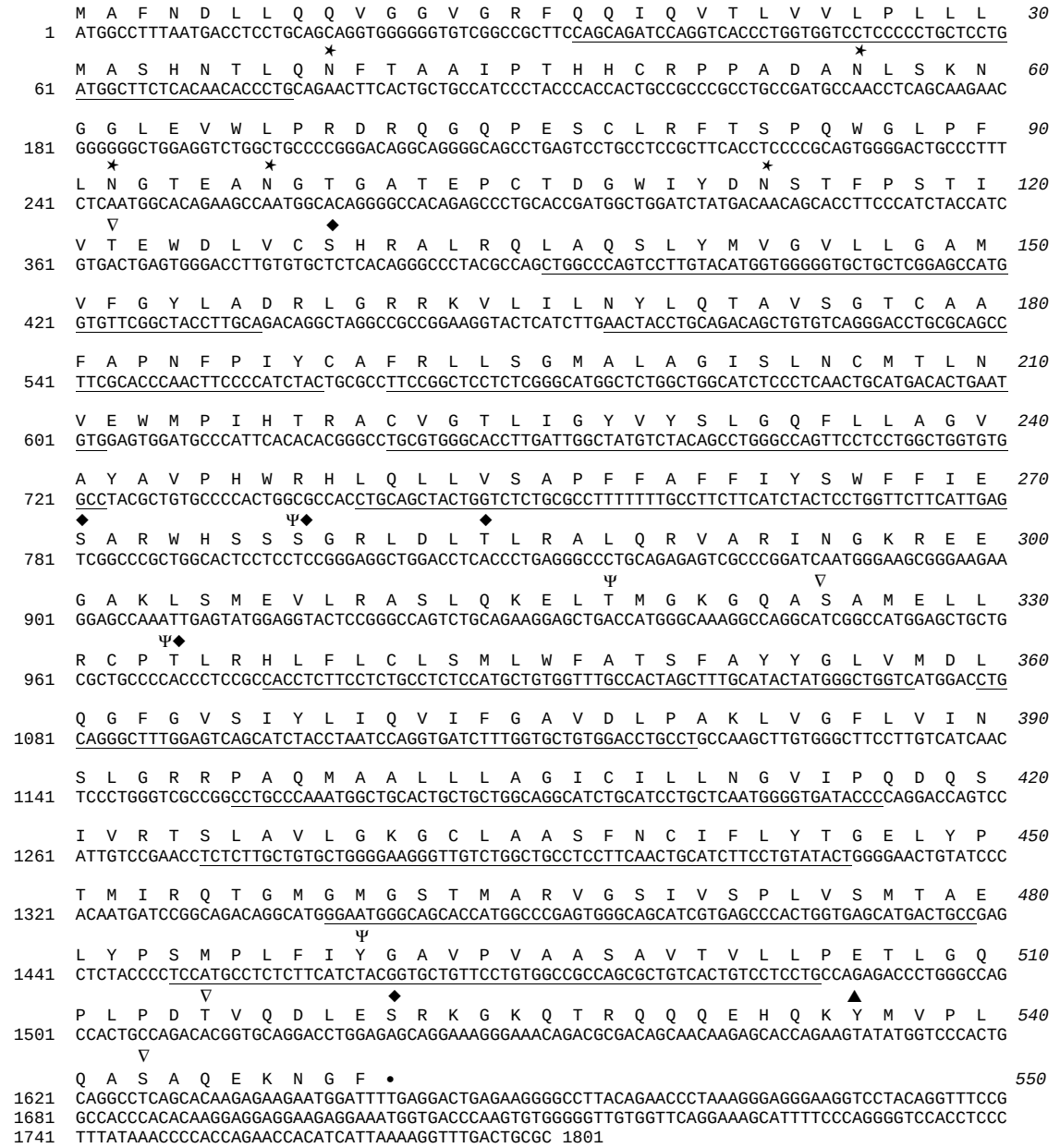

Figure 4.3: hROAT1 open reading frame: nucleotide and amino acid sequence. The hROAT1 cDNA sequence (numbers in the left-hand column) and the amino acid sequence (numbers in the right-hand column) of the 550 amino acid open reading frame. Transmembrane domains predicted by the TopPred 2 program are underlined. Symbols represent consensus sequence sites for N-linked glycosylation (✶), and phosphorylation by protein kinase C (◆), protein kinase A (Ψ), tyrosine kinase (▲), and casein kinase II (∇).

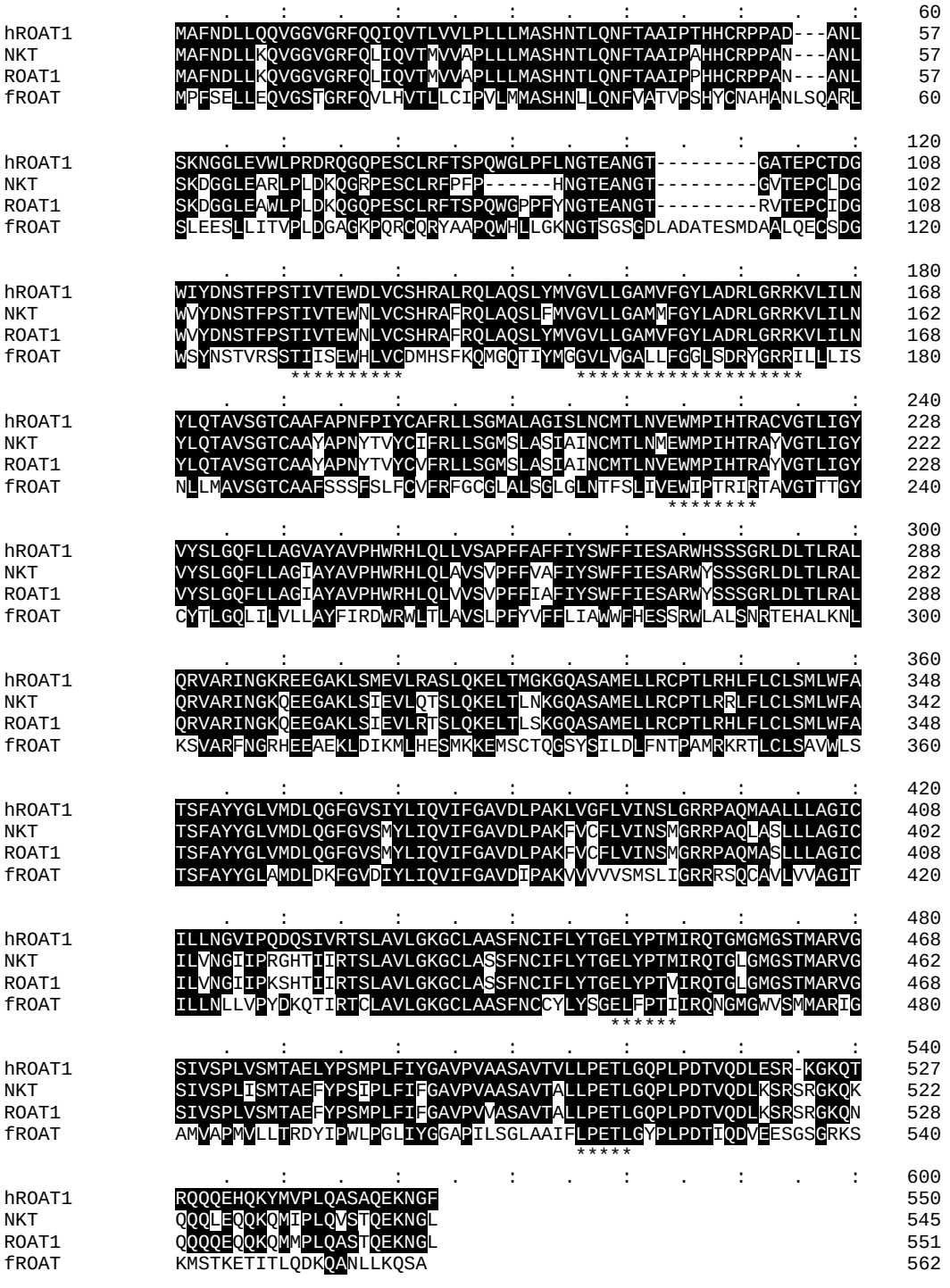

Figure 4.4: Alignment of hROAT1 with other OAT1 homologues. Residues shaded black are those identical in the human, mouse, rat and flounder homologues. Asterisks below the sequence represent the motifs conserved in members of the amphiphilic solute facilitator family (see text for details).

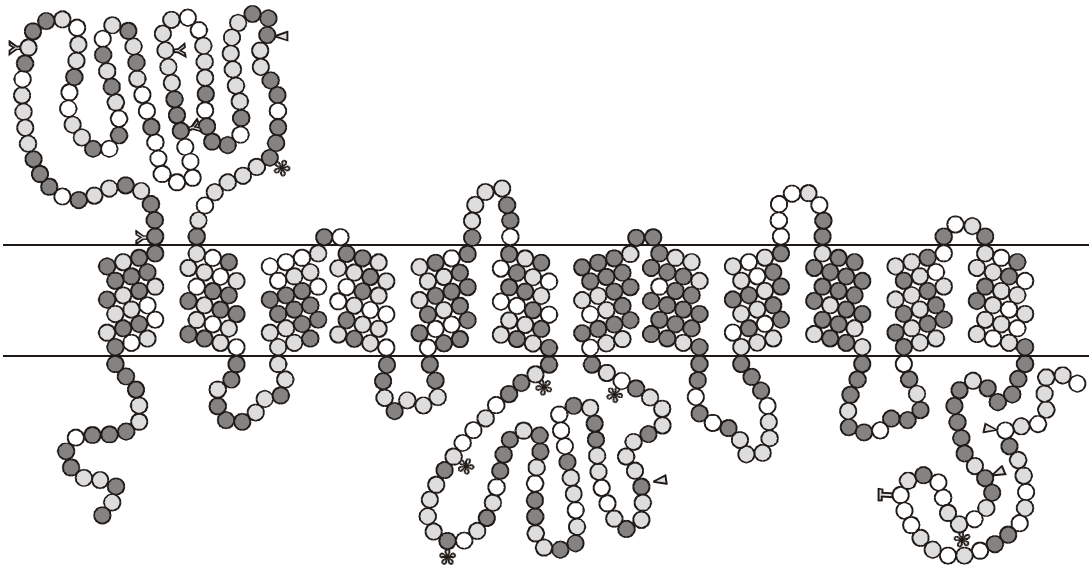

Figure 4.5: Model of the predicted secondary structure of hROAT1. This model represents the topology of the hROAT1 as predicted by TopPred 2. Shaded residues represent amino acid residues conserved in mammalian OAT1s (light and dark) and all OAT1s (dark)). The consensus sites for enzymatic modification are also shown: Y = N-glycosylation, * = protein kinase C, ∇ = protein kinase A, = casein kinase II, T = tyrosine kinase.

hROAT1 also contains motifs common to members of the amphiphilic solute facilitator (ASF) family of solute transporters (Schömig et al 1998), which belongs to the major facilitator superfamily (MFS) (Marger and Saier 1993). These sequences include: $GX_3GX_4GX_3DRXGRRK$ in the second transmembrane domain and the first intracellular loop (G^{144}-K^{163}); EX_6R (E^{212}-R^{219}) in the second intracellular loop; TIXXEWDLVC (T^{119}-C^{128}) in the large external loop between transmembrane domains 1 and 2; ELYPTL (E^{447}-M^{452}; substitution of M for terminal L) between transmembrane domains 10 and 11; and LPETL (L^{504}-L^{508}) after transmembrane domain 12. Table 4.2 shows the amino acid consensus sites for potential modification shared by the human, rat, mouse and flounder OAT1 homologues. Whether any of these sites are involved in regulation of physiological function of these transporters has yet to be elucidated.

OAT homologue	N-glycosylation	protein kinase C	casein kinase II
hROAT1	56, 92	Ser271, Ser278	Ser325, Thr515
NKT	56, 86	Ser265, Ser272	Ser319, Thr509
ROAT1	56, 92	Ser271, Ser278	Ser319, Thr515
fROAT	54, 95	Ser283, Ser290	Ser337, Thr527

Table 4.2: Potential modification sites identical in all OAT homologues. Numbers denote position of consensus site within the amino acid sequence of the respective OAT homologue.

4.1.1.5 Comparison of hROAT1 with other cloned human OAT1 homologues

During the course of this study other reports appeared in the literature concerning the cloning of human organic anion transporter homologues. A comparison of all independently cloned human organic anion transporters is presented in Table 4.3. As seen from the table, five independently cloned versions of hROAT1 (hROAT1 (this study), hOAT1-2 (Hosoyamada et al 1999), hOAT1 (Cihlar et al 1999), hPAHT (Lu et al 1999), and hOAT1 (Race et al 1999)) now exist in the GenBank sequence database, all representing the same protein. A further cDNA, hOAT1-1, the open reading frame of which predicts a protein thirteen amino acids longer than all others, has also been cloned (Hosoyamada et al). A Blast comparison of the nucleotide sequences revealed that hROAT1 is greater than 99% identical to each of the other clones, with 3 to 7 non-identical nucleotides throughout the entire open reading frame. On the protein level, the only differences between hROAT1 and the other human OAT1 clones is the exchange of the last leucine residue for a phenylalanine in hROAT1, and the presence of a serine residue at position 14 in hPAHT, which is a glycine residue in all other open reading frames. Importantly, none of these sequence differences leads to a change in the predicted secondary structure of the protein; neither glycine/serine at position 14, nor leucine/phenylalanine at position 550, occur within a predicted transmembrane domain or conserved sequence motif.

human OAT1 clone[a]	nucleotide identity in ORF	Accession number	Appearance in GenBank	Authors
hROAT1	1653/1653	AF057039	04.11.98	Reid et al (1998), this study
hPAHT	1646/1653	AF104038	28.01.99	Lu et al (1999)
hOAT1-2	1650/1653	AB009698	16.02.99	Hosoyamada et al (1999)
hOAT1	1649/1653	NM_004790	07.05.99	Race et al (1999)
hOAT1	1650/1653	AF124373	16.09.99	Cihlar et al (1999)

Table 4.3: Comparison of human OAT1 clones in the GenBank database. a = Since the first report of the cloning of a human OAT1 (hROAT1), the same clone has appeared four more times in the GenBank database and has four distinct names.

4.1.2 Construction of an hROAT1 functional clone

As mentioned above, the entire reading frame plus 3'UTR of hROAT1 was amplified from human kidney cRNA using specific primers based on the contig sequence. This amplification product was cloned and verified by sequencing. As described above, the 5'RACE reaction terminated prematurely at the end of the start codon, and no sequence from the 5'UTR was obtained. For expression, both 5' and 3' UTRs are necessary for cRNA translation, thus PCR amplification of this region was attempted. Using primers based on the most conserved regions of the 5' UTRs from the mouse and rat homologues, it was possible to amplify approximately 200 bp corresponding to the 5' UTR of hROAT1. This sequence, shown in figure 4.6, has 75 % and 76 % identity to the rat and mouse OAT1 5'UTRs, and also supported the supposition that the earlier 5' RACE had reached the start codon, as the sequence showed 100 % homology from the 3rd nucleotide of the open reading frame.

```
          .    :    .    :    .    :    .    :    .    :
-244   cgaagtgaggagaagctgcaagggaaaagggagggacagatcagggagac
          .    :    .    :    .    :    .    :    .    :
-194   cggggaagaaggaggagcagccaaggaggctgctgtccccccacagagca
          .    :    .    :    .    :    .    :    .    :
-144   gctcggactcagctcccggagcaacccagctgcggaggcaacggcagtgc
          .    :    .    :    .    :    .    :    .    :
 -94   tgctcctccagcgaaggacagcaggcaggcagacagacagaggtcctggg
          .    :    .    :    .    :    .    :   +1   :
 -44   actggaaggcctcagcccccagccactgggctgggcctggccaATG
```

Figure 4.6: hROAT1 5'UTR sequence. The above sequence was PCR-amplified using primers based on the rat and mouse 5'UTRs. The ATG start codon is shown at +1, and the 5'UTR is labelled –1 to -244

From this additional sequence data (Figure 4.6) and the sequence already known from the 3' RACE reactions (Figure 4.3), a further sequence specific primer was designed with which to amplify an entire clone containing both 5' and 3' UTRs to be used as an expression clone. Despite several attempts, it was not possible to specifically amplify the desired product from the cDNA template, perhaps due to diminished template integrity after repeated freeze thaw cycles.

As a full-length expression clone proved recalcitrant to cloning using PCR amplification, it was decided to use a *Xenopus*-specific expression vector. The vector

pGEMHE (see Material) a *Xenopus*-specific vector containing the 5' and 3' UTRs from the *Xenopus laevis* β-globin gene, was used with kind permission from E. Liman (Mass. General Hospital, Boston, Liman et al 1992). The hROAT1 coding region was reamplified with primers incorporating *Bam*HI and *Xba*I sites, and then both the vector and the hROAT1 coding region were sequentially digested with *Bam*HI and *Xba*I. Several attempts to ligate these products produced no positive clones, and neither dephosphorylation of the vector by CIP-treatment, nor the incorporation of additional restriction sites in the multiple cloning site by linker addition, enabled insertion of the hROAT1 open reading frame. Thus, construction of an hROAT1 expression clone was not possible using pGEMHE.

The next strategy used in an attempt to construct a functional clone involved the modification of a flounder sodium dicarboxylate cotransporter, fNaDC-3, which is expressed to very high levels in oocytes. The fNaDC-3 clone, a gift from J. Steffgen, (Dept. of Nephrology, Uni Klinik Göttingen, Steffgen et al 1999) was manipulated to enable the fNaDC-3 coding region to be replaced by the hROAT1 coding region (Figure 4.7). This was carried out by first disrupting the *Bam*HI and *Xba*I sites of the vector using site-directed mutagenesis (Figure 4.7B), then PCR-amplifying the entire fNaDC-3 clone away from the coding region (Figure 4.7C). The primers used in this amplification incorporated *Bam*HI and *Xba*I as close as was practical to the start and stop codons, respectively, to enable subsequent subcloning. Both the fNaDC-3 amplification product and the previously constructed hROAT1 coding region flanked by *Bam*HI and *Xba*I sites, were then sequentially digested with *Bam*HI and *Xba*I and ligated together. This yielded a construct consisting of the hROAT1 coding region flanked by the 5' and 3' UTRs of fNaDC-3 (Figure 4.7A). The full sequence of this expression clone is found in the appendix.

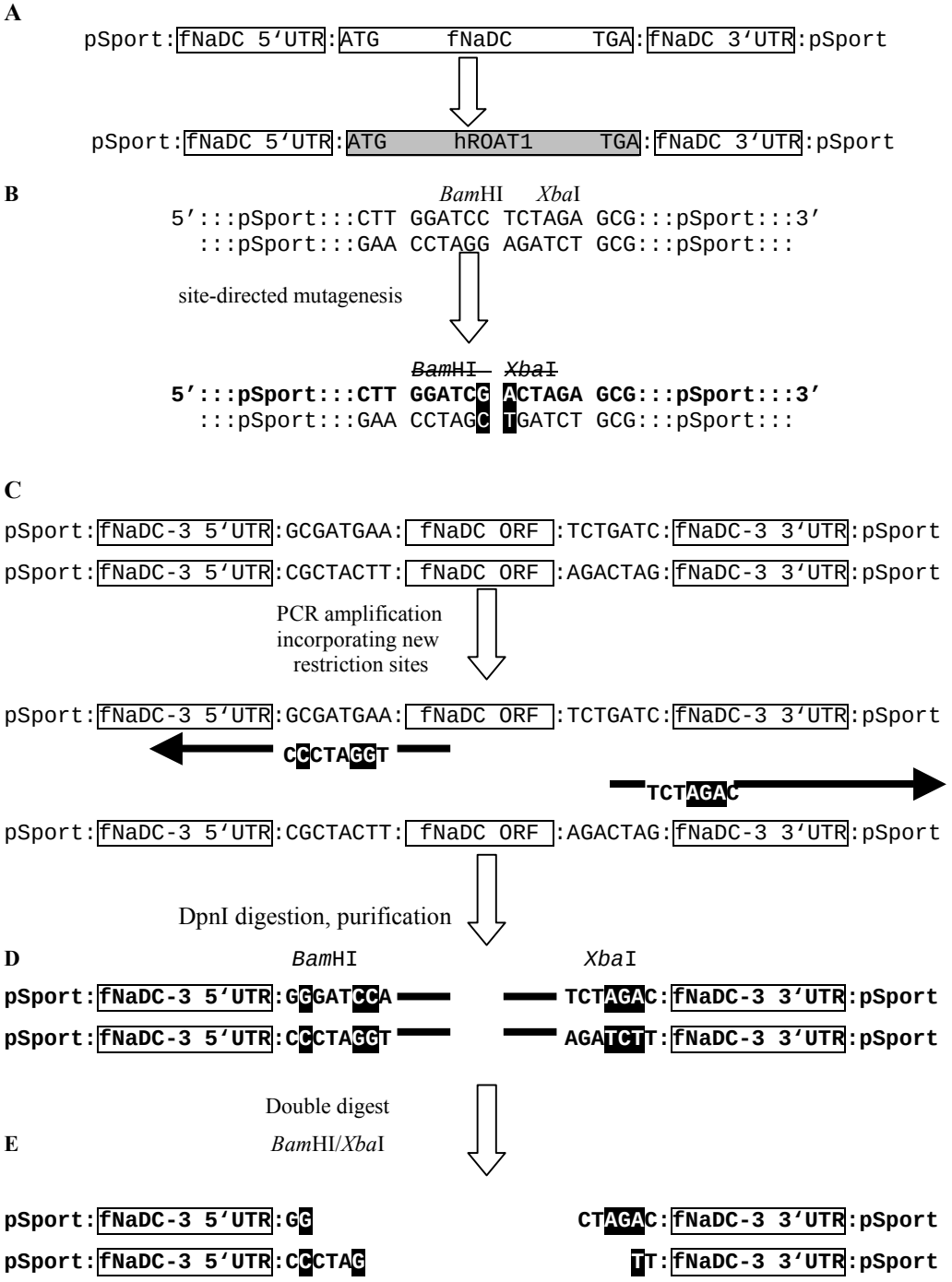

Figure 4.7: Modification of fNaDC-3 A. Outline of proposed method, showing replacement of the coding region (ORF) of the fNaDC-3 cDNA with the hROAT1 coding region, to yield a clone with the hROAT1 coding region flanked by the 5' and 3' UTRs of the fNaDC-3. B. Part of the multiple cloning site of the pSport vector, into which fNaDC-3 was cloned; site-directed mutagenesis was used to disrupt the BamHI and XbaI restriction sites. C. Using PCR to create new restriction sites (C), using primer oligomers (solid arrows) corresponding to the junctions between the fNaDC-3 UTRs and the coding region (partial sequence shown) and also containing mismatches (nucleotides shaded black). PCR amplification was directed away from the fNaDC-3 coding region (C), leading to amplification of the UTRs and the entire vector (D, in bold), with terminal restriction sites. After restriction digestion of the amplification product (E), the amplified vector was ready to receive the hROAT1 coding region.

4.1.3 Functional characterization of hROAT1

The function of hROAT1 was investigated by injection of *Xenopus laevis* oocytes with cRNA derived from the expression clone created in 4.1.2. As seen in Figure 4.8, hROAT1-cRNA injected oocytes incubated in uptake medium containing 10 µM total PAH took up 2.5 pmol PAH/oocyte per hour, a three-fold increase in PAH uptake as compared with water injected control oocytes. This uptake was completely inhibited by the presence of 1 mM of either probenecid or glutarate in the uptake medium. The observed uptake values for hROAT1 were, however, considerably lower than those previously reported for the OAT1/ROAT and fROAT homologues (Sekine et al 1997, Sweet et al 1997, Wolff et al 1997). In an attempt to increase this low activity, two strategies were adopted. First, the oocytes were incubated with glutarate, either 200 µM overnight or 1 mM for 2 hours prior to the transport assay. Secondly, oocytes were co-injected with hROAT1 and fNaDC-3 cRNA. The second approach lead to an increase in uptake of PAH (data not shown), but the overall uptake remained low relative to the rat and flounder clones.

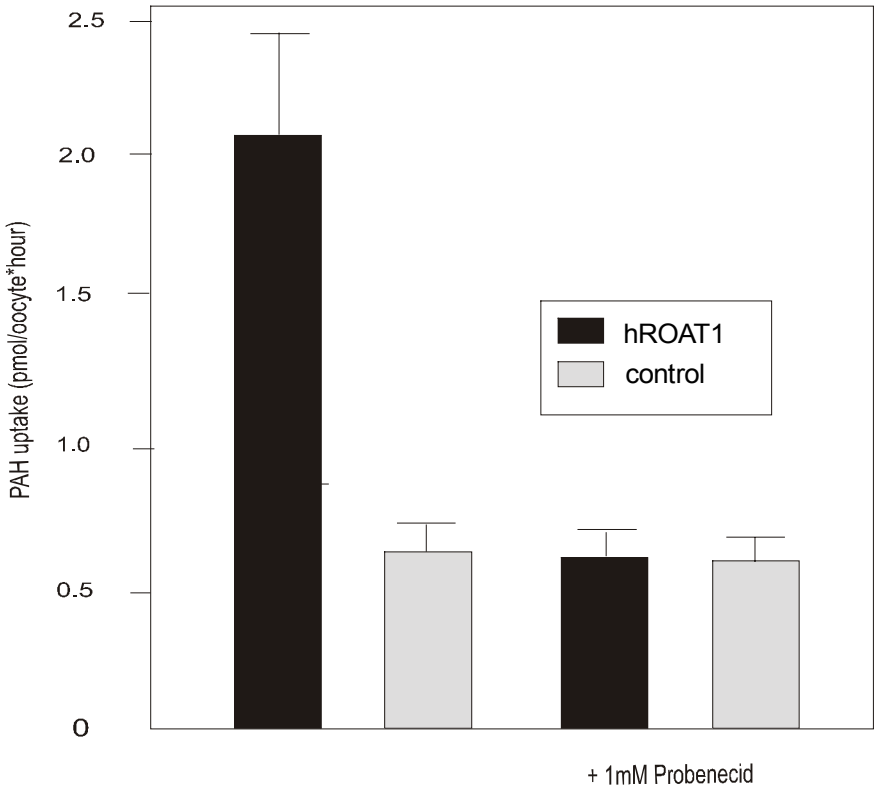

Figure 4.8: hROAT1-mediated PAH uptake. Uptake of PAH by the hROAT1 expression clone, compared with water-injected controls, in the presence and absence of 1 mM probenecid. The figure shows a representative of two independent experiments. Values are mean +/- SE for 9-12 oocytes.

Subsequent analysis of the sequence of the hROAT1 coding region contained within the expression clone revealed a single amino acid substitution, an exchange of a lysine residue for a proline residue (Figure 4.9). Moreover, this proline lies in a predicted transmembrane domain and is conserved in both OATs and OCTs. The amino acid substitution was reversed via site-directed mutagenesis, and the restored wild-type sequence was again tested for function by injection of oocytes with hROAT1 cRNA. Figure 4.10 compares PAH uptake by the restored clone with the original expression clone, demonstrating a substantial increase in the uptake activity of the restored clone - 12 pmol/oocyte*hr compared with 2 pmol/oocyte*hr for the original clone.

A.

```
Query: 246 ctgtgccccactggcgccacctgcagctactggtctctgcgctttttttgccttcttca 305
           ||||||||||||||||||||||||||||||||||||||||| ||||||||||||||||
Sbjct: 728 ctgtgccccactggcgccacctgcagctactggtctctgcgcctttttttgccttcttca 787
```

➔ C770T nucleotide exchange resulting in an amino acid exchange:P257L

B.

hROAT1	GTLIGYVYSLGQFLLAGVAYAVPHWRHLQLLVSAPFFAFFIYSWFFIESARWHSSSGRLD	282
NKT	GTLIGYVYSLGQFLLAGIAYAVPHWRHLQLAVSVPFFVAFIYSWFFIESARWYSSSGRLD	276
ROAT1	GTLIGYVYSLGQFLLAGIAYAVPHWRHLQLVVSVPFFIAFIYSWFFIESARWYSSSGRLD	282
fROAT	GTTTGYCYTLGQLILVLLAYFIRDWRWLTLAVSLPFYVFFLIAWWFHESSRWLALSNRTE	294
NLT/rOAT2	GVISTVFWSGGVLLLALVGYLIRSWRWLLLAATLPCVPGIISIWWVPESARWLLTQGRVE	290
hOCT1	AIMYQMAFTVGLVALTGLAYALPHWRWLQLAVSLPTFLFLLYYWCVPESPRWLLSQKRNT	296
rOCT1	AILYQMAFTVGLVGLAGVAYAIPDWRWLQLAVSLPTFLFLLYYWFVPESPRWLLSQKRTT	297
mOCT1	AILYQVAFTVGLVGLAGVAYAIPDWRWLQLAVSLPTFLFLLYYWFVPESPRWLLSQKRTT	297
hOCT2	GIFYQVAYTVGLLVLAGVAYALPHWRWLQFTVALPNFFFLLYYWCIPESPRWLISQNKNA	297
mOCT2	GICYQIAFTVGLLILAGVAYALPNWRWLQFAVTLPNFCFLLYFWCIPESPRWLISQNKNA	297
rOCT2	GICYQIAFTVGLLILAGVAYVIPNWRWLQFAVTLPNFCFLLYFWCIPESPRWLISQNKIV	297

C.

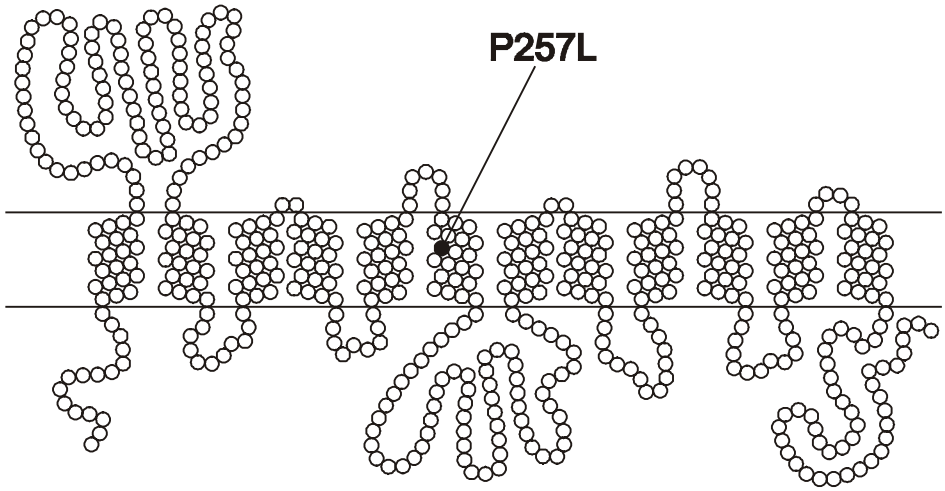

Figure 4.9: Amino acid exchange in hROAT1 resulting from PCR amplification. A. Part of the Blast comparison of the PCR-amplified hROAT1 expression clone sequence and the original hROAT1 sequence, showing the C770T nucleotide exchange (bold), which results in the P257L amino acid exchange. B. Partial OAT/OCT alignment showing the absolute conservation of the Pro257 (white) within the sixth transmembrane domain (grey). C. The position of the P257L amino acid exchange in a secondary structure model of hROAT1, showing the predicted transmembrane location. The mutation was corrected by site-directed mutagenesis.

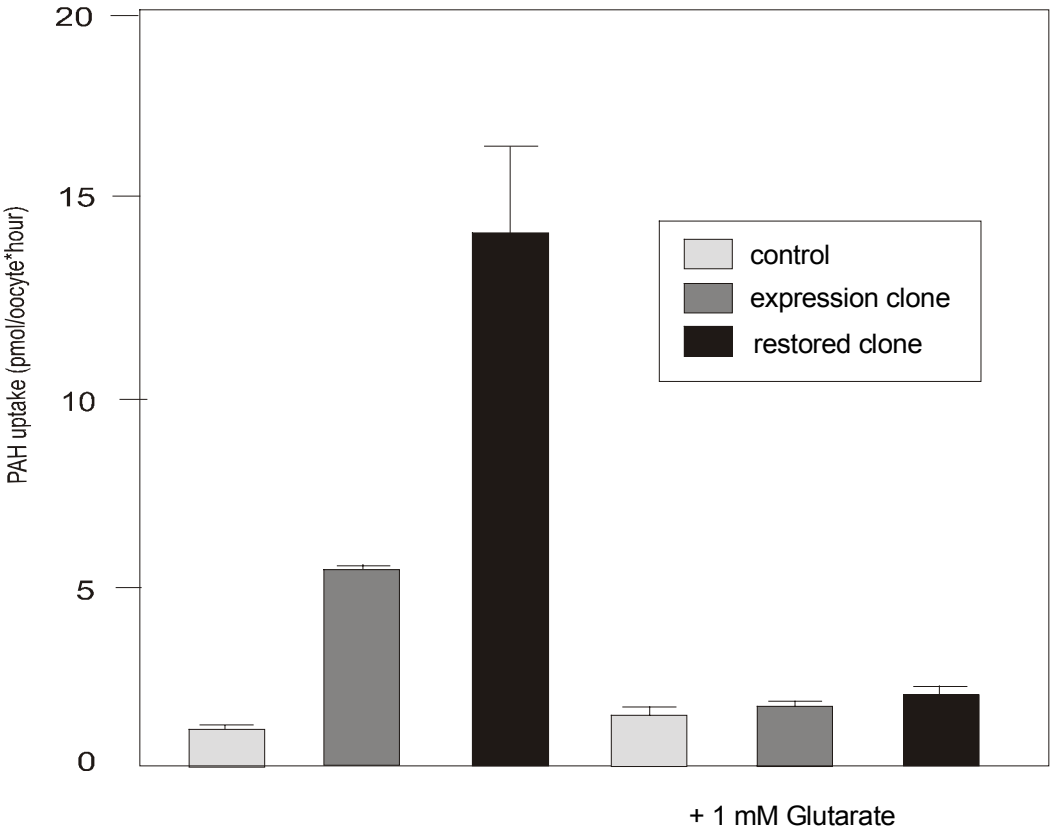

Figure 4.10: PAH uptake mediated by the restored hROAT1 clone. Uptake of PAH by the first expression clone and the restored clone, compared with water-injected controls, in the presence and absence of 1 mM glutarate. The figure shows a representative of two independent experiments. Values are mean +/- SE for 9-12 oocytes.

4.1.3.1 Determination of K_m of hROAT1 for PAH

The uptake of PAH into hROAT1-injected oocytes was found to be a linear process from 0-15 minutes (data not shown), therefore a period of 10 minutes was chosen to determine the K_m of the transporter for PAH.

Figure 4.11 shows a representative from three independent determinations of the K_m for PAH of hROAT1-injected oocytes. The Km value of approximately 10 µM calculated using the EZ-Fit enzyme kinetics software program (Perrella Scientific, Inc), is consistent with that reported for the other human OAT1 clones (Hosoyamada et al 1999, Lu et al 1999), and is also similar to that obtained with the rat OAT1 clone (Sekine et al 1997).

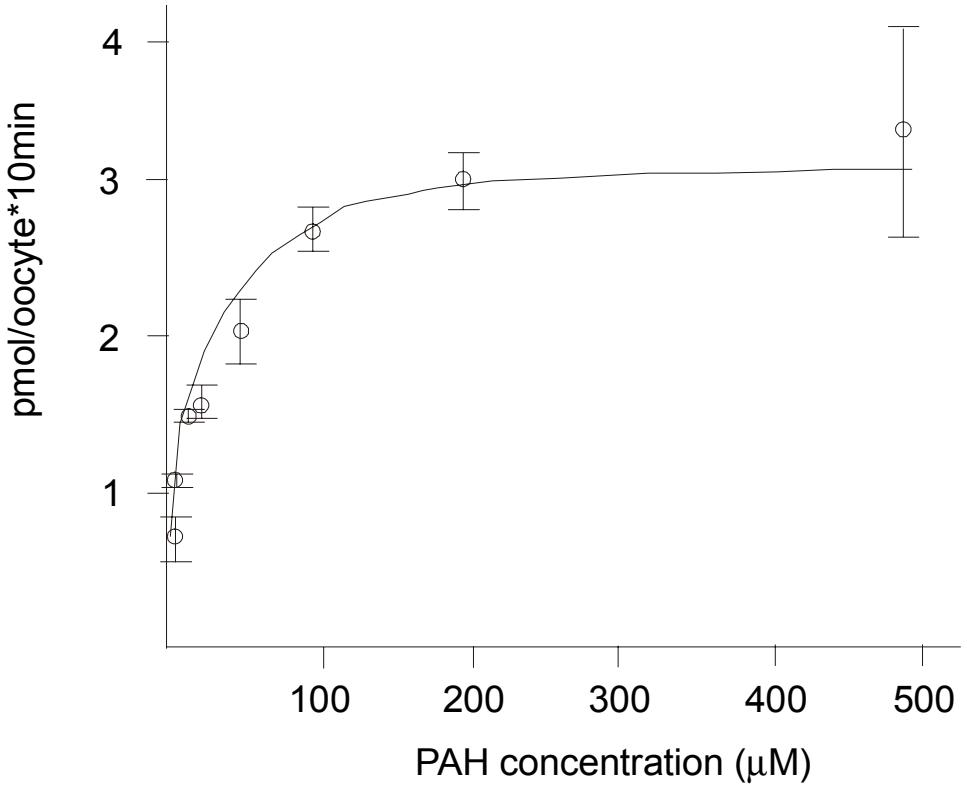

Figure 4.11: Determination of the K_m of hROAT1 for PAH. Concentration-dependent PAH uptake is shown in a representative of three independent experiments. PAH uptake was determined for 1, 5, 10, 20, 50, 100, 200 and 500 µM total PAH. Values shown are mean +/- SE for 7-11 oocytes.

4.1.3.2 Ion dependence of hROAT1-mediated PAH uptake

Many features of the multispecific organic anion system were known from functional studies using the various systems outlined in the introduction. The process had been shown to be pH-independent and electroneutral with an indirect requirement for sodium ions and also some involvement of chloride ions in the transport process (Pritchard and Miller 1993). To test whether the hROAT1 clone shared these properties, uptake experiments were carried out with altered transport media. Chloride dependence was demonstrated using ORI in which chloride was replaced by gluconate, and as seen in Figure 4.12, this decreased PAH uptake by approximately 80 %. In ORI medium in which sodium was replaced with choline, there was also a slight decrease of approximately 30 % in PAH uptake in hROAT1-injected oocytes (Figure 4.12). To test the effect of membrane depolarization on hROAT1-mediated PAH transport, oocytes were pre-incubated in ORI containing 23 mM KCl instead of the usual 3 mM, with a 20 mm reduction in NaCl concentration to 70 mM. Subsequent uptake in the same

medium resulted in an unexpected increase of approximately 60 % in PAH uptake (Figure 4.12).

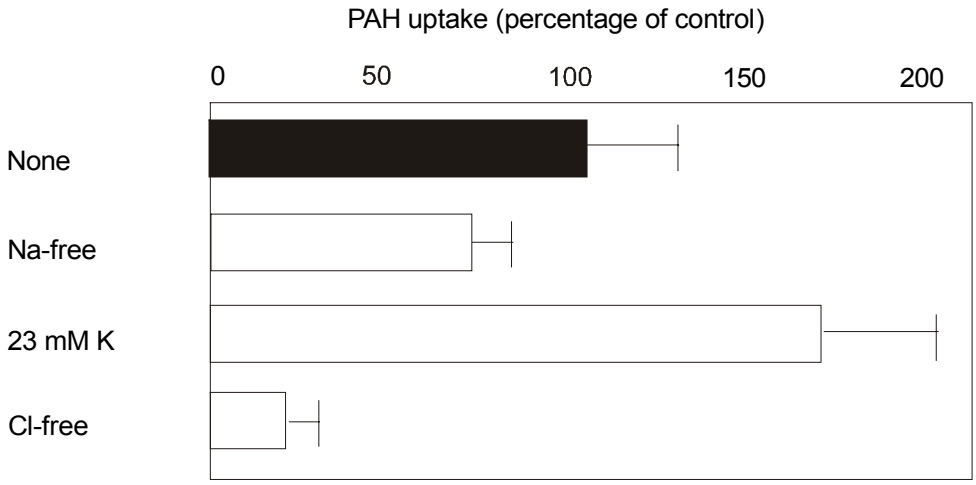

Figure 4.12: Inorganic ion dependence of hROAT1-mediated PAH uptake. The effect of changes in the composition of the uptake medium on hROAT1 mediated PAH uptake is shown. Control levels of PAH uptake are represented by the bar labelled None. Na-free and Cl-free indicate uptake experiments in transport medium where sodium and chloride were replaced by choline and gluconate, respectively. 23 mM K represents uptake in medium containing 23 mM KCl and 70 mM NaCl, which leads to membrane depolarization in the oocyte.

4.1.3.3 Cis-inhibition of hROAT1-mediated PAH uptake

In order to associate hROAT1 more closely with one of the renal organic anion transporting systems that had already been functionally characterized, a number of organic anions were tested for their ability to inhibit hROAT1-mediated PAH uptake. As seen previously, both probenecid, the classical inhibitor of the multispecific organic anion transporting system, and glutarate, a dicarboxylate, inhibited PAH uptake in hROAT1-injected oocytes by more than 95 %. In further cis-inhibition studies, the effects of a number of organic anions on hROAT1-mediated PAH uptake were tested, including clinically relevant compounds such as loop diuretics and sulfated bile acids, as well as a range of dicarboxylates.

As hROAT1 appears to be an organic anion / dicarboxylate exchanger, cis-inhibition studies were carried out with various dicarboxylates in order to determine dicarboxylates that could serve as possible exchange partners. Candidate dicarboxylates tested included unsubstituted dicarboxylates with carbon backbone of 2-8 carbon atoms,

as well as members of the tricarboxylic acid cycle. hROAT1-dependent PAH uptake was carried out in the presence of 1 mM of each dicarboxylate, the results of which are shown in the following two figures.

As seen in Figure 4.13, oxalate, malonate and succinate (with 2, 3 or 4 carbon atoms, respectively) did not significantly inhibit hROAT1-dependent PAH uptake. All unsubstituted dicarboxylates with a carbon backbone ≥ 5 carbon atoms reduced PAH uptake by at least 90 %. This is consistent with inhibition studies of fROAT, which is inhibited by glutarate and suberate, but not malonate or succinate (Wolff et al 1997).

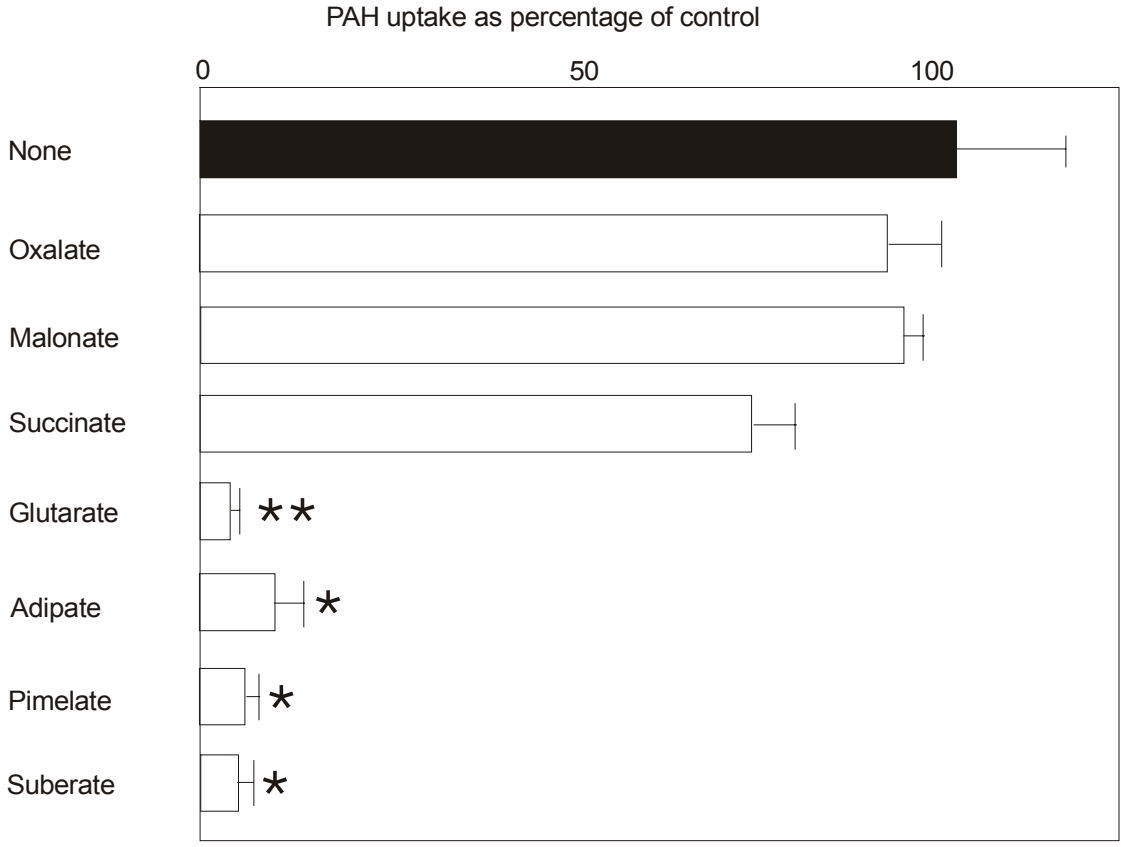

Figure 4.13: Cis-inhibition of hROAT1-mediated PAH uptake by unsubstituted dicarboxylates of increasing length. The effect on control levels of hROAT1-mediated PAH uptake (None) of is shown. The dicarboxylates were present in the uptake medium at a concentration of 1 mM. Control uptake levels were set to 100 %. Uptake in the presence of each dicarboxylate are shown as percentage of control uptake, +/- SE. Results were obtained from 3 independent experiments with 7-12 oocytes per group (* = $P < 0.05$, ** = $P < 0.01$).

Figure 4.14 shows the effect on PAH uptake by members of the TCA cycle. Malate, fumarate, succinate and oxalacatate did not significantly inhibit PAH uptake, consistent with previous studies of fROAT (Wolff et al 1997), whereas α-ketoglutarate reduced

hROAT1-dependent uptake by approximately 90 %, consistent with the assertion that α-ketoglutarate functions as the physiological counterion in basolateral PAH uptake in the proximal tubule (Pritchard and Miller 1993). Citrate, which has a substituted 5 carbon atom backbone, did not inhibit PAH uptake.

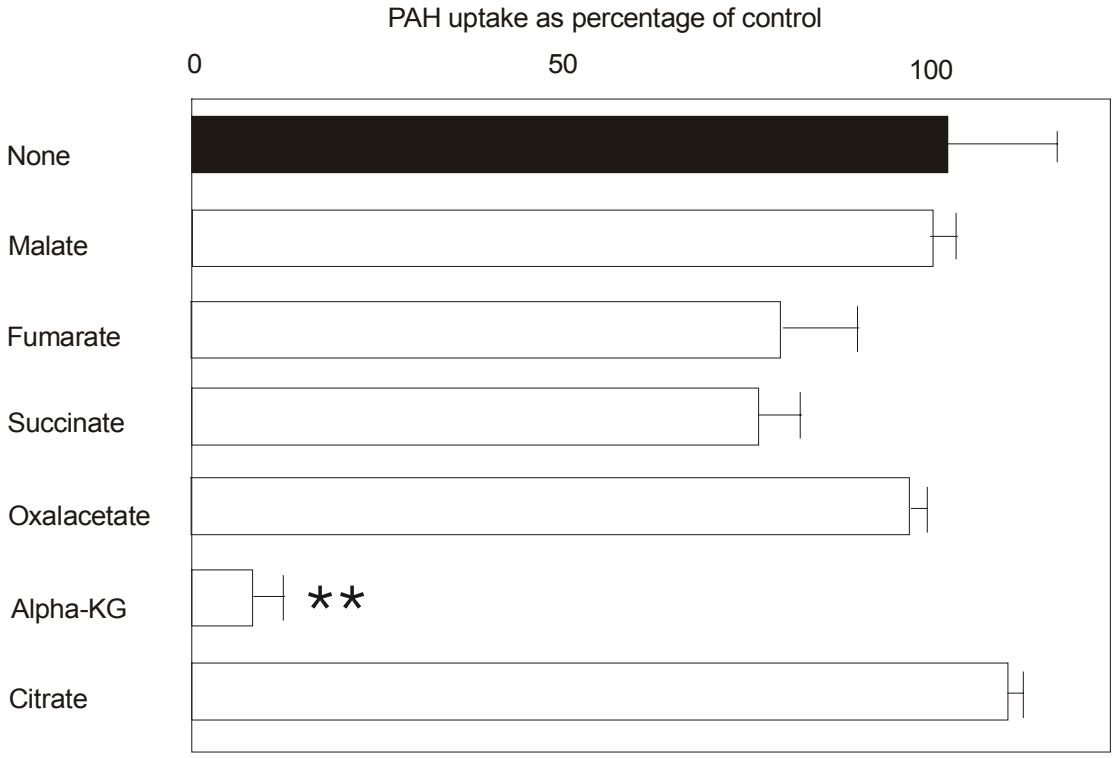

Figure 4.14: Cis-inhibition of hROAT1-mediated PAH uptake by TCA cycle intermediates. The effect on control levels of hROAT1-mediated PAH uptake (None) is shown. The dicarboxylates were present in the uptake medium at a concentration of 1 mM. Control uptake levels were set to 100 %. Uptake in the presence of each dicarboxylate are shown as percentage of control uptake, +/- SE. Results were obtained from 3 independent experiments with 7-12 oocytes per group (** = $P < 0.005$).

Several clinically relevant compounds were also tested for their ability to cis-inhibit hROAT1-mediated PAH uptake. The loop diuretics bumetanide and furosemide had previously been shown to interact with the organic anion transporting system (Møller and Sheikh, 1983), and urate, the end product of purine catabolism, is thought to share the transport system for PAH in many species (Pritchard and Miller 1993). In addition, lithocholic acid derivatives are excreted by the kidney to a greater extent than other bile acids (Palmer 1971).

Figure 4.15 shows that both bumetanide and furosemide strongly inhibit (>95 %) the uptake of PAH by hROAT1-injected oocytes. Urate also inhibits this process to a lesser extent (50 %). Taurolithocholate (TLC) slightly inhibited PAH uptake, an effect

increased by sulfation (TLC-S), whereas neither form of glycolithocholate (GLC and GLC-S) affected hROAT1-mediated PAH uptake.

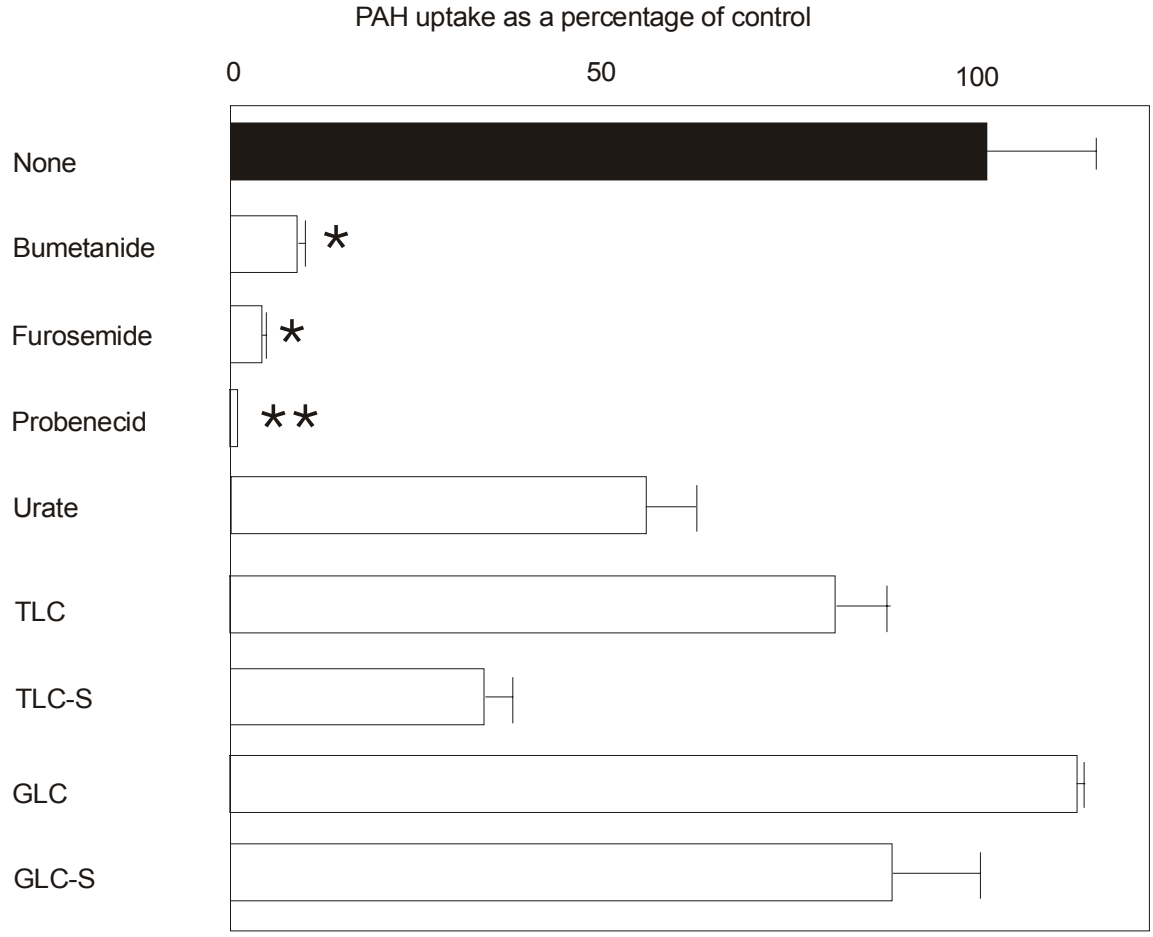

Figure 4.15: Effect of various organic anions on hROAT1-mediated PAH uptake. The effect organic anions on control levels of hROAT1-mediated PAH uptake (None) of is shown. The substances were present in the uptake medium at a concentration of 1 mM (100 µM for bile acids). Control uptake levels were set to 100 %. Uptake in the presence of each dicarboxylate are shown as percentage of control uptake, +/- SE. Results were obtained from 3 independent experiments with 7-12 oocytes per group (* = $P < 0.05$, ** = $P < 0.01$).

4.1.3.1 hROAT1-mediated bumetanide uptake

As the PAH uptake in oocytes expressing hROAT1 was inhibited by more than 95 % by the loop diuretics bumetanide and furosemide, uptake experiments with radioactively-labelled bumetanide were carried out. During a 1 hour incubation, no significant uptake of bumetanide by hROAT1-injected oocytes was observed in comparison with water controls (3.5 ± 0.4 pmol/hr*oocyte versus 3.4 ± 0.4 pmol/hr*oocyte).

4.1.4 Mutational analysis

Mutational analysis of hROAT1 was undertaken in an attempt to identify those regions of the protein involved in the transport process. To this end a combination of point mutations and deletions were generated, and the effect of these alterations on the hROAT1-mediated PAH uptake was observed.

4.1.4.1 hROAT1 point mutants

Upon closer examination of the alignment of the related OATs and OCTs it became apparent that certain charged amino acid residues identical in all members of one group are substituted in all members of the other group for a residue of opposite or neutral charge. Three positions satisfy this criterion: the positively charged residues at positions 34 (histidine), 382 (lysine) and 466 (arginine) in hROAT1 align with isoleucine (neutral), alanine (neutral) and aspartate (positive) residues found at the corresponding positions in all OCTs. Of these single amino acid differences, lysine at position 382 and arginine at position 466 were chosen for further study (Figure 4.16). Using site-directed mutagenesis, the lysine at position 382 of hROAT1 was replaced by an alanine, the amino acid residue found at this position in all OCTs, and the arginine at position 466 was replaced by an aspartic acid, as found in all OCTs. These mutants, K382A and R466D, were sequenced to ensure polymerase fidelity, and expressed in oocytes.

```
hROAT1     LCLSMLWFATSFAYYGLVMDLQGFGVSIYLIQVIFGAVDLPAKLVGFLVINSLGRRPAQM   399
NKT/mOAT   LCLSMLWFATSFAYYGLVMDLQGFGVSMYLIQVIFGAVDLPAKFVCFLVINSMGRRPAQL   393
ROAT1      LCLSMLWFATSFAYYGLVMDLQGFGVSMYLIQVIFGAVDLPAKFVCFLVINSMGRRPAQM   399
fROAT      LCLSAVWLSTSFAYYGLAMDLDKFGVDIYLIQVIFGAVDIPAKVVVVVSMSLIGRRRSQC   411
NLT-rOAT2  LCCMMVWFGVNFSYYGLTLDVSGLGLNVYQTQLLFGAVELPSKIMVYFLVRRLGRRLTEA   405
hOCT1      FILMYLWFTDSVLYQGLILHMGATSGNLYLDFLYSALVEIPGAFIALITIDRVGRIYPMA   407
rOCT1      VILMYLWFSCAVLYQGLIMHVGATGANLYLDFFYSSLVEFPAAFIILVTIDRIGRIYPIA   408
mOCT1      LILMYLWFSCAVLYQGLIMHVGATGANLYLDFFYSSLVEFPAAFIILVTIDRIGRIYPIA   408
hOCT2      MILMYNWFTSSVLYQGLIMHMGLAGDNIYLDFFYSALVEFPAAFMIILTIDRIGRRYPWA   408
mOCT2      LILMYNWFTSSVLYQGLIMHMGLAGDNIYLDFFYSALVEFPAAFIIILTIDRIGRRYPWA   408
rOCT2      LILMYNWFTSSVLYQGLIMHMGLAGDNIYLDFFYSALVEFPAAFIIILTIDRVGRRYPWA   408
                    tmd 7                          tmd 8

hROAT1     MGSTMARVGSIVSP-LVSMTAELYPSMPLFIYGAVPVAASAVTVLLPETLGQPLPDTVQD   518
NKT/mOAT   MGSTMARVGSIVSP-LISMTAEFYPSIPLFIFGAVPVAASAVTALLPETLGQPLPDTVQD   512
ROAT1      MGSTMARVGSIVSP-LVSMTAEFYPSMPLFIFGAVPVVASAVTALLPETLGQPLPDTVQD   518
fROAT      WVSMMARIGAMVAP-MVLLTRDYIPWLPGLIYGGAPILSGLAAIFLPETLGYPLPDTIQD   530
NLT/rOAT2  LTALMGRLGASLAR-LAALLDGVWLLLPKVAYGGIALVAACTALLLPETKKAQLPETIQD   524
hOCT1      VCSSLCDIGGIITPFIVFRLREVWQALPLILFAVLGLLAAGVTLLLPETKGVALPETMKD   527
rOCT1      VCSALCDLGGIFTPFMVFRLMEVWQALPLILFGVLGLTAGAMTLLLPETKGVALPETIEE   528
mOCT1      VCSALCDLGGIFTPFMVFRLMEVWQALPLILFGVLGLSAGAVTLLLPETKGVALPETIEE   528
hOCT2      ICSSMCDIGGIITPFLVYRLTNIWLELPLMVFGVLGLVAGGLVLLLPETKGKALPETIEE   528
mOCT2      VCSSMCDIGGIVTPFLVYRLTDIWLEFPLVVFAVVGLVAGGLVLLLPETKGKALPETIED   528
rOCT2      VCSSMCDIGGIITPFLVYRLTDIWMEFPLVVFAVVGLVAGALVLLLPETKGKALPETIED   528
                    tmd 11                         tmd 12
```

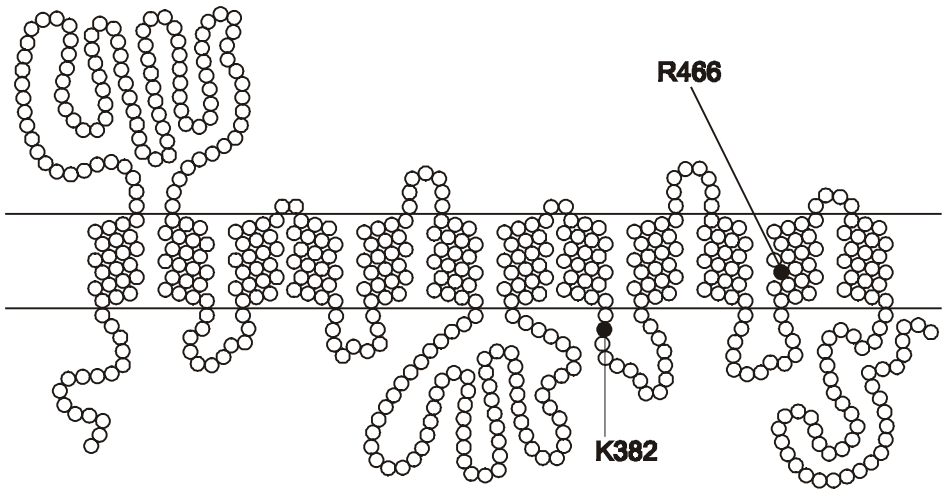

Figure 4.16: Construction of two hROAT1 point mutants. Top: An alignment of the cloned OATs (above) and OCTs (below), showing the position of the conserved lysine and arginine chosen for mutational analysis. Residues shaded grey represent transmembrane domains. Transporter names are as for Figure 4.1. Bottom: Position of these amino acids in the secondary structure model of hROAT1.

The results of uptake experiments involving each mutant are shown in Figure 4.17. In comparison with wild-type hROAT1, neither K382A nor R466D could mediate uptake PAH uptake – these amino acid substitutions completely disrupted the function of the transporter.

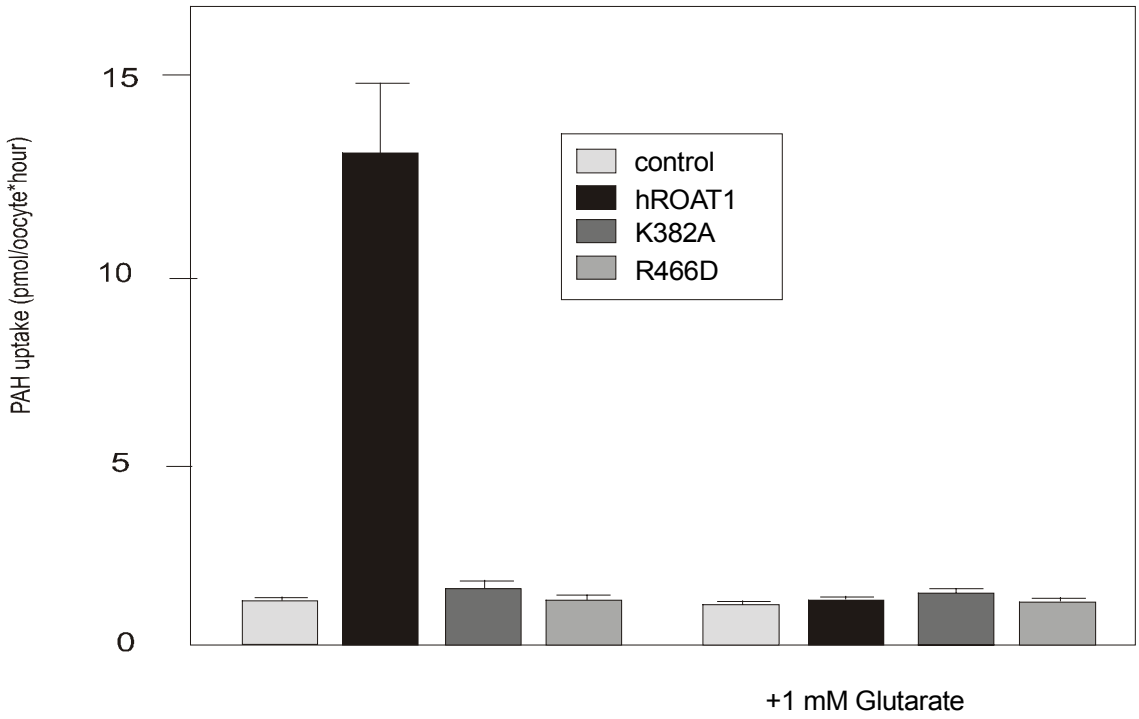

Figure 4.17 PAH uptake by two hROAT1 point mutants. Uptake of PAH by the two hROAT1 point mutants, K382A and R466D, compared with hROAT1 and water controls, in the absence and presence of 1 mM glutarate. The values represent the mean +/- SE for 8-12 oocytes in a representative of three independent experiments.

4.1.4.2 hROAT1 deletion mutants

To determine whether the entire hROAT1 open reading frame is required for transport activity, deletion mutants were generated. These N- and C-terminal mutants were generated by PCR from the hROAT1 expression clone with artificially introduced start or stop codons, respectively, as detailed in Methods. That the entire coding region may not be essential to the transport function of hROAT1 was first suggested by the observation that rOCT1, a member of the related organic cation transporter family, is also expressed as an alternatively spliced short form, rOCT1A. This isoform is missing the N-terminal portion of the protein corresponding to the first two transmembrane domains, but still mediates transport function (Zhang et al 1997). To test whether hROAT1 could mediate PAH uptake without the first two transmembrane domains, an artificially shortened open reading frame was generated with PCR techniques. Figure 4.18 shows the results of uptake experiments with oocytes injected with the shortened hROAT1 cRNA with the wild-type hROAT1 as control. In contrast to the functional rOCT1A, a similarly shortened hROAT1 was not able to mediate transport above control levels.

Transcripts from the hOAT1 gene are also alternatively spliced, and four distinct isoforms of hROAT1 are known (Hosoyamada et al 1999, Bahn et al 2000). All four isoforms differ in the splicing of exons 9 and 10 (Bahn et al 2000). To determine whether these two exons are essential for transport function, both exon 10 alone and exons 9 and 10 together were artificially removed from the hROAT1 open reading frame. This corresponded to the removal of the terminal 28 and 94 amino acids of the hROAT1 reading frame, as depicted in Figure 4.18. Figure 4.19 shows uptake of PAH by oocytes injected with cRNA synthesized from these deletion mutants, in comparison with wild-type hROAT1 cRNA. The deletion of exons 9 and 10 completely abolished the ability of hROAT1 to mediate PAH uptake. In contrast, deletion of exon 10 alone lead to an increase of approximately two-fold in PAH uptake.

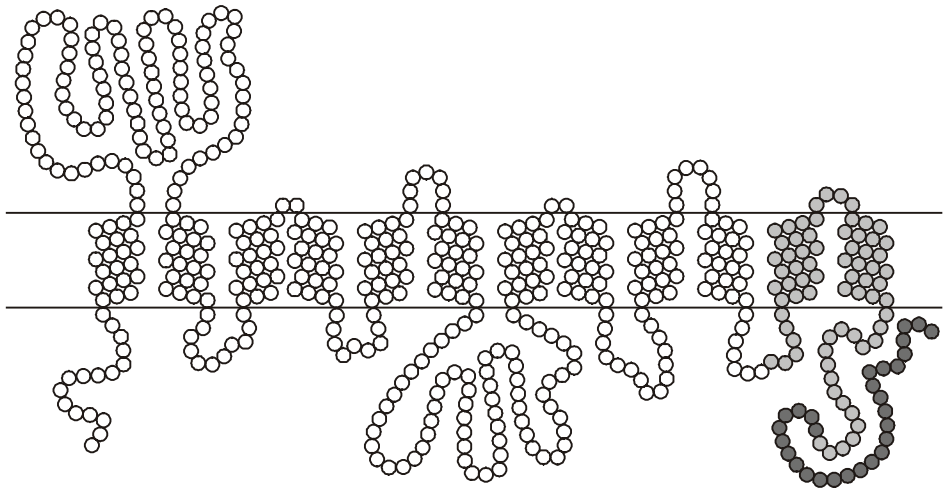

Figure 4.18: Construction of hROAT1 deletion mutants. The location of exon 9 (light shading) and exon 10 (dark shading) superimposed upon the hROAT1 secondary structure. Exon positions are taken from Bahn et al 2000.

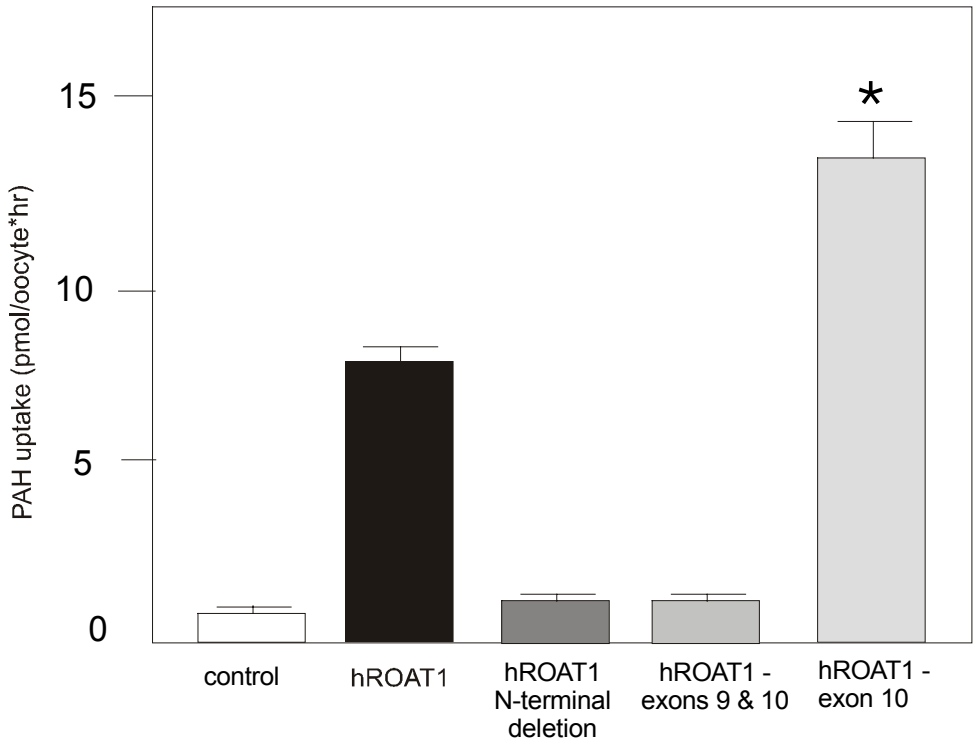

Figure 4.19: PAH uptake mediated by two hROAT1 deletion mutants. PAH uptake mediated by oocytes injected with cRNA derived from hROAT1 with deletion of exon 10, and exons 9 & 10, is shown in comparison with water- and hROAT1-injected controls. The values represent the mean +/- SE for 8-12 oocytes in a representative of three independent experiments. * = $P < 0,05$.

4.2 CLONING AND EXPRESSION OF A HUMAN OAT2 HOMOLOGUE

The cloning of hROAT1, detailed above, represents the first reported cloning of a human OAT1 homologue, a transporter involved in the initial basolateral uptake step in the transepithelial renal secretion of organic anions such as PAH. As outlined in the introduction, this step had already been characterized by functional studies in many species, and the previous cloning of several homologues facilitated the cloning of hROAT1. In contrast, a role in the luminal exit of organic anions secreted in the kidney has yet to be assigned to a known protein. The luminal efflux of PAH has been shown to be a low affinity, uniport system, and a protein with these properties would therefore be a candidate for transport of PAH into the tubular lumen. As the rat NLT/OAT2 satisfies these criteria (Sekine et al 1998), a human homologue was sought.

4.2.1 Human EST-based cloning of hOAT2

4.2.1.1 Retrieval of ESTs from the human dbEST database

The initial step in cloning the human homologue of the rat NLT/rOAT2 consisted of a Blast search of the human expressed sequence tag (EST) database using the rat NLT/OAT2 nucleotide sequence as a search query. This lead to the retrieval of three human ESTs (accession numbers: AI016020, T73363, T68667) with high homology to the rat NLT/OAT2, corresponding to the beginning (EST1: AI016020), middle (EST2: T73363) and end (EST3: T73363) of the rat NLT/OAT2 coding region. Aligning the amino acid sequence derived from each EST to the amino acid of rat NLT/OAT2 revealed 76, 77 and 83 % identity to the rat sequence for EST1, 2 and 3, respectively.

From the amino acid alignment, it was observed that the EST aligning with the 5' end of the rat NLT/OAT2 sequence included the probable start codon of the human NLT/OAT2 homologue. In contrast, the EST corresponding to the 3' region aligned only until amino acid 478 of the predicted reading frame after which the sequences were completely divergent. The nucleotide sequence of the terminally-aligning EST was then edited, based on a comparison with the rat NLT/OAT2 nucleotide sequence, to remove any obvious sequencing errors common in ESTs - additional bases or deletions - that had perhaps caused frameshifts resulting in the sudden divergence seen in the sequence. When the derived amino acid sequence corresponding to the edited EST was aligned

with the rat NLT/OAT2, the homology between the two sequences continued until residue 528 of the rat sequence (Figure 4.20).

```
                .    :    .    :    .    :    .    :    .    :    .    :     60
HNLT-EST1       MGFEELLEQVGGFGPFQLRNVALLALPRVLLPLHFLLPIFLAAVPAHRCALPGAPANFSH     60
NLT/ROAT2       MGFEDLLDKVGGFGPFQLRNLVLMALPRMLLPMHFLLPVFMAAVPAHHCALPGAPANLSH     60

                .    :    .    :    .    :    .    :    .    :    .    :    120
HNLT-EST1       QDVWLEAHLPREPDGTLSSCLRFAYPQALPNTTLGEERQSRGELEDEPATVPCSQGWEYD    120
NLT/ROAT2       QDLWLEAHLPRETDGSFSSCLRFAYPQTVPNVTLGTEVSNSGEPEGEPLTVPCSQGWEYD    120

                .    :    .    :    .    :    .    :    .    :    .    :    180
HNLT-EST1       HSEFSSTIATE_____________________________________________________ 131
NLT/ROAT2       RSEFSSTIATEWDLVCQQRGLNKITSTCFFIGVLVGAVVYGYLSDRFGRRRLLLVAYVSS    180

                _____.    :    .    :    .    :    .    :    .    :    .    :    240
NLT/ROAT2       LVLGLMSAASINYIMFVVTRTLTGSALAGFTIIVLPLELEWLDVEHRTVAGVISTVFWSG    240

                     .    :    .    :    .    :    .    :    .    :    .    :    300
HNLT-EST2       ____________________________QGILSLWWVPESARWLLTQGHVKEAHRYLLHCA     33
NLT/ROAT2       GVLLLALVGYLIRSWRWLLLAATLPCVPGIISIWWVPESARWLLTQGRVEEAKKYLLSCA    300

                .    :    .    :    .    :    .    :    .    :    .    :    360
HNLT-EST2       RLNGRPVCEDSFSQEVWSKVAAGERVVRRPSYLDLFRTPRLRHISLCCVVVWFGVNFSYY     93
NLT/ROAT2       KLNGRPVGEGSLSQEALNNVVTMERALQRPSYLDLFRTSQLRHISLCCMMVWFGVNFSYY    360

                .    :    .    :    .    :    .    :    .    :    .    :    420
HNLT-EST2       GLSLDVSGLGLNVYQTQLLFG___________________________________________ 114
NLT/ROAT2       GLTLDVSGLGLNVYQTQLLFGAVELPSKIMVYFLVRRLGRRLTEAGMLLGAALTFGTSLL    420

                     .    :    .    :    .    :    .    :    .    :    .    :    480
HNLT-EST3       __SDMKSWSTVLAVMGKAFSEAAFTTAYLFTSELYPTVLRQTGMGLTALVGRLGGSLARL     58
NLT/ROAT2       VSLETKSWITALVVVGKAFSEAAFTTAYLFTSELYPTVLRQTGLGLTALMGRLGASLARL    480

                .    :    .    :    .    :    .    :    .    :    .    :    540
HNLT-EST3       AALLDGVXLSLPKLTYGGIXLLAAGTALLLPETRQAQLPETIQDVERK_______         106
NLT/ROAT2       AALLDGVWLLLPKVAYGGIALVAACTALLLPETKKAQLPETIQDVERKSTQEEDV          535
```

Figure 4.20: Alignment of hESTs with NLT/rOAT2. Amino acid alignment of the three hESTs retrieved (top) with NLT/rOAT2 Residues shaded grey are identical in both human EST and rat sequence.

Sequence-specific primers then enabled amplification, from a human liver cDNA template, of a product of 1575 bp representing the first 528 amino acids of a human homologue of the rat NLT/OAT2 (Figure 4.21). This initial amplification product exhibited 78 % identity with the rat clone when the nucleotide sequences were compared, and the derived amino acid sequences showed 85 % identity.

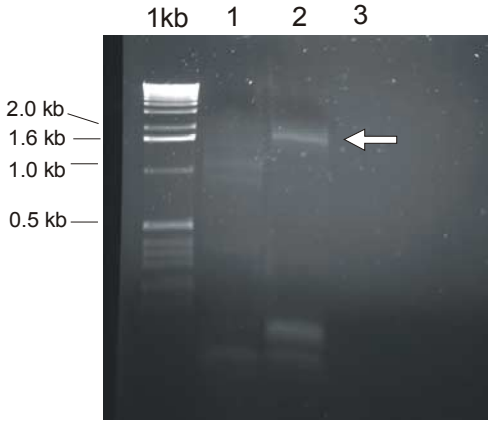

Figure 4.21: Amplification of hOAT2 from human liver cDNA. Lane 1: initial amplification; lane 2: re-amplification; lane 3: negative control. 1 kb: 1kb standard, with band sizes labelled left. The amplification product from which the initial hOAT2 product was cloned is signified by the white arrow

4.2.1.2 3' RACE

To complete the coding region and enable functional characterization, 3'RACE with an hOAT2-specific primer was carried out, again using human liver cDNA as a template. Unfortunately, no successful amplification product was obtained after several attempts with a range of annealing temperatures. The same 3' RACE reaction was then carried out using a human kidney cDNA template, and this yielded a product of approximately 600 bp with an in frame stop codon and poly-A tail. From the sequence of the 3' RACE product amplified from the kidney, it appeared likely that this was expressed from the same gene as the initial product amplified from the liver cDNA, as the overlapping sequence of 240 nucleotides was 100 % identical.

Based on a contig of these two sequences, sequence-specific primers were designed with which to amplify the full-length hOAT2 expressed in the kidney. Following successful amplification of the full-length hOAT2 coding region and verification by sequencing, the hOAT2 sequence was submitted to the GenBank database, where it was assigned the accession number AF210455.

4.2.1.3 Analysis of the hOAT2 sequence

The complete coding sequence of hOAT2 is seen in Figure 4.22. The coding region of the hOAT2 cDNA consists of 1626 nucleotides followed by a 3' UTR of 200 nucleotides (not shown). hOAT2 encodes a protein of 541 amino acids, with a predicted mass of 59 kDa. Based on TopPred2 analysis (window setting of 11-21, upper cut-off 1.0, lower cut-off 0.4), hOAT2 is predicted to contain 12 transmembrane domains with intracellular N- and C-termini, as seen for other members of the OAT family. A model of the predicted secondary structure of hOAT2 including sites for potential enzymatic modification is seen in Figure 4.23. Further analysis of the primary structure revealed a number of conserved motifs. In the large extracellular loop between transmembrane domains 2 and 3 are two consensus sites for N-glycosylation (N^{57} and N^{91}). Also present in the primary amino acid sequence are a number of consensus sites for phosphorylation by various kinases: protein kinase A (S^{333}, T^{405}), protein kinase C (T^{340}, S^{396}), and casein kinase II (S^{333}, T^{522}).

hOAT2, like hROAT1, contains sequence motifs common to the ASF subfamily of the major facilitator superfamily. These motifs are: $GX_3GX_4GX_3DRXGRRK$, with the

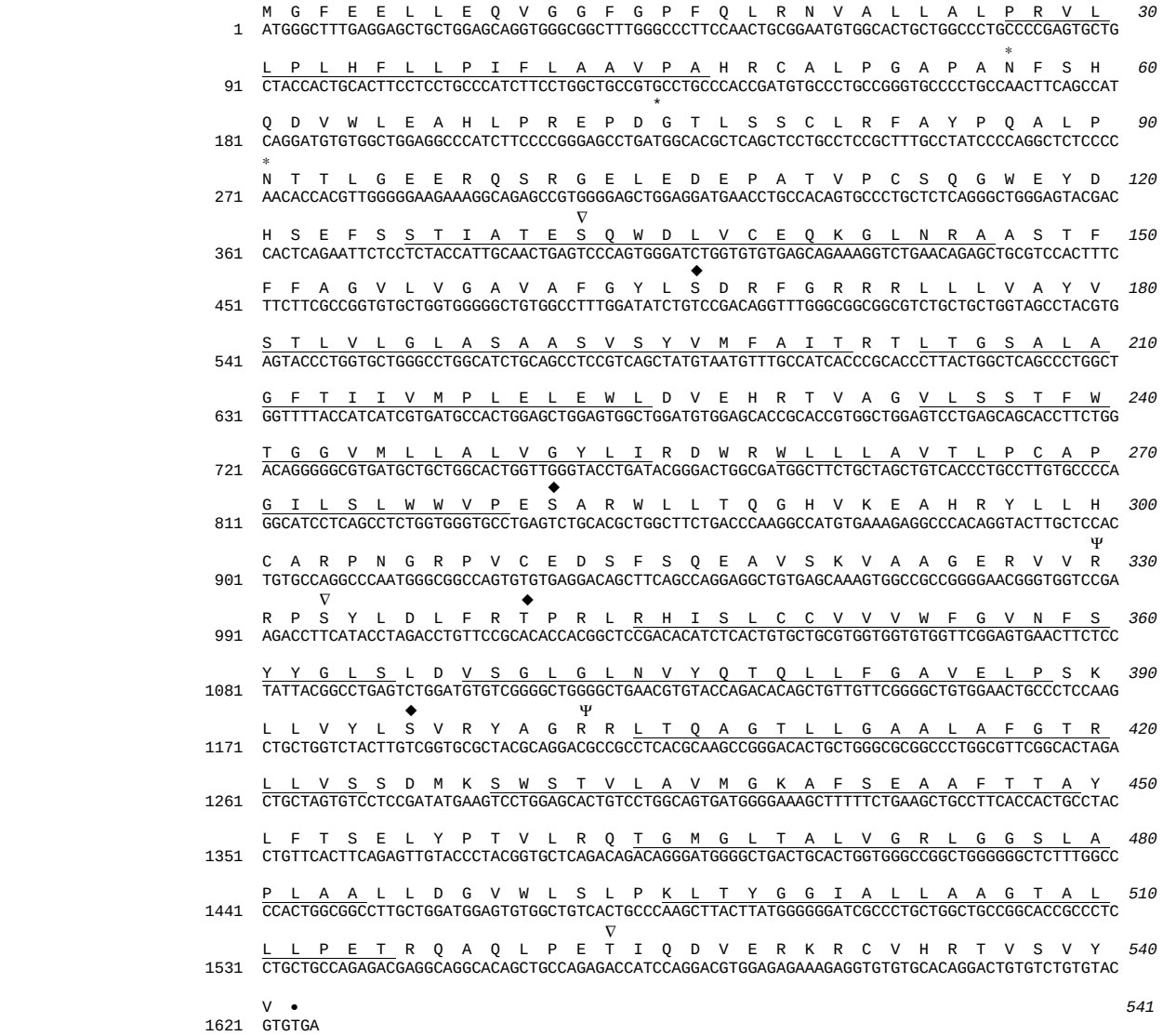

Figure 4.22: hOAT2 nucleotide and amino acid reading frame. The hOAT2 cDNA sequence (left-hand column) and the amino acid sequence (right-hand column) of the 541 amino acid open reading frame. Transmembrane domains predicted by the TopPred 2 programme are underlined. Symbols represent consensus sequence sites for N-linked glycosylation (⋆), and phosphorylation by protein kinase C (◆), protein kinase A (Ψ), and casein kinase II (∇).

exception of a substitution of R at the last position, present in the first intracellular loop; (G^{154}-K^{173}); EX_6R (E^{222}-R^{229}) in the fourth transmembrane domain and second intracellular loop; TIXXEWDLVC (T^{127}-C^{138}) is present in the second transmembrane domain, although it is disrupted by the insertion of serine and glutamine between glutamate and tryptophan; ELYPTL (E^{455}-V^{460}; substitution of V for terminal L) between transmembrane domains 10 and 11; and LPETL (L^{520}-I^{524} ; substitution of I for terminal L) after transmembrane domain 12. As mentioned earlier, the physiological significance of these motifs has yet to be elucidated.

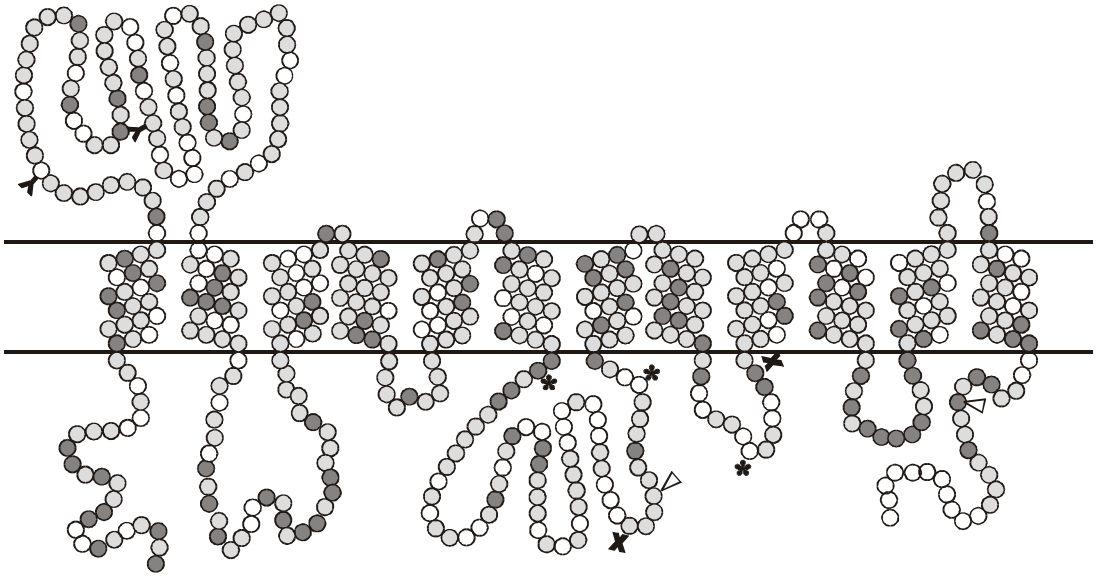

Figure 4.23: Model of the secondary structure of hOAT2. This model shows the secondary structure of hOAT2 as predicted by TopPred2, each circle representing an amino acid. Shaded residues are identical in hOAT2 and the rat OAT2. Darker shading represents those residues also identical in hROAT1. The consensus sites for enzymatic modification are also shown: **Y** = N-glycosylation, * = protein kinase C, **X** = protein kinase A, ∇= casein kinase II.

4.2.1.4 Comparison of hOAT2 with a human OAT2 homologue expressed in the liver

Subsequent to the cloning of hOAT2, a homology search revealed the presence of a second human NLT/rOAT2 homologue in the GenBank database. This clone, termed hNLT, was cloned from human liver cDNA and on the amino acid level is 100 % identical to the hOAT2 cloned in this study until position 528, after which the sequences are completely divergent. Furthermore, the high homology hOAT2 and hNLT to the rat OAT2 sequence ends at the same position. Comparing hOAT2 and hNLT with the rat OAT2 cDNA and genomic sequences predicts that the observed divergence corresponds to the last of 10 predicted exons. To determine whether hNLT is also expressed in the kidney, hNLT-specific primers corresponding to the beginning and end of the hNLT reading frame were used in a PCR with human kidney cDNA as template. Specific amplification using these primers was not observed, in contrast to the amplification of hOAT2 used as a positive control. From this PCR result, it appears that the hNLT is not expressed at detectable levels in human kidney, and as such hOAT2 and hNLT appear to represent kidney- and liver-specific transcripts of the same transporter.

4.2.1.5 Isolation of alternatively spliced hOAT2 transcripts

During amplification of hOAT2 using primers directed against the beginning and end of the predicted open reading frame, three distinct species of cDNA were amplified. In addition to the transcript encoding a predicted protein of 541 amino acids, termed hOAT2, two transcripts encoding shortened open reading frames were also amplified. These transcripts were named hOAT2-2 and hOAT2-3, and contain shortened reading frames encoding proteins of 295 and 271 amino acids, respectively. The differences in the length of the hOAT2-2 and hOAT2-3 open reading frames correspond to three changes on the nucleotide level. The hOAT2-2 transcript has deletions of nucleotides 394-399 and nucleotides 888-952. On the amino acid level, the first deletion corresponds to an in-frame deletion of two amino acids: S^{132} and Q^{133}. The second deletion results in a frame shift: a stop codon (nucleotides 956-958) is brought in frame. The hOAT2-3 transcript also contains these two deletions, but in addition contains an insertion of 116 nucleotides at position 652, which changes the derived amino acid sequence from this point. In both hOAT2-2 and hOAT2-3, translation of these transcripts is predicted to terminate following the second deletion. Comparing hOAT2-2 with the genomic sequence of the rat NLT/OAT2, known as TI-LTP (Simonson and Iwanij 1995), an approximation of the exon organization is obtained (see appendix). This comparison suggests that two internal deletions are a result of alternative splicing events. The first deletion appears to take place during the removal of intron 2, whereas the second deletion seems to be a partial deletion of exon 5 together with intron 5. The extra sequence in hOAT2-3 appears to originate from an unspliced intron between exons 3 and 4 (Appendix 2).

4.2.2 Heterologous expression of hOAT2 in Xenopus oocytes

4.2.2.1 Expression clone construction

To enable the in vitro transcription of hOAT2 cRNA, the hOAT2 open reading frame was subcloned into pSport between the fNaDC-3 5' and 3' UTRs, as detailed for hROAT1. The hOAT2 open reading frame was excised from the Zero Blunt II TOPO vector by double digestion with BamHI and XbaI, and ligated into the similarly restricted pSport::fNaDC-3-UTRs vector, creating a clone in which the hOAT2 open reading frame is flanked by the 5' and 3' UTRs of fNaDC-3.

4.2.2.2 Uptake experiments

The ability of hOAT2 to mediate the uptake of various radioactively-labelled substrates was tested in the *Xenopus laevis* oocyte expression system. As it had already been shown that the rat homologue, NLT/rOAT2, mediates the uptake of glutarate and alpha-ketoglutarate into oocytes, these substrates, as well as PAH, were used in uptake experiments with hOAT2-injected oocytes. As shown in figure 4.24, hOAT2 was not able to mediate uptake of the above mentioned substrates at levels significantly higher than those observed with control oocytes.

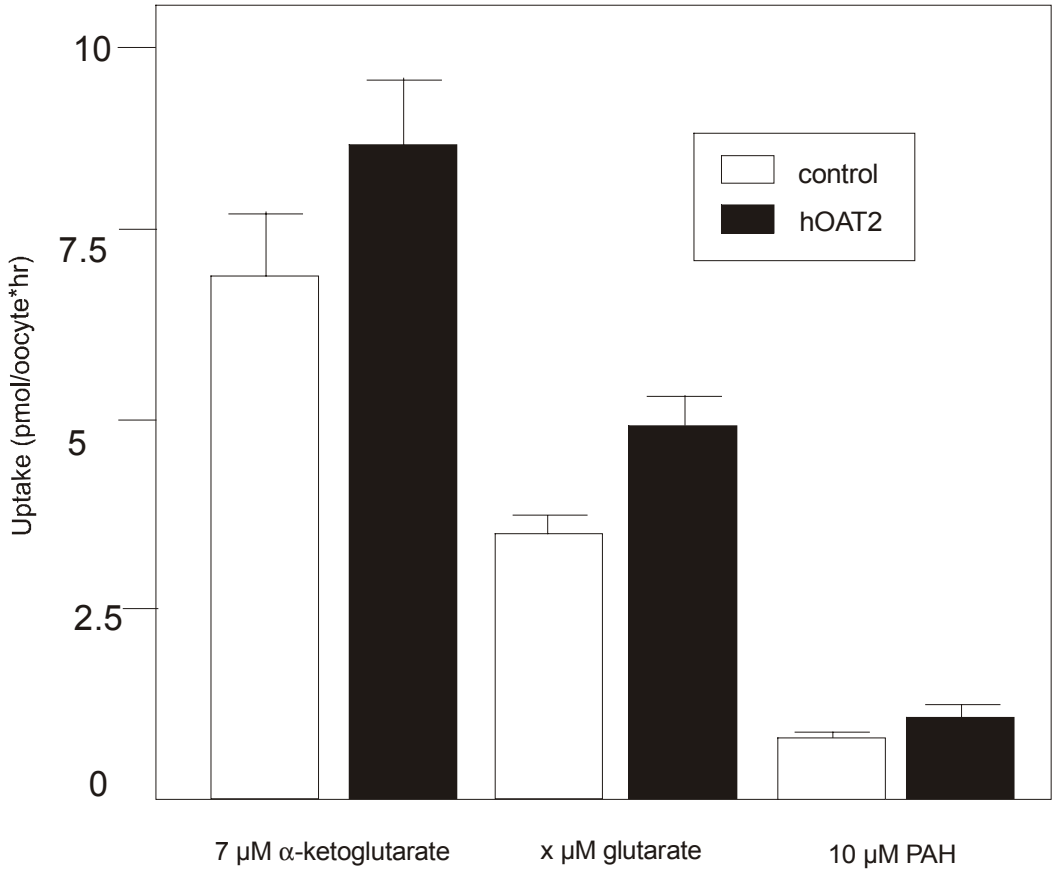

Figure 4.24: Uptake experiments with hOAT2. hOAT2-mediated uptake of a-ketoglutarate, glutarate and PAH into oocytes. The results shown are from a representative of 2 independent experiments, and values are mean +/- SE for 8-12 oocytes.

4.3 CONSTRUCTION OF AN hOAT2:hROAT1 CHIMERA

4.3.1 Chimera construction

Chimeric proteins can often provide insights into the location of functional domains of proteins. This approach has proved successful in the determination of the substrate-binding domains of, among others, MDR (Zhou et al 1999) and MRP (Stride et al 1999) multidrug resistance proteins, the sodium-sulfate and sodium-dicarboxylate cotransporters (Pajor et al 1998) and the sodium-dependent nucleoside transporters (Wang and Giacomini 1997). In an attempt to further characterize the functional domains of the OAT proteins isolated in this study, a chimera of hOAT2 and hROAT1 was constructed by the overlapping PCR technique described in section 3.1.2.6. The amplification product consisted of the first half of hOAT2 (nucleotides 1-831 of the coding region; amino acids M^{1}-P^{277}) fused to the second half of hROAT1 (nucleotides 811-1653 of the coding region; amino acids S^{271}-F^{550}), yielding a chimeric coding region of 1674 nucleotides encoding 558 amino acids. Based on TopPred 2 analysis, the chimera was predicted to contain the first six transmembrane domain of hOAT2 joined to the large internal loop and last six transmembrane domains of hROAT1 (see Figure 4.25).

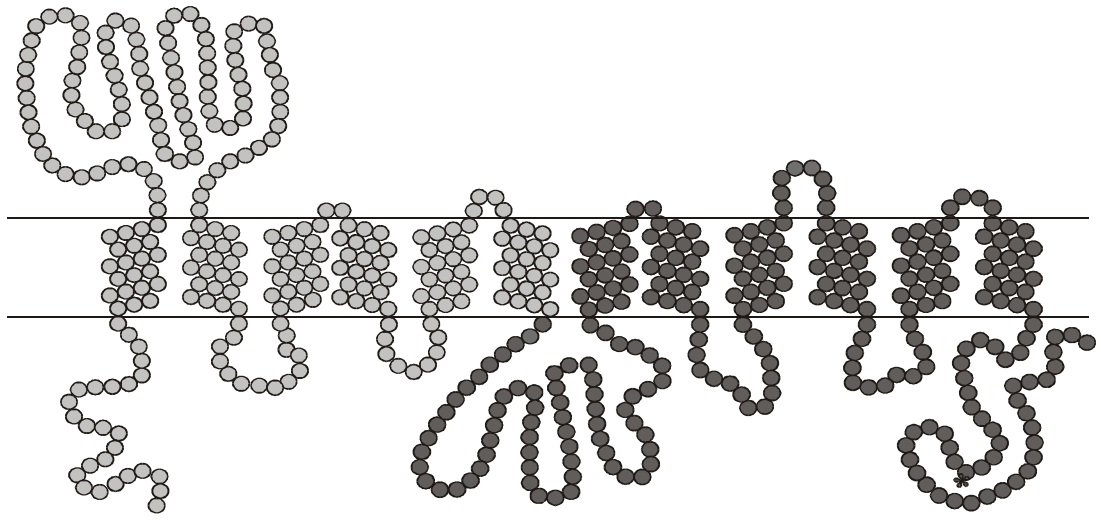

Figure 4.25 Predicted secondary structure of the hOAT2:hROAT1 chimera. The N-terminal part of the molecule (light shading) is derived from hOAT2, and is fused to the C-terminal half of hROAT1 (dark shading).

Analysis of the chimera itself predicted the same twelve transmembrane domains corresponding to those from each half (Figure 4.25). The ability of the hOAT2:hROAT1 chimera to mediate PAH uptake was tested in oocytes. Chimera-injected oocytes were unable to mediate uptake of PAH at levels significantly greater than those in control oocytes (1.53 ± 0.33 pmol / hour*oocyte vs 1.48± 0.25 pmol / hour*oocyte).

5 DISCUSSION

5.1 CLONING AND CHARACTERIZATION OF hROAT1

5.1.1 Cloning and analysis of an hROAT1 cDNA

A vast array of potentially toxic anions of both endogenous and exogenous origin are eliminated from the body by the multispecific organic anion transporting system located in the proximal tubule of the kidney. Shared by almost all vertebrates and invertebrates studied to date, the system consists of the well-defined uptake of the model organic anion PAH at the basolateral membrane in exchange for intracellular α-ketoglutarate. Since the advent of molecular biology and expression cloning techniques, the organic anion transporting system has come under increasing scrutiny.

In 1997, using the *Xenopus laevis* oocyte expression cloning system, cDNAs were isolated from rat (Sekine et al, Sweet et al) and flounder (Wolff et al) which mediated uptake of labeled PAH when expressed in oocytes. All satisfied the functional characteristics of the tertiary active basolateral step of organic anion transport and were named OAT1*. The major goal of this study was to clone and characterize a human homologue of the OAT1. The isolation of the rat and flounder clones, and a non-functional mouse clone, opened the possibility to clone a human OAT1 homologue using a degenerate PCR-based cloning strategy. Using this strategy, it was possible to amplify part of a human OAT1 reading frame, which was completed using RACE. The clone, which was named hROAT1 (human Renal Organic Anion Transporter) represents the first reported cloning of a human OAT1 homologue (Reid et al 1998).

The cloning of hROAT1, concisely reported here, posed a number of problems. Although it was hoped to bypass the labour intensive process of library construction and screening successfully employed to isolate the rat, mouse and flounder homologues, the degenerate PCR approach proved just as time consuming. Considering that the degenerate primers used in the successful amplification comprised a pool of at least 1500 distinct primers, necessitating the higher than normal primer concentration , and that the low annealing temperature gave a low stringency, the successful amplification was probably serendipitous.

* OAT1 is the generic name for the homologues of this transport protein in different species, which has been variously combined with a lower case initial designating the species of origin and occasionally R to denote renal. Isoforms have also been isolated and are represented by -1, -2 etc.

Following the publication of the hROAT1 sequence, four further reports of the cloning of a human OAT1 homologue appeared. Of these clones, hOAT1 (Race et al, 1999) and hPAHT (Lu et al, 1999) were generated by PCR techniques, and hOAT1-1 and 1-2 (Hosoyamada et al, 1999) and hOAT1 (Cihlar et al, 1999) were isolated from cDNA libraries. The sequences deposited in GenBank are greater than 99 % identical on the nucleotide level, and from the seven nucleotide differences, only two amino acid changes result – the serine at position 14 of hPAHT, and the phenylalanine at position 550 in hROAT1. Cihlar et al (1999) suggest that the differences are errors incorporated by the polymerase during PCR. This conclusion is supported by the observation that the open reading frame of their clone is 100 % identical to that of hOAT1-2, which was also isolated by screening a cDNA library (Hosoyamada et al, 1999). The purchase of the poly(A)$^+$ RNA used by each group in library construction from different companies also favours this argument. However, this does not rule out the possibility that the changes observed in hROAT1 result from genetic differences in the patient from which the poly(A)$^+$ RNA used in this study was isolated. This suggestion is based on the independent occurrence of the same three nucleotide changes in both the initial 3'RACE and the subsequent amplification of the full hROAT1 open reading frame. Furthermore, the two amino acid differences found in the PCR-generated clones do not result in a change in any sequence or motif that is absolutely conserved throughout the entire OAT family. Irrespective of the source of these sequence differences, it is apparent from the characterization of the different human OAT1s that these two differences in amino acid sequence do not have a noticeable effect on the function of the transporter.

The reported cloning of human OAT1 homologues by five independent groups and the continual appearance of new members of the OAT family, has lead to a certain confusion in the nomenclature of these proteins. The clone isolated in this study was named hROAT1 to coincide with the previously isolated rat and flounder clones, where R denotes renal expression of this protein. It has since been demonstrated by Northern blot and RT-PCR that the human OAT1 gene is also transcribed in a number of other tissues, including brain (Hosoyamada et al 1999, Race et al 1999) and placenta (Hosoyamada et al 1999). In addition, RT-PCR-derived sequences of four distinct OAT1 transcripts have now been published, which appear to result from alternative splicing events (Hosoyamada et al 1999, Bahn et al 2000). However, although the presence of mRNA isoforms can be detected by RT-PCR, this does not mean that such

transcripts are translated, nor does RT-PCR detect sequence differences in transcripts of similar length. Immunological evidence is required before it can be concluded that these alternative transcripts represent isoforms of the human OAT1 transporter.

5.1.2 Functional characterization of hROAT1

5.1.2.1 Functional clone construction

Using degenerate-PCR and RACE, it was possible to isolate the reading frame and 3'UTR of hROAT1. As functional characterization in the oocyte expression system also requires the 5'UTR, amplification of the hROAT1 5'UTR was carried out to complete this clone. Using primers based on conserved sequences in the rat and mouse 5' UTRs together with a primer specific for the hROAT1 reading frame, a product was amplified with 100 % identity to the hROAT1 reading frame in the 3'-terminal part of the sequence, strongly suggesting that this sequence was in fact the 5'UTR of hROAT1. This assumption was confirmed by comparison of the sequence with the subsequently isolated human OAT1 clones, listed in Table 4.2, which shows greater than 99 % identity between the 5'UTRs. These results make the inability to amplify a full-length cDNA using primers specific to the 5' and 3' UTRs difficult to understand. As it was possible to amplify 5' UTR sequence, this means that the initial RT-PCR successfully produced first-strand cDNAs corresponding to mature mRNAs. The reason for the inability to amplify a product corresponding to a mature mRNA is uncertain, but may have been due to either a degradation of the cDNA template resulting from repeated freeze/thaw cycles, or a lack of specificity of the primers employed in the attempted PCR-amplification.

In the second strategy used in an attempt to construct a functional clone, the *Xenopus*-specific pGEMHE vector was obtained with the goal of subcloning the hROAT1 reading frame between the β-globin UTRs contained within the vector. The use of this vector in particular, and *Xenopus*-specific UTRs in general, has been shown to improve the expression of mammalian cDNAs injected into oocytes (Liman et al 1994, Shih et al 1998). Despite several attempts, the hROAT1 open reading frame could not be subcloned into the pGEMHE vector, and the reasons for this remain unclear. As it was possible to subclone the rat OAT2 open reading frame into pGEMHE using exactly the same strategy, this is even more perplexing. Difficulties in modifying pGEMHE, such as dephosphorylation and linker addition, have been observed in similar applications

(FM Dautzenberg, pers. comm.). The construction of a functional expression clone was ultimately achieved by subcloning the hROAT1 coding region between the UTRs of the flounder sodium dicarboxylate cotransporter, fNaDC-3 (Steffgen et al 1999). This strategy yielded a clone that mediated PAH uptake when expressed in oocytes. The expression was apparently unaffected by the incorporation, immediately upstream from the start codon, of the *Bam*HI site used in the subcloning strategy. This results in a weakened context for translation initiation, as predicted by Kozak, with A and T at positions -3 and -4 (Kozak 1987). Comparison with the wild type cDNA as characterized by other groups suggests that the hROAT1 reading frame functions equally well in different UTR contexts. The fNaDC-3 UTRs may in fact improve the expression of mammalian cDNAs in oocytes, a suggestion based on assays involving a recently cloned rabbit OAT1 clone, rbOAT1 (Bahn et al 2000). In these assays, PAH uptake by a native rbOAT1 clone was approximately 20 % lower than uptake mediated by the open reading frame flanked by the fNaDC-3 UTRs (unpublished results).

5.1.2.2 PAH uptake mediated by hROAT1

The human OAT1 homologue, hROAT1, isolated in this study has functional characteristics of a renal basolateral organic anion/dicarboxylate exchanger. Expressed in oocytes, hROAT1 mediated PAH uptake with a calculated K_m of approximately 10 µM and was inhibitable by probenecid, the classical inhibitor of the system. Although PAH uptake by human basolateral membrane vesicles has been demonstrated, no K_m was determined. However, the K_m value is similar to the range of 14-70 µM reported for the OAT1s isolated from rat, mouse and flounder (Sekine et al 1997, Sweet et al 1997, Wolff et al 1997, Kuze et al 1999), and equivalent to that reported for other human OAT1 clones (Lu et al 1999, Hosoyamada et al 1999). The structural and functional similarity of hROAT1 to the previously cloned OAT1 homologues from rat and flounder, strongly suggests that it represents a human OAT1 homologue mediating organic anion uptake across the basolateral membrane in the human kidney.

The basolateral localization suggested by these functional characteristics is strongly supported by immunological studies of human and rat OAT1 clones. Hosoyamada and coworkers (1999) showed staining of the basolateral membrane of the proximal tubule with an antibody specific for a peptide corresponding to the terminal 14 amino acids of hOAT1. The rat OAT1 was also detected only at the basolateral membrane (Tojo et al

1999). Thus, hROAT1 has both the functional properties and membrane localization of a transporter involved in basolateral PAH uptake in proximal tubule cells.

5.1.2.3 Ion dependence of hROAT1-mediated PAH uptake

The hROAT1-mediated PAH uptake was investigated in a range of media with different ion composition to determine whether it was consistent with the previously determined ion dependence of the organic anion transporting system. Substitution of gluconate for chloride ions in the uptake medium inhibited hROAT1-mediated PAH uptake by 80 %, consistent with previous studies showing a requirement for chloride in basolateral PAH uptake. A study of PAH uptake by rat kidney basolateral membrane vesicles showed a chloride dependence which was sided, meaning that maximal stimulation occurred with chloride on the same side as PAH (Pritchard 1988). However, the nature of the chloride involvement is complex, as PAH uptake was not stimulated by an inwardly directed chloride gradient, nor was chloride cotransported with PAH (Pritchard 1988). Similar decreases in PAH uptake have also been demonstrated for the other human OAT clones when chloride was replaced by gluconate in the transport medium (Race et al 1999, Hosoyamada et al 1999). For hOAT1 cloned by Race and co-workers, replacing chloride with gluconate decreased PAH uptake by 80 % in hOAT1-injected oocytes which were first passively pre-loaded with glutarate (Race et al 1999). The longer human OAT1 splice-variant, hOAT1-1, also exhibited chloride dependence –in oocytes pre-incubated with glutarate, transport of PAH in medium containing gluconate instead of chloride was reduced by 90 % (Hosoyamada et al 1999). Although direct comparison of these results is hindered by the glutarate pre-treatment of the hOAT1- and hOAT1-1-injected oocytes prior to transport, and the use of the longer hOAT1-1 isoform by Hosoyamada and co-workers, the qualitative effect is same.

Previous studies on the influence of potassium on PAH uptake have shown that PAH/ α-ketoglutarate exchange is electroneutral. In bovine basolateral membrane vesicles, PAH/α-ketoglutarate was shown to have a stoichiometry of 1:1, and as PAH carries one negative charge and α-ketoglutarate carries two at physiological pH, this predicts the transfer of one negative charge (Schmitt and Burckhardt 1993). However, the process was found to be electroneutral as it was not stimulated by an inwardly directed potassium gradient, suggesting to the authors that perhaps either monovalent α-ketoglutarate is exchanged, or that an unknown anion or cation is cotransported (Schmitt and Burckhardt 1993). The effect of an inwardly directed potassium gradient

was also investigated in the characterization of the rat OAT1 (Sweet et al 1997). PAH uptake mediated by the rat OAT1 in oocytes was investigated in medium containing increased potassium concentration, which depolarizes the oocyte membrane (Gründemann et al, 1994). Under these conditions no change in rat OAT1-mediated PAH uptake was observed, consistent with the predicted electroneutral nature of PAH/α-ketoglutarate exchange. In light of these results the reason for the observed increase in PAH uptake into hROAT1-injected oocytes in the presence of an increased extracellular potassium concentration is unclear.

According to the accepted model for renal organic anion transport, basolateral PAH uptake has an indirect requirement for sodium in which the sodium gradient drives the basolateral uptake of dicarboxylates in the functionally coupled system (Shimada et al 1987, Pritchard et al 1987). As such, the observed 30 % decrease in PAH uptake into hROAT1-injected oocytes in medium where sodium ions were replaced with choline was unexpected. However, a similar, albeit lesser, reduction of PAH uptake after sodium replacement was reported for the rat OAT1 and the human hOAT1-1 (Sekine et al 1997, Hosoyamada et al 1999). PAH uptake in oocytes injected with the rat OAT1 decreased by approximately 15 % in sodium-free medium, whereas the hOAT1-1-mediated PAH uptake decreased by 10 % (Sekine et al 1997, Hosoyamada et al 1999). In the latter case, the oocytes were passively preloaded by overnight incubation in medium containing 1 mM glutarate (Hosoyamada et al 1999). In addition, Sekine and co-workers showed that passive glutarate uptake into non-injected control oocytes was decreased by half when sodium was replaced by choline (Sekine et al 1997). It has also been shown in studies of fROAT, ROAT1, and hOAT1 that passive glutarate loading of oocytes increases subsequent PAH uptake (Wolff et al 1997, Sweet et al 1997, Cihlar et al 1999). Taken together, these results could indicate that replacing sodium with choline leads to inhibition of an endogenous sodium/dicarboxylate cotransporter in the oocytes. Although the relative importance of re-uptake of exchanged dicarboxylates for transport of PAH by OAT1 in heterologous expression in oocytes is not certain, import of dicarboxylate back into the cells of rabbit proximal tubules has been calculated to contribute approximately 50 % of the dicarboxylate exchange partner for the uptake of the organic anion fluoresecein by this functionally coupled system (Welborn et al 2000). Removal of sodium could thus prevent recycling of exchanged α-ketoglutarate and slowly decrease the intracellular concentration available for continuing PAH uptake into the oocyte.

5.1.2.4 Cis-inhibition of hROAT1-mediated PAH uptake

Various organic anions were tested for the ability to cis-inhibit PAH transport by hROAT1. As hROAT1 is believed to be an organic anion/dicarboxylate exchanger, a range of dicarboxylates were tested for the ability to inhibit hROAT1-mediated PAH uptake. Significant inhibition of hROAT1-mediated PAH uptake was observed with glutarate, adipate, pimelate and suberate, consistent with the predicted model for a minimum charge separation required for inhibition of PAH transport (Ullrich 1997). This is also consistent with in situ inhibition of PAH transport in stopped flow capillary perfusion studies of rat proximal tubules; for unsubstituted dicarboxylates, cis-inhibition was moderate with succinate and stronger for all larger dicarboxylates tested (Ullrich et al 1987). In analysis of the rat OAT1 in oocytes, the inhibition spectrum was similar to the in vivo data with the exception that succinate did not inhibit PAH uptake (Uwai et al 1998). Furthermore, fROAT-mediated PAH uptake was only inhibited by unsubstituted dicarboxylates with a carbon backbone of five or more carbons (Wolff et al 1997).

Inhibition by intermediates of the TCA cycle was also investigated, in order to ascertain whether common physiological dicarboxylates interact with hROAT1. Of this group, only α-ketoglutarate significantly inhibited PAH uptake into hROAT1-injected oocytes. In contrast to the data of Ullrich and co-workers, PAH uptake into hROAT1-injected oocytes was not affected by fumarate (Ullrich et al 1987). Although the potential inhibition of the rat OAT1 by fumarate was not tested, fumarate did not inhibit fROAT-mediated PAH uptake (Wolff et al 1997). Of the aliphatic dicarboxylates tested with the isolated OAT1 clones, only citrate affects PAH uptake in a species-dependent manner. In contrast to its inability to inhibit hROAT1-mediated PAH uptake, citrate was shown to reduce PAH uptake by fROAT by 45 % (Wolff et al 1997). In general however, the inhibition by dicarboxylates of heterologously expressed OAT1 homologues corresponds to the previously obtained data from in situ studies.

Like PAH, urate is also transported in the proximal tubule, but the system does not show the same conservation between species as seen for PAH transport by OAT1. Transport steps are shared by these anions in some species but not others, and furthermore, urate is either reabsorbed or secreted depending on the species investigated (Pritchard and Miller 1993). In basolateral membrane vesicles from human kidney, urate transport was found to be electrogenic, and was not stimulated by α-ketoglutarate in the presence of an inwardly directed NaCl gradient, conditions which stimulated

PAH uptake, suggesting separate transport systems (Guisan and Roch-Ramel 1995). That urate only moderately inhibits hROAT1-mediated PAH transport is consistent with this report, and suggests that urate is not transported by hROAT1. In support of this, PAH uptake by the human OAT1 clone of Race and co-workers was not inhibited by urate, nor was urate transported by hOAT1 (Race et al 1999). In contrast, the longer human OAT1 isoform, hOAT1-1, was inhibited by over 90 %, although urate uptake was not reported (Hosoyamada et al 1999). As the concentrations of PAH and urate applied varied in these studies, direct comparison is difficult. Furthermore, PAH transport by the rat OAT1 was either inhibited (Sekine et al 1997) or unaffected (Sweet et al 1997) by urate. In the former study, urate was also transported at low levels, contradicting the findings in rat basolateral membrane vesicles, where urate uptake was not stimulated by an inwardly directed sodium gradient and α-ketoglutarate,. meaning it could not have been exchanged by the PAH transport system (Polkowski and Grassl 1993).

Another class of compounds, the lithocholic acid derivatives, were tested for the ability to inhibit the transport of PAH by hROAT1. Lithocholic acid is formed from the primary bile acid chenodeoxycholic acid by bacteria in the intestine (MacDonald et al 1983), and is metabolized in humans by conjugation to glycine and taurine in the liver (Palmer and Bolt 1971). Lithocholic acid and its conjugated derivatives are highly cholestatic in animals (van der Meer et al 1988), and although sulfation reduces the toxicity of taurolithocholic acid, it does not affect that of glycolithocholic acid (Dorvil et al 1983). Sulfation of these compounds, which increases polarity, takes place in the human liver (Kuiper et al 1985), and has been shown to increase renal excretion of glycolithocholic acid in rats (Palmer 1971). During cholestasis, hepatic uptake of bile acids is decreased to protect hepatocytes from their toxic effects (Trauner et al 1998), consistent with the increase in serum levels of sulfated lithocholates in children with cholestasis (Balistreri et al 1981). In addition, renal excretion of bile acids in patients with liver cirrhosis increases, and approximately 80 % of the these bile acids are sulfated (Stiehl et al 1975). Thus the potential involvement of hROAT1 in renal excretion of lithocholate derivatives was investigated by cis-inhibition studies. In hROAT1-injected oocytes, taurolithocholate slightly inhibited PAH uptake, and this effect was increased by sulfation, similar to the inhibition of fROAT-mediated PAH transport by these compounds (NA Wolff, pers. comm.) suggesting the possibility of transport by hROAT1. As intestinal reabsorption is not decreased by sulfation, which

lowers biliary excretion (van der Meer et al 1988), hROAT1 may be involved in the observed decrease in the toxicity of taurolithocholate following sulfation. In contrast, neither form of glycolithocholate inhibited hROAT1-mediated PAH uptake. This is consistent with the observations in healthy human probands, in which sulfation of glycolithocholate does not increase renal excretion (Cowen et al 1975).

The loop diuretics bumetanide and furosemide also inhibited hROAT1-mediated PAH uptake into oocytes, consistent with the inhibition of the rat OAT1 and human OAT1 isoform hOAT1-1 by furosemide (Sekine et al 1997, Hosoyamada et al 1999), and the inhibition of fROAT by bumetanide (Wolff et al 1997). The pharmacological effect of loop diuretics is the inhibition of the $Na^+/K^+/2Cl^-$ cotransporter in the luminal membrane of the ascending limb of the loop of Henle (Jackson 1996). As bumetanide and furosemide are extensively bound by plasma proteins yet efficiently cleared by the human kidney, they must be transported through the proximal tubule cell to reach their luminal site of action, and the human OAT1 has already been proposed to be the protein responsible (Jackson 1996, Hosoyamada et al 1999). Although this is supported by the fROAT-mediated bumetanide uptake reported in oocytes (Burckhardt et al 1999), in some species bumetanide and furosemide seem to be transported by different transporters. The excretion of furosemide and bumetanide in cats, where probenecid concentrations inhibiting PAH and furosemide clearance do not effect bumetanide clearance, suggests that furosemide, but not bumetanide, is a substrate of OAT1 (Friedman and Roch-Ramel 1977). In contrast, PAH excretion in dogs was slightly decreased by bumetanide, and the clearance of bumetanide itself was similar to that of PAH and was inhibited by probenecid (Østergaard et al 1972). Moreover, furosemide causes diuresis in rats and inhibits the rat OAT1 (Sekine et al 1997), whereas bumetanide has no diuretic effect and is almost completely metabolized (Østergaard et al 1972). When expressed in oocytes, hROAT1 did not stimulate uptake of labeled bumetanide suggesting that, like probenecid, bumetanide is a non-transportable inhibitor of hROAT1, and reaches the lumen via a system distinct from hROAT1. Whether furosemide is transported by hROAT1 awaits uptake studies with labeled furosemide.

5.1.3 Role of OAT1 in basolateral organic anion uptake

Based on its transport properties, OAT1 appears to have a major role in the basolateral uptake step of renal organic anion transport. Further evidence suggests that basolateral

uptake of organic anions is a more complex process than previously thought, and is mediated by a range of transporters with partly overlapping specificity. As well as the loop diuretics bumetanide and furosemide discussed above, the uricosuric drug probenecid also has a luminal site of action and is secreted by the proximal tubule cell, but it is not transported by OAT1; in rOAT1-injected oocytes, no rOAT1-specific uptake was detected by high performance liquid chromatography following incubation with probenecid (Uwai et al 1998). In addition, the OAT1 homologues from different species display varying spectra of substrate specificity. Expressed in oocytes, the rat OAT1 transports, in addition to PAH, dicarboxylates, urate, and low levels of cyclic nucleotides, folate and its analogue methotrexate, and prostaglandin E_2 (Sekine et al 1997). In contrast, the human OAT1 expressed in HeLa cells transported α-ketoglutarate, but was neither inhibited nor able to transport methotrexate or prostaglandin E_2 (Lu et al 1999), and did not transport urate when expressed in oocytes (Race et al 1999).

In addition to the endogenous substrates listed above, recent studies have demonstrated the transport of exogenous organic anions of diverse structure: β-lactams and non-steroidal anti-inflammatory drugs (NSAIDs) are transported by the rat OAT1 (Jariyawat et al 1999, Apiwattankul et al 1999), and nucleoside analogues are transported by both the rat and human OAT1 (Cihlar et al 1999). Salicylate, acetylsalicylate and indomethacin, are NSAIDs transported by the rat OAT1, shown in a study also demonstrating that OAT1 can act as hetero- and homoexchanger, as PAH efflux was stimulated by PAH, glutarate and NSAIDs (Apiwattankul et al 1999). These results suggest multispecificity of both the extracellular and intracellular substrate binding sites.

Adding to the complexity of renal organic anion transport, a number of recently cloned and/or characterized transporters exhibit low level organic anion transport, and have been added to the OAT subfamily of the organic cation transporter family. The OAT2 transporter (discussed in more detail in section 5.2) cloned from rat liver, is also found in the human liver, and is expressed in the kidney of both species (Simonson et al 1994, Sekine et al, 1998b, author's own unpublished results). The more recently characterized OAT3 from the rat is also expressed in the human kidney, but the human form has yet to be characterized (Kusuhara et al 1999, Race et al 1999). A further member, OAT4, was cloned from human kidney and is also expressed in the placenta (Cha et al 2000).

These OAT proteins also interact with a diverse range of anionic substrates, although the driving force for these proteins has yet to be elucidated (Cha et al 2000); none has been shown to function by an exchange mechanism similar to OAT1. In addition to these transporters, two as yet uncharacterized cDNAs were isolated from the kidney: RST from the mouse (Mori et al 1997) and UST1 from the rat (Schömig et al 1998). These show 49 and 39 % identity to hROAT1, respectively, and are considered members of the OAT family (Sekine et al 2000). The potential involvement of these transporters in basolateral uptake of organic anions in the kidney, however, awaits studies of their subcellular localization, and in some cases function.

5.1.4 Mutational analysis of hROAT1

5.1.4.1 Site-directed mutagenesis

Mutational analysis of hROAT1 was undertaken with the aim of defining regions essential for PAH transport. As previous studies have shown that acidic residues are involved in the translocation of organic cations by a variety of transporters (Pourcher et al 1993, Merickel et al 1995), it is possible that basic residues play a role in interaction between the organic anion transporters and their substrates. Comparing the known members of the organic anion-transporting OATs with the organic cation-transporting OCTs, it became apparent that three positively charged residues conserved in all OATs are negatively charged or neutral in OCTs. The positively charged residues at positions 34 (histidine), 382 (lysine) and 466 (arginine) in hROAT1 align with isoleucine (neutral), alanine (neutral) and aspartate (positive) residues found at the corresponding positions in all OCTs. When these specific lysine and arginine residues in the fROAT were mutated to alanine and aspartate, respectively, PAH transport was reduced by approximately 90 %, suggesting an involvement of these residues in the interaction of fROAT with PAH (Wolff et al 2000). Futhermore, mutation of the arginine residue changed the affinity of the transporter for PAH, and after both mutations, glutarate no longer inhibited PAH uptake (Wolff et al 2000). For this reason, lysine at position 382 and arginine at position 466 in hROAT1 were chosen for further study.

Following site-directed mutagenesis of lysine 382 to alanine and arginine 466 to aspartate, the corresponding residues conserved in all OCTs, total abolition of PAH uptake was observed. This result suggests an involvement of these residues in the interaction of hROAT1 with PAH. However, such a conclusion must be treated with

caution. The major problem with this assumption is lack of evidence for the proper targeting of these hROAT1 mutants to the plasma membrane. Such a demonstration requires immunological evidence, usually obtained via antibody detection of the protein at the membrane, using either protein-specific antibodies or insertion of an epitope tag within the reading frame in conjunction with tag-specific antibodies (Shih et al 1998). Unfortunately, an antibody synthesized against a region of the large extracellular loop of hROAT1 detected multiple bands in solubilized native plasma membrane vesicles, and thus did not have the hoped for specificity (N. A. Wolff, pers. comm.). Any definitive conclusions as to the effect of these point mutations on hROAT1 function await immunological proof of their appearance in the plasma membrane.

Despite the lack of immunological proof for correct routing of the K382A and R466D hROAT1 mutants to the membrane, there is some evidence to suggest that they represent non-functional transporters localized in the membrane. A similar analysis of fROAT, in which the same conserved residues were mutated, also lead to disruption of fROAT function (Wolff et al 2000), and these mutants appear to be properly targeted to the membrane (NA Wolff, pers. comm.). However, the oocytes injected with the fROAT mutants were still able to transport PAH at levels significantly greater than those observed in control oocytes. The overall effect of these mutations was to decrease the rate of PAH uptake by more than 90 %, from ~35 to ~3 pmol/oocyte*hr. In the case of the hROAT1 mutants, such a decrease in PAH uptake would show no significant difference to that of control oocytes.

Similar results were observed in a study of the rat OCT1, in which the conserved aspartate residue at position 475 was mutated to a basic residue (Gorboulev et al 1999). These mutants, when expressed in the HEK 293 cell line, were detected at the plasma membrane. In this study, V_{max} values for the transport of various organic cations were decreased by 89-98 %. However, the high original values of transport mediated by wild-type rOCT1 meant that uptake by mutant-expressing cells, although greatly reduced, was still significantly higher than controls. As such, expression of the K382A and R466D mutants in an appropriate cell line may provide more meaningful results. In preliminary results with transiently transfected COS-7 cells for example, hROAT1 mediated PAH uptake at levels more than 100-fold over that obtained in cells transfected with vector only (authors own observations). Using this expression system

it may be possible to observe function of these mutants that is beyond detection in oocytes, which would in turn be complemented by immunological studies.

5.1.4.2 Deletion mutants

In addition to the point mutations discussed above, deletion mutants of hROAT1 were also created. An N-terminal deletion mutant was constructed to resemble rOCT1A, an alternatively spliced isoform of the rat organic cation transporter rOCT1 that was shown to mediate organic cation transport despite the predicted loss of the first two transmembrane domains (Zhang et al 1997). In contrast to the retention of function by rOCT1A, this shortened hROAT1 mutant was unable to mediate PAH uptake when expressed in oocytes. As discussed previously for the two hROAT1 point mutants, it is not certain that the shortened hROAT1 cRNA directed the synthesis of a polypeptide that was correctly inserted into the plasma membrane of the oocyte. Also, rOCT1A is a splice variant rather than a simple deletion mutant. Translation of rOCT1A is predicted to begin in an alternate reading frame before returning to the reading frame that it shares with rOCT1 following the splicing event linking exons 1 and 2 (Zhang et al 1997). Thus, the initial 46 amino acids of rOCT1A show no homology to rOCT1, and therefore rOCT1A is not simply a deletion mutant. If a similar removal of exon 2 from the hROAT1 reading frame occurred, it would yield a shortened protein due to an in frame stop codon, with no homology to hROAT1 following the splicing event. Further investigation of the role in transport of the N-terminal part of hROAT1 awaits the ability to detect such mutants in the membrane.

As mentioned earlier, the expression of four distinct transcripts from the human OAT1 gene has been detected in the kidney. All four appear to be generated by alternative splicing events involving exons 9 and 10. To determine whether these exons contain regions essential to the transport process, two C-terminal deletion mutants were constructed in which either exon 10 alone (terminal 28 amino acids) or exons 9 and 10 together (terminal 97 amino acids) were removed. Following removal of both exons 9 and 10, hROAT1 was no longer able to mediate PAH uptake. Once more, it is not certain whether this mutant reaches the membrane. If correct membrane insertion is assumed, the lack of function is not surprising as this region contains the conserved arginine at position 466 that appears to be involved in the transport process, and suggests that the first eight exons do not encode a polypeptide capable of mediating

PAH transport. Again, further investigation of this mutant requires the ability to detect its presence in the membrane.

The deletion from hROAT1 of exon 10 alone was more interesting. This manipulation resulted in a two-fold increase in PAH uptake, strongly suggesting that this mutant reaches the membrane. The intracellular location of the C-terminal 26 amino acids encoded by exon 10 would suggest that they are not involved in substrate binding, and exon 10 is also the least conserved between members of the OAT family. Although conclusions concerning the molecular basis of this effect require further investigation, the increased transport of PAH by removal of exon 10 may be due a disruption in the post-translational regulation of hROAT1. The amino acid sequences of the OAT1 homologues from all species contain consensus sites for phosphorylation by several protein kinases. Protein kinase-mediated down-regulation of the organic anion transporting system has been documented in a variety of systems (Roch-Ramel 1998). For example, recent studies have shown that activation of PKC leads to down-regulation of PAH transport by the human and rat OAT1 homologues (Lu et al 1999, Uwai et al 1998). The presence of PKC consensus sites in the cloned OAT1 homologues has lead to the suggestion that PKC-dependent OAT1 down-regulation results from direct phosphorylation (Uwai et al 1998).

The mechanism responsible for this effect, however, has yet to be elucidated. Although phosphorylation of the mouse OAT1 homologue at serine residues does occur, as evidenced by an increased phosphorylation state following inhibition of protein phosphatase by okadaic acid, direct phosphorylation of the mouse OAT1 homologue by PKC was not observed (You et al 2000). In any case, exon 10 does not encode consensus sites for phosphorylation by PKC, suggesting that the effect of deleting exon 10 is not related to a change in PKC-dependent phosphorylation. A consensus site for tyrosine kinase (TK) is found in this region, but the activation of this kinase showed no effect on hOAT1-mediated PAH uptake in transiently-transfected cells (Lu et al 1999). Furthermore, inhibition of TK in isolated S2 segments of the rabbit proximal tubule lead to a decrease of 25 % in PAH uptake (Gabriëls et al 1999). Neither of these observations correspond to the effect of deleting exon 10 from hROAT1, suggesting that the mechanism responsible is also unrelated to phosphorylation involving TK. The study by Gabriëls and co-workers also showed that inhibition of phosphatidylinositol 3-kinase (PI3K) and mitogen-activated protein kinase (MAPK) decreased PAH uptake by

20-30 %, however, the hROAT1 amino acid sequence contains no predicted consensus sites for phosphorylation by these kinases.

Also present in exon 10 is a consensus site for casein kinase II (CKII)-dependent phosphorylation, found in all members of the OAT family (Sweet and Pritchard 1999). The major roles of this kinase appear to be in signal transduction and regulation of the cell cycle. A recent review of the literature suggests that a role for CKII in the regulation of renal organic anion transport has not been investigated. Interestingly, CKII has been shown to phosphorylate the vesicular monoamine transporter VMAT2, a monoamine neurotransmitter transporter found in the rat brain (Krantz et al 1997). This phosphorylation occurs at sites near the end of the C-terminus, similar to the location of the CKII site found within the exon 10-encoded C-terminus of hROAT1, and is abrogated by mutation of the serine residues in the casein kinase II consensus sequence. In contrast, the related monoamine transporter VMAT1, which displays different subcellular localization, is not phosphorylated at the C-terminus by CKII (Krantz et al 1997). Furthermore, phosphorylation by CKII has been demonstrated to change the intracellular location of the endoprotease furin (Takahashi et al 1995). Although the effect of CKII-dependent phosphorylation on the transport properties of VMAT2 has yet to be determined, it would be of interest to investigate whether mutation of the CKII site in the tenth exon of hROAT1 and/or specific inhibition of CKII have the same effect on transport as complete deletion of exon 10. This would raise the possibility that CKII is responsible for the observed phosphorylation of mOAT1 at serine residues, as mOAT1 also has a CKII site at the C-terminal end.

5.2 CLONING OF hOAT2

5.2.1 Cloning and expression of an OAT2 homologue from human kidney

In comparison with the active basolateral uptake of organic anions, efflux at the luminal membrane is poorly understood. There are several possible reasons for this discrepancy. Whereas a highly conserved system couples organic anion uptake to the sodium gradient at the basolateral membrane, such conservation is not observed in luminal efflux in which urate-secreting and urate-reabsorbing species differ. Furthermore, the high intracellular accumulation of organic anions in proximal tubule cells suggests that the luminal system has low affinity for transported substrates.

Isolation of proteins involved in luminal efflux using expression cloning is hindered by the lack of a sensitive assay that is not masked by OAT1-mediated PAH uptake, and in addition, both systems are inhibited by probenecid.

As mentioned in previous sections, a number of recently cloned and characterized transporters are related to OAT1 on the sequence level. One of these, NLT, was initially cloned from rat liver, but no function could be demonstrated (Simonson et al 1994). NLT was later characterized as an organic anion transporter, and consequently renamed rOAT2 (Sekine et al 1998). Expressed in oocytes, rOAT2 mediated low affinity PAH transport and could not be trans-stimulated by dicarboxylates, properties consistent with one of the luminal efflux systems for PAH observed in brush border membrane vesicles (Roch-Ramel 1998). Northern blot analysis revealed highest levels of expression in the liver with lower levels present in the kidney (Simonson et al 1994, Sekine et al 1998). To investigate the possibility that an OAT2 homologue has a role in the luminal efflux step of organic anion transport, it was first determined whether an OAT2 homologue is expressed in the human kidney.

The expression of a human OAT2 homologue in human kidney was demonstrated using an EST-based cloning strategy, and lead to the isolation of a cDNA encoding a 541 amino acid protein that was named hOAT2. This cDNA sequence was deposited in GeneBank with the accession number AF210455, and is the first evidence for the presence of an OAT2 homologue in the human kidney. Following subcloning of the open reading frame between the fNaDC-3 UTRs, the ability of hOAT2 to mediate the transport of organic anions was tested in oocytes. Uptake of PAH, glutarate or α-ketoglutarate was not enhanced in oocytes injected with hOAT2, in contrast to the results obtained for the rOAT2 for which PAH and α-ketoglutarate uptake was demonstrated (Sekine et al 1998). There are several possible explanations for this discrepancy. Firstly, the affinity of the human and rat OAT2 clones for the substrates tested may not be identical. Such a difference was also observed for the uptake of nucleoside analogues by the human and rat OAT1 homologues. The calculated K_m values of the rat OAT1 for cidofovir and adefovir are 6 and 9 times greater, respectively, than those of the human OAT1 (Cihlar et al 1999). In addition, unlike the expression cloning strategy used to clone the OAT1 homologues, NLT was originally cloned by immunological screening of an expression library to identify clones recognized by a monoclonal antibody specific for a hepatocyte membrane protein

(Simonson et al 1994). The cDNAs encoding UST1 and RST from rat and mouse kidney, respectively, were also identified by sequence-based cloning strategies rather than expression cloning, and have yet to be functionally characterized (Schömig et al 1998, Mori et al 1997). The advantage of the expression cloning approach is that a suitable substrate for the transporter is already known. In the case of hOAT2, a high affinity substrate has yet to be identified.

Another possible explanation for the inability of hOAT2 to mediate transport of the organic anions tested is the disruption of the TIXXEWDLVC motif in the second transmembrane domain. This motif is common to members of the ASF subfamily of the major facilitator superfamily, and is present in the sequences of all OATs isolated to date (Schömig et al 1998, personal observation). In the reading frames of hOAT2 and hNLT this motif is interrupted by the insertion of serine and glutamine between the glutamate and tryptophan residues. The importance of the conserved ASF motifs for the structure and/or function of these transporters has yet to be investigated, but it is of interest to note that the reading frame of rOAT2, the only functionally characterized OAT2 to date, does contain this sequence perturbance (Simonson et al 1994, Sekine et al 1998).

Three distinct hOAT2 transcripts of similar size were isolated from human kidney cDNA, with predicted open reading frames encoding 541, 295 and 271 amino acids, respectively. These transcripts appear to be the result of alternative splicing events. The synthesis of alternatively spliced transcripts has previously been reported for the human and rat OAT1 genes (Hosoyamada et al 1999, Bahn et al 2000, Jariyawat et al 1999), and the related rat OCT1 (Zhang et al 1997). Furthermore, a transcript very similar to the human OAT3 cloned by Race and co-workers recently appeared in the GenBank database. From comparison of the two OAT3 nucleotide sequences, they also appear to be splice variants generated from the same gene, although confirmation of this suggestion awaits genomic characterization of the OAT3 gene. In all of these examples, the size of the reading frame remains relatively constant in contrast to the dramatic shortening of the hOAT2 reading frame. The characterization of the function, if any, of these shorter reading frames awaits the identification of a suitable substrate for hOAT2 with which to compare all three isoforms, and demonstration of the synthesis of the respective proteins in vivo.

5.2.2 Comparison of hOAT2 with a liver-specific OAT2 homologue

As detailed in the results, the initial amplification of a human OAT2 sequence was carried out with a liver cDNA template, and was then cloned in its entirety from human kidney cDNA. This was done to maximize the chance of amplifying an OAT2 homologue, since it was previously shown in the rat that OAT2 is expressed at higher levels in the liver than in the kidney (Simonson et al 1994, Sekine et al 1998). Similar to the difficulties reported for hROAT1, it was not possible to amplify the remainder of the OAT2 reading frame from the same liver cDNA template using the RACE technique. Again, this result is probably due to degradation of the template, as amplification of a GAPDH internal standard was also unsuccessful in subsequent PCRs. Shortly after the isolation of the OAT2 sequence from human kidney, a second OAT2 homologue, termed hNLT, appeared in the GenBank database. The sequence represents a full OAT2 open reading frame from human liver, and is identical on both nucleotide and amino acid level to kidney-derived hOAT2 until the predicted start of exon 10, after which both sequences are fully divergent, predicting proteins with non-homologous C-termini. The perfect homology between the first nine exons of the two nucleotide sequences and the inability to amplify the hNLT transcript from human kidney, suggests that hNLT is a liver-specific alternative transcript from the same gene.

Divergence in exon 10 sequence, in comparison to the overall homology of the human and rat OAT2 clones, is consistent with analysis of sequence data from OAT1 homologues, in which exon 10 is also the least conserved between species. However, there is no precedence for the difference in sequence between two OAT cDNAs isolated from different tissues of the same species. The four human OAT1 isoforms isolated to date all originate from the kidney (Hosoyamada et al 1999, Bahn et al 2000). Human OAT1 has also been detected by Northern blots in placenta and brain (Hosoyamada et al 1999) and by RT-PCR in pancreas, eye and brain (A Bahn pers. comm.), but possible tissue-specific sequence differences have yet to be investigated. Interestingly, the amino acid sequences of the C-termini of hOAT2, hNLT and rOAT2 differ with respect to the protein kinase sites they encode. Casein kinase II (CKII) sites present in the C-termini of hNLT and rOAT2 (Simonson et al 1994), both isolated from the liver, are absent from the C-terminus of hOAT2. As discussed previously, CKII phosphorylates the serine residues in the C-terminus of the monoamine transporter VMAT2, but does not phosphorylate the C-terminus of the related VMAT1 (Krantz et al 1997).

Furthermore, these proteins exhibit different subcellular localization and phosphorylation has been implicated in this process. Thus, the involvement of alternative tissue-specific C-termini in regulation of the human OAT2 is an attractive hypothesis that requires further investigation.

5.2.3 Apical proteins mediating organic anion transport

As discussed earlier in this section, the ultimate goal of cloning hOAT2 to assess a possible role in luminal efflux of organic anions from the proximal tubule cell, must await functional characterization as well as studies of the subcellular localization in the kidney. Interestingly, NPT1 and MRP2, two transporters localized to the luminal membrane in the proximal tubule cells, have recently been shown to transport PAH (Uchino et al 2000, Leier et al 2000). NPT1was initially cloned and characterized as a sodium-dependent inorganic phosphate transporter (Miyamoto et al 1995). PAH transport mediated by NPT1 was shown to be of low affinity, with a K_m of 2.66 mM, and was influenced by chloride ions and pH. The effect of increasing chloride concentration was a decrease in PAH uptake, consistent with the proposed in vivo efflux of PAH in the presence of an inwardly directed chloride gradient (Uchino et al 2000). MRP2 is a multidrug resistance protein which is located apically in polarized cells (Schaub et al 1997). In membrane vesicles derived from HEK293 cells expressing MRP2, ATP-dependent PAH transport took place, with a calculated K_m of 880 μM (Leier et al 2000). Furthermore, this transport was inhibited by the mycotoxin ochratoxin A, which itself was shown to be transported by MRP2 (Leier et al 2000). Interestingly, based on its substrate specificity and apical localization, several authors have previously proposed a role for MRP2 in luminal efflux of the nephrotoxic nucleoside analogues and β-lactams (Cihlar et al 1999, Jariyawat et al 1999). Transport of PAH by NPT1 and MRP2, therefore, represents the first reports of PAH transport by proteins located in the luminal membrane of proximal tubule cells, although their role in vivo awaits further investigation.

5.3 CONSTRUCTION OF AN hROAT1: hOAT2 CHIMERA

A chimera consisting of the N-terminal half of hOAT2 fused to the C-terminal half of hROAT1 was constructed. The rational for creating this chimeric protein was based on evidence from studies of related transporters suggesting that the C-terminal half of these

proteins may have a significant role in the transport process. Firstly, the C-terminal half of hROAT1 contains two of the three positively charged residues conserved in all OATs and negatively charged or neutral in OCTs. As discussed previously, the conserved lysine and arginine residues in the eighth and eleventh transmembrane domains, respectively, appear to be involved in substrate interaction based on mutagenesis studies in fROAT (Wolff et al 2000). Further support for this suggestion comes from a study of rOCT1A, an isoform of the rat organic cation transporter rOCT1 (Zhang et al 1997). In this study, an artificially shortened reading frame was constructed that corresponded to one of the three possible reading frames of the rOCT1A cDNA. This reading frame, termed Pro3, was predicted to encode a 354 amino acid protein resembling rOCT1 without the first 202 amino acids encoded by the rOCT1 cDNA, corresponding to the first three transmembrane domains (Zhang et al 1997). When expressed in oocytes, Pro3 not only mediated organic cation uptake, but did so at levels almost twice those mediated by rOCT1 itself (Zhang et al 1997). It was therefore hoped that fusing the N-terminal half of hOAT2 to the C-terminal half of hROAT1 may produce a functional transporter.

When expressed in oocytes, the hOAT2:hROAT1 chimera was not able to mediate PAH uptake. Whether this results from an inherent lack of function of the chimera, or failure to reach the membrane remains to be elucidated. If found to be non-functional at the membrane, it may be that the parent transporters are too functionally distinct to yield functional chimeric proteins. Although many functional chimera have been constructed from related transport proteins providing insights into the location of functional domains and substrate binding sites, these have tended to be more closely related on either the functional or structural level. For example, functional chimera were generated from N1 and N2 type Na^+-dependent nucleoside transporters. These transporters have different substrate specificities (purine and pyrimidine selective, respectively) but both transport their respective substrate via cotransport with sodium and are structurally similar (Wang and Giacomini 1997). Chimera between the rabbit Na^+/dicarboxylate transporter from the rabbit and the Na^+/sulfate transporter of the rat, which have only 43 % sequence identity, were nevertheless functional, probably because the respective substrates are similarly cotransported with sodium (Pajor et al 1998).

5.4 OUTLOOK

The human OAT1 homologue cloned and functionally characterized in this study is probably involved in the uptake of organic anions at the basolateral membrane during the excretion process. The potential involvement of the human OAT2 homologue awaits functional characterization, which in turn requires the identification of a well-transported substrate for this transporter. The hROAT1 point mutants may be useful in further studies to determine regions of the transporter important for its multiple specificity. Using the overlapping PCR technique, further chimera between hROAT1 and hOAT2 could be constructed to aid this approach. It may be possible to better characterize these mutants by expression in a mammalian system, for example the COS-7 cell line. Epitope tagging of mutants and chimera will facilitate immunological studies to determine whether the mutants are correctly targeted to the membrane. Characterization of the hROAT1 deletion mutants suggest a possible regulatory role of the C-terminus encoded by exon 10. This exon also appears to have a tissue specific expression in hOAT2. Further mutational studies are needed to clarify the possible regulatory role of the C-termini of both transporters.

6 REFERENCES

Apiwattanakul N, Sekine T, Chairoungdua A, Kanai Y, Nakajima N, Sophasan S and Endou H (1999) Transport properties of nonsteroidal anti-inflammatory drugs by organic anion transporter 1 expressed in *Xenopus laevis* oocytes. *Mol Pharmacol* **55:**847-854.

Aronson PS (1989) The renal proximal tubule: a model for diversity of anion exchangers and stilbene-sensitive anion transporters. *Annu Rev Physiol* **5**:419-441.

Bahn A, Pravitt D, Enklaar T, Reid G, Wolff NA and Burckhardt G (2000) Genomic cloning and characterization of the human renal organic anion transporter gene (hOAT1). *FASEB J* **14**:A106.

Balistreri WF, Suchy FJ, Farrell MK and Heubi JE (1981) Pathologic versus physiologic cholestasis: elevated serum concentration of a secondary bile acid in the presence of hepatobiliary disease. *J Pediatr* **98**:399-402.

Berner W and Kinne R (1976) Transport of p-aminohippuric acid by plasma membrane vesicles isolated from rat kidney cortex. *Pflüg Arch* **361**:269-277.

Boyd TA and Goldstein L (1979) Kidney metabolite levels and ammonium production in acute acid-base alterations in the rat. *Am J Physiol* **236**:E289-E294.

Burckhardt BC, Wolff NA and Burckhardt G (1999) Electrophysiologic characterization of an organic anion transporter cloned from winter flounder kidney (fROAT). *J Am Soc Physiol* **11**:9-17.

Cha SH, Sekine T, Kusuhara H, Yu E, Kim JY, Kim DK, Sugiyama Y, Kanai Y and Endou H (2000) Molecular cloning and characterization of multispecific anion transporter 4 expressed in the placenta. *J Biol Chem* **275**:4507-4512.

Chambers R and Kempton RT (1933) Indications of function of the chick mesonephros in tissue culture and phenol red. *J Cell Comp Physiol* **6**:131-160.

Chatsudthipong V and Dantzler WH (1991) PAH/α-KG countertransport stimulates PAH uptake and net secretion in isolated snake renal tubules. *Am J Physiol* **261**:F858-F867.

Chatsudthipong V and Dantzler WH (1992) PAH/α-KG countertransport stimulates PAH uptake and net secretion in isolated rabbit renal tubules. *Am J Physiol* **263**:F384-F391.

Cihlar T, Lin DC, Pritchard JB, Fuller MD, Mendel DB and Sweet DH (1999) The antiviral nucleotide analogs cidofovir and adefovir are novel substrates for human and rat renal organic anion transporter 1. *Mol Pharmacol* **56**:570-580.

Cortney MA, Mylle M, Lassiter WE and Gottschalk CW (1965) Renal tubular transport of water, solute and PAH in rats loaded with isotonic saline. *Am J Physiol* **209**:1199-1205.

Cowen AE, Korman MG, Hofmann AF and Cass OW (1975) Metabolism of lithocholate in healthy man. I. Biotransformation and biliary excretion of intravenously administered lithocholate, lithocholylglycine and their sulfates. *Gastroenterology* **69**:59-66.

Crawford JM and Gollan JL (1991) Transcellular transport of organic anions in hepatocytes: still a long way to go. *Hepatology* **14**:192-197.

Dantzler WH (1974) PAH transport by snake proximal renal tubules: differences from urate transport. *Am J Physiol* **226**:634-641.

Dantzler WH (1989) Organic acid (or anion) and organic base (or cation) transport by renal tubules of nonmammalian vertebrates. *J Exp Zool* **249**:247-257

Dantzler WH and Wright SH (1997) Renal tubular secretion of organic anions. *Advan Drug Delivery Rev* **25**:217-230.

Dorvil NP, Yousef IM, Tuchweber B and Roy CC (1983) Taurine prevents cholestasis induced by lithocholic acid sulfate in guinea pigs. *Am J Clin Nutr* **37**:221-232.

Endou H (1998) Recent advances in molecular mechanisms of nephrotoxicity. *Toxicol Lett* **102-103**:29-33

Eveloff J, Kinne R and Kinter WB (1979) p-Aminohippuric acid transport in brush border vesicles isolated from flounder kidney. *Am J Physiol* **237**:F291-F298.

Eveloff J (1987) *p*-Aminohippurate transport in basal-lateral membrane vesicles from rabbit renal cortex: stimulation by pH and sodium gradients. *Biochim Biophys Acta* **897**:474-480.

Friedman PA and Roch-Ramel F (1977) Hemodynamic and natriuretic effects of bumetanide and furosemide in the cat. *J Pharmacol Exp Ther* **203**:82-91.

Frohman MA, Dush MK, Martin GR (1988) Rapid production of full-length cDNAs from rare transcripts. Amplification using a single gene-specific oligonucleotide primer. *Proc Nat Acad Sci USA* **85**:8998-9002.

Forster RP (1948) Use of thin kidney slices and isolated renal tubules for the study of cellular transport kinetics. *Science* **108**:65-67.

Gabriëls G, Werners A, Mauss S and Greven J (1999) Evidence for differential regulation of renal proximal tubular *p*-aminohippurate and sodium-dependent dicarboxylate transport. *J Pharmacol Exp Ther* **290**:710-715.

Gemba M, Kawaguchi M, Konishi S, Nakanishi J and Matsushima Y (1983) Inhibition of *p*-aminohippurate transport by cycli GMP in rat kidney cortical slices. *J Pharmacobio-Dyn* **6**:621-626.

Gorboulev V, Volk C, Arndt P, Akhoundova A and Koepsell H (1999) Selectivity of the polyspecific cation transporter rOCT1 is changed by mutation of aspartate 475 to glutamate. *Mol Pharmacol* **56**:1254-1261.

Gründemann D, Gorboulev V, Gambaryan M and Koepsell H (1994) Drug excretion mediated by a new prototype of polyspecific transporter. *Nature* **372**:549-552

Guisan and Roch-Ramel (1995) Urate and *p*-aminohippurate transport by human basolateral membrane vesicles (BLMV) of proximal tubules. *Experentia* **53**:A93.

Hosoyamada M, Sekine T, Kanai Y and Endou H (1999) Molecular cloning and functional expression of a multispecific organic anion transporter from human kidney. *Am J Physiol* **276**:F122-F128.

Irish JM III (1979) Secretion of prostaglandin E2 by rabbit proximal tubules. *Am J Physiol* **237**:F268-F273.

Ishii T, Zerr P, Xia X-M, Bond CT, Maylie J and Adelmann JP (1998) Site-directed mutagenesis. *Methods Enzymol* **293**:53-71.

Jackson (1996) Diuretics. In: Goodman and Gilman's the pharmacological basis of therapeutics, 9th edition, Hardman JG (ed), New York: McGraw-Hill, pp.685-713.

Jariyawat S, Sekine T, Takeda M, Apirwattanakul N, Kanai Y, Sophasan S and Endou H (1999) The interaction and transport of B-lactam antibiotics with the cloned rat renal organic anion transporter 1. *J Pharmacol Exp Ther* **290**:672-677.

Jung KY and Endou H (1989) Nephrotoxicity assessment by measuring cellular ATP content. II. Intranephron site of ochratoxin A nephrotoxicity. *Toxicol Appl Pharmacol* **100**:383-390.

Kasher JS, Holohan PD and Ross CR (1983) Na+ gradient-dependent *p*-aminohippurate (PAH) transport in rat basolateral membrane vesicles. *J Pharmacol Exp Ther* **227**:122-129

Kinsella JL, Holohan PD, Pessah NI and Ross CR (1979) Transport of organic anions in renal cortical luminal and antiluminal membrane vesicles. *J Pharmacol Exp Ther* **209**:443-450.

Kippen I and Klinenberg JR (1978) Effect of renal fuels on uptake of PAH and Uric acid by separated renal tubules of the rabbit. *Am J Physiol* **235**:F137-F141.

Kozak M (1987) An analysis of 5'-noncoding sequences from 699 vertebrate messenger RNAs. *Nucl Acids Res* **15**:8125-8148.

Krantz DE, Peter D, Liu Y and Edwards RH (1997) Phosphorylation of a vesicular monoamine transporter by casein kinase II. *J Biol Chem* **272**:6752-6759.

Kuipers F, Bijleveld CMA, Kneepkens CMF, van Zantan A, Fernandes J and Vonk J (1985) Sulphated lithocholic acid conjugates in serum from children with hepatic and intestinal diseases. *Scand J Gastroenterol* **20**:1255-1261.

Kusuhara H, Sekine T, Utsunomiya-Tate N, Tsuda M, Kojima R, Cha SH, Sugiyama Y, Kanai Y and Endou H (1999) Molecular cloning and characterization of a new multispecific organic anion transporter from rat brain. *J Biol Chem* **274**:13675-13680.

Kuze K, Graves P, Leahy A, Wilson P, Stuhlmann H and You G (1999) Heterologous expression and functional characterization of a mouse renal organic anion transporter in mammalian cells. *J Biol Chem* **274**:1519-1524.

Leier I, Hummel-Eisenbeiss J, Cui Y, Keppler D (2000) ATP-dependent para-aminohippuratetransport by multidrug resistance protein MRP2. *Kidney Int* **57**:1636-1642

Lemieux G, Pichette C, Viany P and GouGoux A (1980) Cellular mechanisms of the ammoniagenic effect of the ketone bodies in the dog. *Am J Physiol* **239**:F420-F426.

Liman ER, Tytgat J, Hess P (1992) Subunit stoichiometry of a mammalian K+ channel determined by construction of multimeric cDNAs. *Neuron* **9**:861-871.

Lopez-Nieto CE, You G, Bush KT, Barros EJG, Beier DR and Nigam SK (1997) Molecular cloning and characterization of NKT, a gene product related to the organic cation transporter family that is almost exclusively expressed in the kidney. *J Biol Chem* **272**:6471-6478.

Lu R, Chan BS and Schuster VL (1999) Cloning of the human kidney PAH transporter: narrow substrate specificity and regulation by protein kinase C. *Am J Physiol* **276**:F295-F303.

MacDonald IA, Bokkenheuser VD, Winter J, McLernon AM and Mosbach EH (1983) Degradation of steroids in the human gut. *J Lipid Res* **24**:675-700.

Malvin RL, Wilde WS and Sullivan LP (1958) Localization of nephron transport by stop-flow analysis. *Am J Physiol* **194**:135-142.

Marger MD and Saier Jr MH (1993) A major superfamily of transmembrane facilitators that catalyse uniport, symport and antiport. *Trends Biochem Sci* **18**:13-20.

Marshall EK Jr and Grafflin AL (1928) The structure and function of the kidney of *Lophius piscatorius*. *Bull Johns Hopkins Hosp* **43**:205-235.

Martin M, Ferrier B and Baverel G (1989) Transport and utilization of α-ketoglutarate by the rat kidney in vivo. *Pflüg Arch* **413**:217-224.

Martinez F, Manganel M, Montrose-Rafizadeh C, Werner D and Roch-Ramel F (1990) Transport of urate and p-aminohippurate in rabbit renal brush-border membranes. *Am J Physiol* **258**:F1145-F1153.

Maxild J (1978) Effect of externally added ATP and related comounds on active transport of *p*-aminohippurate and metabolism in cortical slices of the rabbit kidney. *Arch Int Physiol Biochem* **86**:509-530.

Merickel A, Rosandich P, Peter D and Edwards RH (1995) Identification of residues involved in substrate recognition by a vesicular monoamin transporter. *J Biol Chem* **270**:25798-25804.

Miller DS, Stewart DE and Pritchard JB (1993) Intracellular compartmentation of organic anions within renal cells. *Am J Physiol* **264**:R882-R890.

Møller JV and Sheikh I (1983) Renal organic anion transport system: Pharmacological, physiological and biochemical aspects. *Pharmacol Rev* **34**:315-358.

Mori K, Ogawa Y, Ebihara K, Aoki T, Tamura N, Sugawara A, Kuwahara T, Ozaki S, Mukoyama M, Tashiro K, Tanaka I and Nakao K (1997) Kidney-specific expression of a novel mouse organic cation transporter-like protein. *FEBS Lett* **417:**371-374.

Mullis KB (1990) The unusual origin of the polymerase chain reaction. *Sci Am* **262**:56-61

Okuda M, Saito H, Urakami Y, Takano M and Inui K-I (1996) cDNA cloning and functional expression of a novel rat kidney organic anion transporter, OCT2. *Biochem Biophys Res Comm* **224**:500-507.

Østergaard EH, Magnussen MP, Nielsen CK, Eilertsen E and Frey H-H (1972) Pharmacological properties of 3-n-butylamino-4-phenoxy-5-sulfamylbenzoic acid (bumetanide), a new potent diuretic. *Arzneim Forsch (Drug Res)* **22**:66-72.

Pajor AM, Sun N, Bai, L, Markovich D and Sule P (1998) The substrate specificity domain in the Na^+ / dicarboxylate and Na^+ / sulfate cotransporters is located in the carboxy-terminal portion of the protein. *Biochim Biophys Acta* **1370**:98-106.

Palmer RH (1971) Bile acid sulfates. II. Formation, metabolism, and excretion of lithocholic acid in the rat. *J Lipid Res* **12**:680-687.

Palmer RH and Bolt MG (1971) Bile acid sulfates. I. Synthesis of lithocholic acid sulfates and their identification in human bile. *J Lipid Res* **12**:671-679.

Podevin RA and Boumendil-Podevin EF (1975) Inhibition by cyclic AMP and dibutyryl cyclic AMP of transport of organic acids in kidney cortex. *Biochim Biophys Acta* **375**:106-114.

Podevin RA and Boumendil-Podevin EF (1977) Monovalent cation and ouabain effects on PAH uptake by rabbit kidney slices. *Am J Physiol* **232**:F239-F247.

Polkowski CA and Grassl SM (1993) Uric acid transport in rat renal basolateral membrane vesicles. *Biochim Biophys Acta* **1146**:145-152.

Pourcher T, Zani M-L and Leblanc G (1993) Mutagensis of acidic residues in putative membrane-spanning segments of the melibiose permease of *Eschericia coli*. I. Effect on Na+-dependent transport and binding properties. *J Biol Chem* **268**:3209-3215.

Prescott LF, Freestone S, McAuslane JA (1993) The concentration-dependent disposition of intravenous *p*-aminohippurate in subjects with normal and impaired renal function. *Br J Clin Pharmacol* **35**:20-29.

Pritchard JB (1987) Luminal and peritubular steps in renal transport of *p*-aminohippurate. *Biochim Biophys Acta* **906**:295-308.

Pritchard JB (1988) Coupled transport of p-aminohippurate by rat basolateral membrane vesicles. *Am J Physiol* **255**:F594-F604.

Pritchard JB (1990) Rat renal cortical slices demonstrate p-aminohippurate/glutarate exchange and sodium/glutarate coupled p-aminohippurate transport. *J Pharmacol Exp Ther* **255**:969-975.

Pritchard JB and Miller DS (1991) Comparitive insights into the mechanisms of renal organic anion and cation secretion. *Am J Physiol* **261**:R1329-1340.

Pritchard JB and Miller DS (1993) Mechanisms mediating renal secretion of organic anions and cations. *Physiol Rev* **73**:765-796.

Race JE, Grassl SM, Williams WJ and Holtzman EJ (1999) molecular cloning and characterization of two novel human renal organic anion transporters (hOAT1 and hOAT3). *Biochem Biophys Res Comm* **255**:508-514.

Reid G, Wolff NA, Dautzenberg FM and Burckhardt G (1998) Cloning of a human renal p-aminohppurate transporter, hROAT1. *Kidney Blood Press Res* **21**:233-237.

Rocchiccioli F, Leroux JP and Cartier PH (1984) Microdetermination of 2-ketoglutaric acid in plasma and cerebrospinal fluid by capillary gas chromatography mass spectroscopy: applications in pediatrics. *Biomed Mass Spectrom* **11**:24-28.

Roch-Ramel F (1998) Renal transport of organic anions. *Curr Opinion Nephrol Hyperten* **7**:517-524.

Roch-Ramel F, Guisan B and Schild L (1996) Indirect coupling of urate and p-aminohippurate transport to sodium in human brush-border membrane vesicles. *Am J Physiol* **270**:F61-F68.

Roch-Ramel F and Diezi J (1997) Renal transport of organic anions and uric acid. In: *Diseases of the Kidney,* 6th edition, Schrier RW and Gottschalk CW (eds). Boston: Little, Brown and Company, pp. 231-249.

Ross CR and Weiner IM (1972) Adenine nucleotides and PAH transport in slices of renal cortex. *Am J Physiol* **222**:356-359.

Schaub TP, Kartenbeck J, König J, Vogel O, Witzgall R, Kriz W and Keppler D (1997) Expression of the conjugate export pump encoded by the mrp2 gene in the apical membrane of kidney proximal tubule cells. *J Am Soc Nephrol* **8**:1213-1221.

Schmitt C and Burckhardt G (1993) *p*-Aminohippurate/2-oxoglutarate exchange in bovine renal brush-border and basolateral membrane vesicles. *Pflüg Arch* **423**:280-90.

Schömig E, Spitzenberger F, Engelhardt M, Martel F, Örding N and Gründemann D (1998) Molecular cloning and characterization of two novel transport proteins from rat kidney. *FEBS Lett* **425**:79-86.

Sekine T, Watanabe N, Hosoyamada M, Kanai Y and Endou H (1997) Expression cloning and characterization of a novel multispecific organic anion transporter. *J Biol Chem* **272**:18526-18529.

Sekine T, Cha SH, Tsuda M, Apiwattanakul N, Nakajima N, Kanai Y and Endou H (1998b) Identification of multispecific organic anion transporter 2 expressed predominantly in the liver. *FEBS Lett* **429**:179-182.

Sekine T, Cha SH, Endou T (2000) The multispecific organic anion transporter (OAT) family. *Pflüg Arch*, in press.

Shannon JA (1938) The renal excretion of phenol red by the aglomerular fishes *Opsanus tau* and *Lophius piscatorius*. *J Cell Comp Physiol* **11**:315-323.

Sheikh MI, Maxild J and Møller JV (1981) Effect on vanadate on the renal accumulation of *p*-aminohippurate in the rabbit kidney tubules in vitro. *Biochem Pharmacol* **30**:2141-2146.

Shih TM, Smith RD, Toro L and Goldin AL (1998) High-level expression and detection of ion channels in Xenopus oocytes. *Methods Enzymol* **293**:529-555.

Shimada H, Moewes B and Burckhardt G (1987) Indirect coupling to Na of *p*-aminohippuric acid into rat basolateral membrane vesicles. *Am J Physiol* **253**:F795-F801.

Simonson GD, Vincent AC, Roberg KJ, Huang Y and Iwanij V (1994) Molecular cloning and characterization of a novel liver-specific transport protein. *J Cell Sci* **107**:1065-1077.

Simonson GD and Iwanij V (1995) Genomic organization and promoter sequence of a gene encoding a rat liver-specific type-I transport protein. *Gene* **154**:243-247.

Steffgen J, Burckhardt BC, Langenberg C, Kühne L, Müller GA, Burckhardt G and Wolff NA (1999) Expression cloning and characterization of a novel sodium-dicarboxylate cotransporter from winter flounder kidney. *J Biol Chem* **274**:20191-20196.

Stiehl A, Earnest DL, Admirant WH (1975) Sulfation and renal excretion of bile salts in patients with cirrhosis of the liver. *Gastoenterology* **68**:534-544.

Stride BD, Cole SPC, Deeley, RG (1999) Localization of a substrate specificity domain in the multidrug resistance protein. *J Biol Chem* **274**:22877-22883.

Sullivan LP and Grantham JJ (1992) Specificity of basolateral organic anion exchanger in proximal tubule for cellular and extracellular solutes. *J Am Soc Nephrol* **2**:1192-1200.

Sweet DH, Wolff NA and Pritchard JB (1997) Expression cloning and characterization of ROAT1, the basolateral organic anion transporter in rat kidney. *J Biol Chem* **272**:30088-30095.

Sweet DH and Pritchard JB (1999) The molecular biology of renal organic anion and cation transporters. *Cell Biochen Biophys* **31**:89-118.

Takahashi S, Nakagawa T, Banno T, Watanabe T, Murakami K and Nakayama K (1995) Localization of furin to the trans-Golgi network and recycling from the cell surface involves Ser and Tyr residues within the cytoplasmic domain. *J Biol Chem* **270**:28397-28401.

Terlouw SA, Tanriseven O, Russel FGM and Masereeuw (2000) Metabolite anion carriers mediate the uptake of the anionic drug fluorescein in renal cortical mitochondria. *J Pharmacol Exp Ther* **292**:968-973.

Tojo A, Sekine T, Nakajima N, Hosoyamada M, Kanai Y, Kimura K and Endou H (1999) Immunohistochemical localization of multispecific renal organic anion transporter 1 in rat kidney. *J Am Soc Nephrol* **10**:464-471.

Trauner M, Meier PJ and Boyer JL (1998) Molecular pathogenesis of cholestasis. *New Engl J Med* **339**:1217-1227.

Ullrich KJ, Rumrich G, Fritzsch G and Klöss S (1987) Contraluminal para-aminohippurate (PAH) transport in the proximal tubule of the rat kidney. II. Specificity: aliphatic dicarboxylic acids. *Pflüg Arch* **408**:38-45.

Ullrich KJ (1997) Renal transporters for organic anions and organic cations. Strucural requirements for substrates. *J Membrane Biol* **158**:95-107.

Uwai Y, Okuda M, Takami K, Hashimoto Y and Inui K-I (1998) Functional characterization of the rat multispecific organic anion transporter OAT1 mediating basolateral uptake of anionic drugs in the kidney. *FEBS Lett* **438**:321-324.

van der Meer R Vonk RJ and Kuipers F (1988) Cholestais and the interactions of sulfated glyco- and taurolithocholate with calcium. *Am J Physiol* **254**:G644-G649.

von Heijne G (1992) Membrane protein structure prediction, hydrophobicity analysis and the positive-inside rule. *J Mol Biol* **225**:487-494.

Wang J and Giacomini KM (1997) Molecular determinants of substarte selectivity in Na^+-dependent nucleoside transporters. *J Biol Chem* **272**:28845-28848.

Welborn JR, Shpun S, Dantzler WH and Wright SH (1998) Effect of α-ketoglutarate on organic anion transport in single rabbit renal proximal tubules. *Am J Physiol* **274**:F165-F174.

Wolff NA, Werner A, Burckhardt S and Burckhardt G (1997) Expression cloning and characterization of a renal organic anion transporter from winter flounder. *FEBS Lett* **417:**287-297.

Wolff NA, Grünwald B, Godehardt S and Burckhardt G (2000) Mutational analysis of the flounder renal organic anion transporter. *FASEB J* **14**:A109.

You G, Kuze K, Kohanski RA, Amsler K and Henderson S (2000) Regulation of mOAT-mediated organic anion transport by okadaic acid and protein kinase C in LLC-PK_1 cells. *J Biol Chem* **275**:10278-10284.

Zhang L, Dresser MJ, Chun JK, Babbitt PC and Giacomini KM (1997) Cloning and functional characterization of a rat renal organic cation transporter isoform (rOCT1A). *J Biol Chem* **272:**16548-16554.

Zhou Y, Gottesman MM, Pastan I (1999) Domain exchangeability between the multidrug transporter (MDR1) and phosphatidylcholine flippase (MDR2). *Mol Pharmacol* **56**:997-1004.

7 APPENDIX

agcagagcaggttcctctcagctgcctgcagctcctttcccttcaaacggagccaaacta
*ctttcctctgg***ggatcc**ATGGCCTTTAATGACCTCCTGCAGCAGGTGGGGGGTGTCGGCC
GCTTCCAGCAGATCCAGGTCACCCTGGTGGTCCTCCCCCTGCTCCTGATGGCTTCTCACA
ACACCCTGCAGAACTTCACTGCTGCCATCCCTACCCACCACTGCCGCCCGCCTGCCGATG
CCAACCTCAGCAAGAACGGGGGGCTGGAGGTCTGGCTGCCCCGGGACAGGCAGGGGCAGC
CTGAGTCCTGCCTCCGCTTCACCTCCCCGCAGTGGGGACTGCCCTTTCTCAATGGCACAG
AAGCCAATGGCACAGGGGCCACAGAGCCCTGCACCGATGGCTGGATCTATGACAACAGCA
CCTTCCCATCTACCATCGTGACTGAGTGGGACCTTGTGTGCTCTCACAGGGCCCTACGCC
AGCTGGCCCAGTCCTTGTACATGGTGGGGGTGCTGCTCGGAGCCATGGTGTTCGGCTACC
TTGCAGACAGGCTAGGCCGCCGGAAGGTACTCATCTTGAACTACCTGCAGACAGCTGTGT
CAGGGACCTGCGCAGCCTTCGCACCCAACTTCCCCATCTACTGCGCCTTCCGGCTCCTCT
CGGGCATGGCTCTGGCTGGCATCTCCCTCAACTGCATGACACTGAATGTGGAGTGGATGC
CCATTCACACACGGGCCTGCGTGGGCACCTTGATTGGCTATGTCTACAGCCTGGGCCAGT
TCCTCCTGGCTGGTGTGGCCTACGCTGTGCCCCACTGGCGCCACCTGCAGCTACTGGTCT
CTGCGCCTTTTTTTGCCTTCTTCATCTACTCCTGGTTCTTCATTGAGTCGGCCCGCTGGC
ACTCCTCCTCCGGGAGGCTGGACCTCACCCTGAGGGCCCTGCAGAGAGTCGCCCGGATCA
ATGGGAAGCGGGAAGAAGGAGCCAAATTGAGTATGGAGGTACTCCGGGCCAGTCTGCAGA
AGGAGCTGACCATGGGCAAAGGCCAGGCATCGGCCATGGAGCTGCTGCGCTGCCCCACCC
TCCGCCACCTCTTCCTCTGCCTCTCCATGCTGTGGTTTGCCACTAGCTTTGCATACTATG
GGCTGGTCATGGACCTGCAGGGCTTTGGAGTCAGCATCTACCTAATCCAGGTGATCTTTG
GTGCTGTGGACCTGCCTGCCAAGCTTGTGGGCTTCCTTGTCATCAACTCCCTGGGTCGCC
GGCCTGCCCAAATGGCTGCACTGCTGCTGGCAGGCATCTGCATCCTGCTCAATGGGGTGA
TACCCCAGGACCAGTCCATTGTCCGAACCTCTCTTGCTGTGCTGGGGAAGGGTTGTCTGG
CTGCCTCCTTCAACTGCATCTTCCTGTATACTGGGGAACTGTATCCCACAATGATCCGGC
AGACAGGCATGGGAATGGGCAGCACCATGGCCCGAGTGGGCAGCATCGTGAGCCCACTGG
TGAGCATGACTGCCGAGCTCTACCCCTCCATGCCTCTCTTCATCTACGGTGCTGTTCCTG
TGGCCGCCAGCGCTGTCACTGTCCTCCTGCCAGAGACCCTGGGCCAGCCACTGCCAGACA
CGGTGCAGGACCTGGAGAGCAGGAAAGGGAAACAGACGCGACAGCAACAAGAGCACCAGA
AGTATATGGTCCCACTGCAGGCCTCAGCACAAGAGAAGAATGGATTTTGAgg**tctaga***cc*
ctcgcagaggagaagggtcagaggatcatcgtgtgaaggttcaacactaaacgtggactc
acgtcaacactgtgtcgctctgggagcttcagctttcacctgttgtgacgcttttcacaa
gcttttacattcaagtgtctttttaggctctcgaaagtgtcaagatttcattcagaacaa
gttcaaaacagctcgagctctgaagagttcgttttctatattttgaaactccagtgtga
ctgcagagggcgctgtttgtattgatgaagaatgagagagaggcatctgtgaataattct
tttaaaaatatatatatatatttgggttgaaatcacccacagatcacgttacttgtgta
tttgttgtgttttaaatcttgtctgtattagcagatgaatcctgattaatgaacgtgtac
attttgttacagagtgatttgcaggtaatgcagtataaatgctgttacaaggaaaaaaaa
aaaaaaaaaaaaaaaaaaaaa

Appendix 1: Full nucleotide sequence of the hROAT1 expression clone. The hROAT1 sequence is denoted by capital letters (start and stop codons underlined), and the fNaDC-3 5‘ and 3‘ UTRs sequences are italicized. The BamHI and XbaI sites incorporated to enable subcloning are in bold.

Appendix 2 (overleaf): Alignment of the hOAT2, hNLT and rOAT2 with the rat OAT2 gene, TI-LTP. The TI-LTP sequence is shaded grey, and intron sequences are in lower case. The last homologous sequence shared by all three transcripts is shaded black.

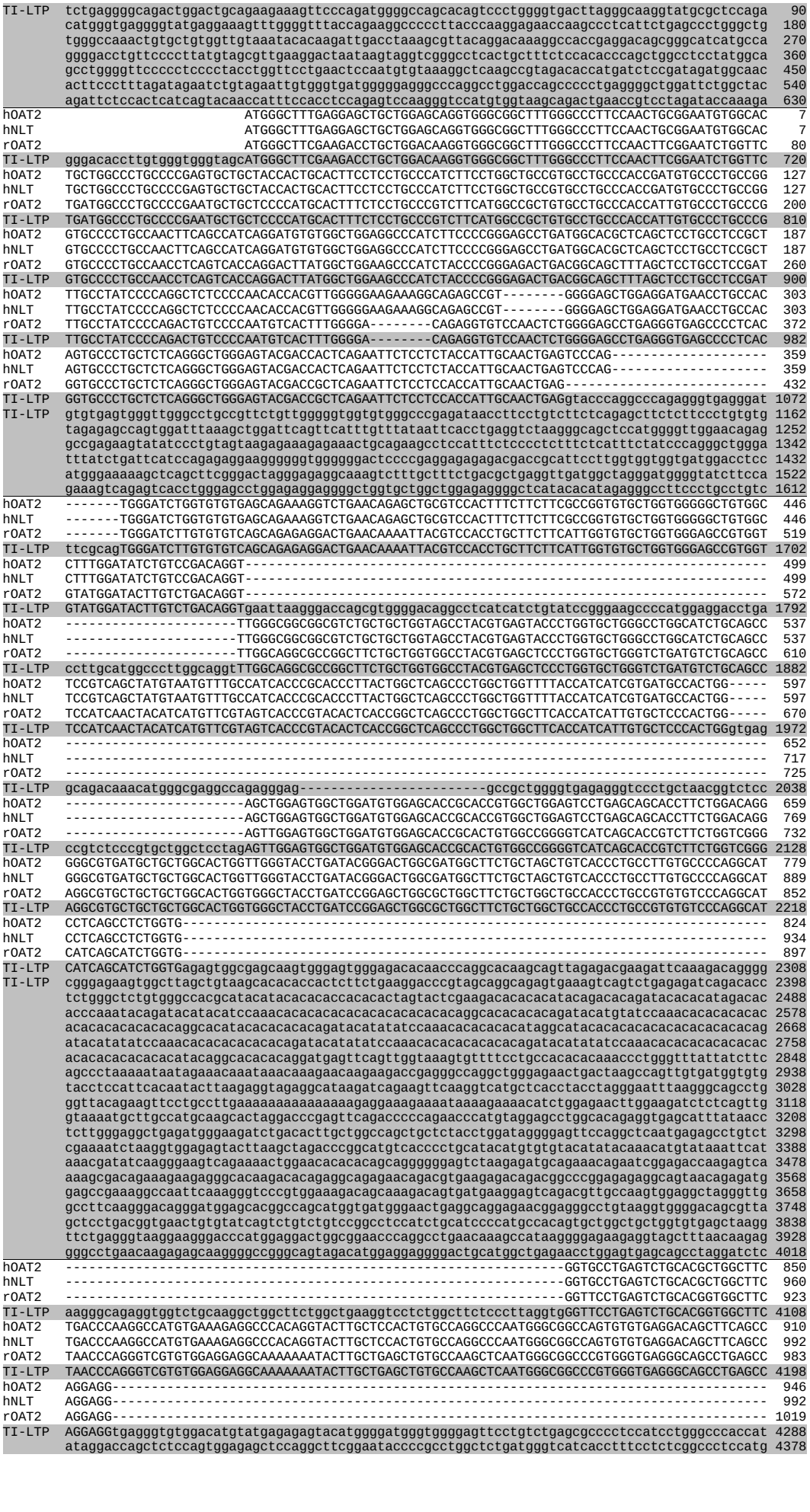

```
TI-LTP  tctgaggggcagactggactgcagaagaaagttcccagatggggccagcacagtccctggggtgacttagggcaaggtatgcgctccaga   90
        catgggtgaggggtatgaggaaagtttggggtttaccagaaggccccccttacccaaggagaaccaagccctcattctgagccctgggctg  180
        tgggccaaactgtgctgtggttgtaaatacacaagattgacctaaagcgttacaggacaaaggccaccgaggacagcgggcatcatgcca  270
        ggggacctgttccccttatgtagcgttgaaggactaataagtaggtcgggcctcactgctttctccacacccagctggcctcctatggca  360
        gcctggggttccccctcccctacctggttcctgaactccaatgtgtaaaggctcaagccgtagacaccatgatctccgatagatggcaac  450
        acttccctttagatagaatctgtagaattgtgggtgatggggagggcccaggcctggaccagccccctgaggggctggattctggctac  540
        agattctccactcatcagtacaaccatttccacctccagagtccaagggtccatgtggtaagcagactgaaccgtcctagataccaaaga  630
hOAT2                          ATGGGCTTTGAGGAGCTGCTGGAGCAGGTGGGCGGCTTTGGCCCTTCCAACTGCGGAATGTGGCAC    7
hNLT                           ATGGGCTTTGAGGAGCTGCTGGAGCAGGTGGGCGGCTTTGGCCCTTCCAACTGCGGAATGTGGCAC    7
rOAT2                          ATGGGCTTCGAAGACCTGCTGGACAAGGTGGGCGGCTTTGGCCCTTCCAACTTCGGAATCTGGTTC   80
TI-LTP  gggacaccttgtgggtgggtagcATGGGCTTCGAAGACCTGCTGGACAAGGTGGGCGGCTTTGGCCCTTCCAACTTCGGAATCTGGTTC  720
hOAT2   TGCTGGCCCTGCCCCGAGTGCTGCTACCACTGCACTTCCTCCTGCCCATCTTCCTGGCTGCCGTGCCTGCCCACCGATGTGCCCTGCCGG  127
hNLT    TGCTGGCCCTGCCCCGAGTGCTGCTACCACTGCACTTCCTCCTGCCCATCTTCCTGGCTGCCGTGCCTGCCCACCGATGTGCCCTGCCGG  127
rOAT2   TGATGGCCCTGCCCCGAATGCTGCTCCCCATGCACTTTCTCCTGCCCGTCTTCATGGCCGCTGTGCCTGCCCACCATTGTGCCCTGCCCG  200
TI-LTP  TGATGGCCCTGCCCCGAATGCTGCTCCCCATGCACTTTCTCCTGCCCGTCTTCATGGCCGCTGTGCCTGCCCACCATTGTGCCCTGCCCG  810
hOAT2   GTGCCCCTGCCAACTTCAGCCATCAGGATGTGTGGCTGGAGGCCCATCTTCCCCGGGAGCCTGATGGCACGCTCAGCTCCTGCCTCCGCT  187
hNLT    GTGCCCCTGCCAACTTCAGCCATCAGGATGTGTGGCTGGAGGCCCATCTTCCCCGGGAGCCTGATGGCACGCTCAGCTCCTGCCTCCGCT  187
rOAT2   GTGCCCCTGCCAACCTCAGTCACCAGGACTTATGGCTGGAAGCCCATCTACCCCGGGAGACTGACGGCAGCTTTAGCTCCTGCCTCCGAT  260
TI-LTP  GTGCCCCTGCCAACCTCAGTCACCAGGACTTATGGCTGGAAGCCCATCTACCCCGGGAGACTGACGGCAGCTTTAGCTCCTGCCTCCGAT  900
hOAT2   TTGCCTATCCCCAGGCTCTCCCCAACACCACGTTGGGGGAAGAAAGGCAGAGCCGT--------GGGGAGCTGGAGGATGAACCTGCCAC  303
hNLT    TTGCCTATCCCCAGGCTCTCCCCAACACCACGTTGGGGGAAGAAAGGCAGAGCCGT--------GGGGAGCTGGAGGATGAACCTGCCAC  303
rOAT2   TTGCCTATCCCCAGACTGTCCCCAATGTCACTTTGGGGA--------CAGAGGTGTCCAACTCTGGGGAGCCTGAGGGTGAGCCCCTCAC  372
TI-LTP  TTGCCTATCCCCAGACTGTCCCCAATGTCACTTTGGGGA--------CAGAGGTGTCCAACTCTGGGGAGCCTGAGGGTGAGCCCCTCAC  982
hOAT2   AGTGCCCTGCTCTCAGGGCTGGGAGTACGACCACTCAGAATTCTCCTCTACCATTGCAACTGAGTCCCAG--------------------  359
hNLT    AGTGCCCTGCTCTCAGGGCTGGGAGTACGACCACTCAGAATTCTCCTCTACCATTGCAACTGAGTCCCAG--------------------  359
rOAT2   GGTGCCCTGCTCTCAGGGCTGGGAGTACGACCGCTCAGAATTCTCCTCCACCATTGCAACTGAG-------------------------  432
TI-LTP  GGTGCCCTGCTCTCAGGGCTGGGAGTACGACCGCTCAGAATTCTCCTCCACCATTGCAACTGAGgtacccaggcccagagggtgagggat 1072
TI-LTP  gtgtgagtgggttgggcctgccgttctgttgggggtggtgtgggcccgagataaccttcctgtcttctcagagcttctcttccctgtgtg 1162
        tagagagccagtggatttaaagctggattcagttcatttgtttataattcacctgaggtctaagggcagctccatggggttggaacagag 1252
        gccgagaagtatatccctgtagtaagagaaagagaaactgcagaagcctccatttctcccctctttctcatttctatcccagggctggga 1342
        tttatctgattcatccagagaggaagggggtgggggactccccgaggagagagacgaccgcattccttggtggtggtgatggacctcc 1432
        atgggaaaaagctcagcttcgggactagggagaggcaaagtctttgctttctgacgctgaggttgatggctagggatggggtatcttcca 1522
        gaaagtcagagtcacctgggagcctggagaggaggggctggtgctggctggagaggggctcatacacatagagggccttccctgcctgtc 1612
hOAT2   -------TGGGATCTGGTGTGTGAGCAGAAAGGTCTGAACAGAGCTGCGTCCACTTTCTTCTTCGCCGGTGTGCTGGTGGGGGCTGTGGC  446
hNLT    -------TGGGATCTGGTGTGTGAGCAGAAAGGTCTGAACAGAGCTGCGTCCACTTTCTTCTTCGCCGGTGTGCTGGTGGGGGCTGTGGC  446
rOAT2   -------TGGGATCTTGTGTGTCAGCAGAGAGGACTGAACAAAATTACGTCCACCTGCTTCTTCATTGGTGTGCTGGTGGGAGCCGTGGT  519
TI-LTP  ttcgcagTGGGATCTTGTGTGTCAGCAGAGAGGACTGAACAAAATTACGTCCACCTGCTTCTTCATTGGTGTGCTGGTGGGAGCCGTGGT 1702
hOAT2   CTTTGGATATCTGTCCGACAGGT-------------------------------------------------------------------  499
hNLT    CTTTGGATATCTGTCCGACAGGT-------------------------------------------------------------------  499
rOAT2   GTATGGATACTTGTCTGACAGGT-------------------------------------------------------------------  572
TI-LTP  GTATGGATACTTGTCTGACAGGTgaattaagggaccagcgtggggacaggcctcatcatctgtatccgggaagccccatggaggacctga 1792
hOAT2   ----------------------TTGGGCGGCGGCGTCTGCTGCTGGTAGCCTACGTGAGTACCCTGGTGCTGGGCCTGGCATCTGCAGCC  537
hNLT    ----------------------TTGGGCGGCGGCGTCTGCTGCTGGTAGCCTACGTGAGTACCCTGGTGCTGGGCCTGGCATCTGCAGCC  537
rOAT2   ----------------------TTGGCAGGCGCCGGCTTCTGCTGGTGGCCTACGTGAGCTCCCTGGTGCTGGGTCTGATGTCTGCAGCC  610
TI-LTP  ccttgcatggcccttggcaggtTTGGCAGGCGCCGGCTTCTGCTGGTGGCCTACGTGAGCTCCCTGGTGCTGGGTCTGATGTCTGCAGCC 1882
hOAT2   TCCGTCAGCTATGTAATGTTTGCCATCACCCGCACCCTTACTGGCTCAGCCCTGGCTGGTTTTACCATCATCGTGATGCCACTGG-----  597
hNLT    TCCGTCAGCTATGTAATGTTTGCCATCACCCGCACCCTTACTGGCTCAGCCCTGGCTGGTTTTACCATCATCGTGATGCCACTGG-----  597
rOAT2   TCCATCAACTACATCATGTTCGTAGTCACCCGTACACTCACCGGCTCAGCCCTGGCTGGCTTCACCATCATTGTGCTCCCACTGG-----  670
TI-LTP  TCCATCAACTACATCATGTTCGTAGTCACCCGTACACTCACCGGCTCAGCCCTGGCTGGCTTCACCATCATTGTGCTCCCACTGGgtgag 1972
hOAT2   ------------------------------------------------------------------------------------------  652
hNLT    ------------------------------------------------------------------------------------------  717
rOAT2   ------------------------------------------------------------------------------------------  725
TI-LTP  gcagacaaacatgggcgaggccagagggag------------------------gccgctggggtgagagggtccctgctaacggtctcc 2038
hOAT2   -----------------------AGCTGGAGTGGCTGGATGTGGAGCACCGCACCGTGGCTGGAGTCCTGAGCAGCACCTTCTGGACAGG  659
hNLT    -----------------------AGCTGGAGTGGCTGGATGTGGAGCACCGCACCGTGGCTGGAGTCCTGAGCAGCACCTTCTGGACAGG  769
rOAT2   -----------------------AGTTGGAGTGGCTGGATGTGGAGCACCGCACTGTGGCCGGGGTCATCAGCACCGTCTTCTGGTCGGG  732
TI-LTP  ccgtctcccgtgctggctcctagAGTTGGAGTGGCTGGATGTGGAGCACCGCACTGTGGCCGGGGTCATCAGCACCGTCTTCTGGTCGGG 2128
hOAT2   GGGCGTGATGCTGCTGGCACTGGTTGGGTACCTGATACGGGACTGGCGATGGCTTCTGCTAGCTGTCACCCTGCCTTGTGCCCCAGGCAT  779
hNLT    GGGCGTGATGCTGCTGGCACTGGTTGGGTACCTGATACGGGACTGGCGATGGCTTCTGCTAGCTGTCACCCTGCCTTGTGCCCCAGGCAT  889
rOAT2   AGGCGTGCTGCTGCTGGCACTGGTGGGCTACCTGATCCGGAGCTGGCGCTGGCTTCTGCTGGCTGCCACCCTGCCGTGTGTCCCAGGCAT  852
TI-LTP  AGGCGTGCTGCTGCTGGCACTGGTGGGCTACCTGATCCGGAGCTGGCGCTGGCTTCTGCTGGCTGCCACCCTGCCGTGTGTCCCAGGCAT 2218
hOAT2   CCTCAGCCTCTGGTG---------------------------------------------------------------------------  824
hNLT    CCTCAGCCTCTGGTG---------------------------------------------------------------------------  934
rOAT2   CATCAGCATCTGGTG---------------------------------------------------------------------------  897
TI-LTP  CATCAGCATCTGGTGagagtggcgagcaagtgggagtgggagacacaacccaggcacaagcagttagagacgaagattcaaagacagggg 2308
TI-LTP  cgggagaagtggcttagctgtaagcacacaccactcttctgaaggacccgtagcaggcagagtgaaagtcagtctgagagatcagacacc 2398
        tctgggctctgtgggccacgcatacatacacacaccacacactagtactcgaagacacacacatacagacacagatacacacatagacac 2488
        acccaaatacagatacatacatccaaacacacacacacacacacacaggcacacacacagatacatgtatccaaacacacacacac 2578
        acacacacacacacaggcacatacacacacacagatacatatatccaaacacacacacataggcatacacacacacacacacacacacag 2668
        atacatatatccaaacacacacacacacagatacatatatccaaacacacacacacacagatacatatatccaaacacacacacacacac 2758
        acacacacacacacatacaggcacacacaggatgagttcagttggtaaagtgttttcctgccacacacaaaccctgggtttattatcttc 2848
        agccctaaaaataatagaaacaaataaacaaagaacaagaagaccgagggccaggctgggagaactgactaagccagttgtgatggtgtg 2938
        tacctccattcacaatacttaagaggtagaggcataagatcagaagttcaaggtcatgctcacctacctagggaatttaagggcagcctg 3028
        ggttacagaagttcctgccttgaaaaaaaaaaaaaaagaggaaagaaaataaaagaaaacatctggagaacttggaagatctctcagttg 3118
        gtaaaatgcttgccatgcaagcactaggacccgagttcagaccccagaacccatgtaggagcctggcacagaggtgagcatttataacc 3208
        tcttgggaggctgagatgggaagatctgacacttgctggccagctgctctacctggataggggagttccaggctcaatgagagcctgtct 3298
        cgaaaatctaaggtggagagtacttaagctagacccggcatgtcacccctgcatacatgtgtgtacatatacaaacatgtataaattcat 3388
        aaacgatatcaagggaagtcagaaaactggaacacacacagcagggggggagtctaagagatgcagaaacagaatcggagaccaagagtca 3478
        aaagcgacagaaagaagagggcacaagacacagaggcagagaacagacgtgaagagacagacggcccggagagaggcagtaacagagatg 3568
        gagccgaaaggccaattcaaagggtcccgtggaaagacagcaaagacagtgatgaaggagtcagacgttgccaagtggaggctagggttg 3658
        gccttcaagggacagggatggagcacggccagcatggtgatgggaactgaggcaggagaacggagggcctgtaaggtggggacagcgtta 3748
        gctcctgacggtgaactgtgtatcagtctgtctgtccggcctccatctgcatccccatgccacagtgctggctgctggtgtgagctaagg 3838
        ttctgagggtaaggaagggacccatggaggactggcggaacccaggcctgaacaaagccataaggggagaagaggtagctttaacaagag 3928
        gggcctgaacaagagagcaaggggccgggcagtagacatggaggaggggactgcatggctgagaacctggagtgagcagcctaggatctc 4018
hOAT2   ----------------------------------------------------------------GGTGCCTGAGTCTGCACGCTGGCTTC  850
hNLT    ----------------------------------------------------------------GGTGCCTGAGTCTGCACGCTGGCTTC  960
rOAT2   ----------------------------------------------------------------GGTTCCTGAGTCTGCACGGTGGCTTC  923
TI-LTP  aagggcagaggtggtctgcaaggctggcttctggctgaaggtcctctggcttctcccttaggtgGGTTCCTGAGTCTGCACGGTGGCTTC 4108
hOAT2   TGACCCAAGGCCATGTGAAAGAGGCCCACAGGTACTTGCTCCACTGTGCCAGGCCCAATGGGCGGCCAGTGTGTGAGGACAGCTTCAGCC  910
hNLT    TGACCCAAGGCCATGTGAAAGAGGCCCACAGGTACTTGCTCCACTGTGCCAGGCCCAATGGGCGGCCAGTGTGTGAGGACAGCTTCAGCC  992
rOAT2   TAACCCAGGGTCGTGTGGAGGAGGCAAAAAAATACTTGCTGAGCTGTGCCAAGCTCAATGGGCGGCCCGTGGGTGAGGGCAGCCTGAGCC  983
TI-LTP  TAACCCAGGGTCGTGTGGAGGAGGCAAAAAAATACTTGCTGAGCTGTGCCAAGCTCAATGGGCGGCCCGTGGGTGAGGGCAGCCTGAGCC 4198
hOAT2   AGGAGG------------------------------------------------------------------------------------  946
hNLT    AGGAGG------------------------------------------------------------------------------------  992
rOAT2   AGGAGG------------------------------------------------------------------------------------ 1019
TI-LTP  AGGAGGtgagggtgtggacatgtatgagagagtacatggggatgggtggggagttcctgtctgagcgcccctccatcctgggcccaccat 4288
        ataggaccagctctccagtggagagctccaggcttcggaatacccgcctggctctgatgggtcatcacctttcctctcggccctccatg 4378
```

```
        tgtactcccagcccaggactgctgaggacacagagaagcagagagaacacactggctcctgagacaagctctaaggtggaaatcttgctt 4468
hOAT2   ---------------CTGTGAGCAAAGTGGCCGCCGGGGAACGGGTGGTCCGAAGACCTTCATACCTAGACCTGTTCCGCACACCACGGC  991
hNLT    ---------------CTGTGAGCAAAGTGGCCGCCGGGGAACGGGTGGTCCGAAGACCTTCATACCTAGACCTGTTCCGCACACCACGGC 1037
rOAT2   ---------------CCCTGAACAACGTGGTCACCATGGAAAGGGCGTTGCAAAGACCCTCATACTTAGACCTGTTCCGAACATCTCAGC 1064
TI-LTP  tcttccccaaccaggCCCTGAACAACGTGGTCACCATGGAAAGGGCGTTGCAAAGACCCTCATACTTAGACCTGTTCCGAACATCTCAGC 4558
hOAT2   TCCGACACATCTCACTGTGCTGCGTGGTGGTGTGGT---------------------------------------------------- 1051
hNLT    TCCGACACATCTCACTGTGCTGCGTGGTGGTGTGGT---------------------------------------------------- 1097
rOAT2   TCCGACATATCTCACTGTGCTGCATGATGGTGTGGT---------------------------------------------------- 1124
TI-LTP  TCCGACATATCTCACTGTGCTGCATGATGGTGTGGTaagatggggtcgagttgtatctggtggagtgagggtgtgggagggaggggccaa 4648
        gattgtaactggggagggtagagtgatcatcctggagctgggaaggggaaatctgactaccacaggtccagtgtagtcggcaacggagac 4738
        acgtaggcccaactttaggctctatgacttccttaccgtgtgaccctggacaactgtctaaccactctgatccttaacatctatttttgt 4828
        aaaacgagcagttttctgttaattcctgtgtcacagggttgctgctaagattggggtaaaggtgctttggccactggtatctacttgggg 4918
        attgtggatggctgggggaagaggggcagagcctgggctgcggtctctgaagtgccaagtggcaggagagggttcttgaggggcactgca 5008
hOAT2   -------------TCGGAGTGAACTTCTCCTATTACGGCCTGAGTCTGGATGTGTCGGGGCTGGGGCTGAACGTGTACCAGACACAGCTG 1104
hNLT    -------------TCGGAGTGAACTTCTCCTATTACGGCCTGAGTCTGGATGTGTCGGGGCTGGGGCTGAACGTGTACCAGACACAGCTG 1150
rOAT2   -------------TTGGAGTGAACTTTTCCTACTACGGCCTGACTCTGGACGTGTCTGGGCTGGGGCTGAACGTGTACCAGACACAGCTG 1177
TI-LTP  actccattcaggtTTGGAGTGAACTTTTCCTACTACGGCCTGACTCTGGACGTGTCTGGGCTGGGGCTGAACGTGTACCAGACACAGCTG 5098
hOAT2   TTGTTCGGGGCTGTGGAACTGCCCTCCAAGCTGCTGGTCTACTTGTCGGTGCGC--TACGCAGGACGCCGCCTCACGCAAGCCGGGACAC 1164
hNLT    TTGTTCGGGGCTGTGGAACTGCCCTCCAAGCTGCTGGTCTACTTGTCGGTGCGC--TACGCAGGACGCCGCCTCACGCAAGCCGGGACAC 1210
rOAT2   CTGTTTGGGGCTGTGGAGCTCCCCTCCAAAATTATGGTCTACTTCCTTGTGCGCCGTCTG--GGACGCCGTCTCACGGAGGCTGGGATGC 1237
TI-LTP  CTGTTTGGGGCTGTGGAGCTCCCCTCCAAAATTATGGTCTACTTCCTTGTGCGCCGTCTG--GGACGCCGTCTCACGGAGGCTGGGATGC 5186
hOAT2   TGCTGGGCGCGGCCCTGGCGTTCGGCACTAGACTGCTAGTGTCCTCCGATATG---------------------------------- 1275
hNLT    TGCTGGGCGCGGCCCTGGCGTTCGGCACTAGACTGCTAGTGTCCTCCGATATG---------------------------------- 1321
rOAT2   TGCTGGGCGCTGCTCTGACCTTTGGCACCAGCCTGCTGGTATCCT------TGG---------------------------------- 1343
TI-LTP  TGCTGGGCGCTGCTCTGACCTTTGGCACCAGCCTGCTGGTATCCT------TGGgtaagccaggcctggcagttccttctgccctctgtg 5270
hOAT2   ------------------------------------------------------------------------AAGTCCTGGAGCACTGT 1292
hNLT    ------------------------------------------------------------------------AAGTCCTGGAGCACTGT 1338
rOAT2   ------------------------------------------------------------------AGACTAAGTCATGGATCACTGC 1365
TI-LTP  gggactctgcctcacatccaggggctcctggctccatcccctccctgaggaatccctttccctccagAGACTAAGTCATGGATCACTGC 5360
hOAT2   CCTGGCAGTGATGGGGAAAGCTTTTTCTGAAGCTGCCTTCACCACTGCCTACCTGTTCACTTCAGAGTTGTACCCTACGGTGCTCAG--- 1352
hNLT    CCTGGCAGTGATGGGGAAAGCTTTTTCTGAAGCTGCCTTCACCACTGCCTACCTGTTCACTTCAGAGTTGTACCCTACGGTGCTCAG--- 1398
rOAT2   TCTGGTGGTGGTGGGGAAAGCTTTTTCTGAAGCTGCTTTTACTACGGCCTACCTGTTCACGTCCGAGTTGTACCCTACTGTGCTCAG--- 1425
TI-LTP  TCTGGTGGTGGTGGGGAAAGCTTTTTCTGAAGCTGCTTTTACTACGGCCTACCTGTTCACGTCCGAGTTGTACCCTACTGTGCTCAGgta 5450
        agccagggacccaggcgactgcctgccttaacctaggtgtctgtgttcacacactgcccacccattctttagctatagccagatacatcg 5540
        atgcaccatgggtatttgtccaaatcttggggagcacagggaacttgatcttctgtactgggattgcctgcacaggaggggagccttgtg 5630
hOAT2   -------------------------------ACAGACAGGGATGGGGCTGACTGCACTGGTGGGCCGGCTGGGGGGCTCTTTGGCCCCAC 1438
hNLT    -------------------------------ACAGACAGGGATGGGGCTGACTGCACTGGTGGGCCGGCTGGGGGGCTCTTTGGCCCCAC 1484
rOAT2   -------------------------------ACAGACAGGATTGGGACTTACTGCACTCATGGGCAGGCTAGGGGCCTCTCTGGCCCGAC 1511
TI-LTP  acgaacggccccctcttcctttcctgaacagACAGACAGGATTGGGACTTACTGCACTCATGGGCAGGCTAGGGGCCTCTCTGGCCCCAC 5720
hOAT2   TGGCGGCCTTGCTGGATGGAGTGTGGCTGTCACTGCCCAAGCTTACTTATGGGGGGATCGCCCTGCTGGCTGCCGGCACCGCCCTCCTGC 1498
hNLT    TGGCGGCCTTGCTGGATGGAGTGTGGCTGTCACTGCCCAAGCTTACTTATGGGGGGATCGCCCTGCTGGCTGCCGGCACCGCCCTCCTGC 1544
rOAT2   TGGCGGCCTTGCTGGATGGAGTGTGGCTGTTGCTGCCCAAAGTTGCTTACGGGGGGATTCCCTGGTGGCTGCCTGCACTGCACTCCTGCG 1571
TI-LTP  TGGCGGCCTTGCTGGATGGAGTGTGGCTGTTGCTGCCCAAAGTTGCTTACGGGGGGATTGCCCTGGTGGCTGCCTGCACTGCACTCCTGC 5810
hOAT2   TGCCAGAGACGAGGCAGGCACAGCTGCCAGAGACCATCCAGGACGTGGAGAGAAAGAG---------------------------------- 1558
hNLT    TGCCAGAGACGAGGCAGGCACAGCTGCCAGAGACCATCCAGGACGTGGAGAGAAAGAG---------------------------------- 1604
rOAT2   TGCCTGAGACGAAGAAGGCACAGCTGCCAGAGACCATCCAGGATGTGGAGAGGAAGAG---------------------------------- 1631
TI-LTP  TGCCTGAGACGAAGAAGGCACAGCTGCCAGAGACCATCCAGGATGTGGAGAGGAAGAGgtatgtgtgcagtgcgtgcgtgtgtgcgtgtg 5900
        tgtgtgtgtgagtgcgtgtgtgtgtgtgcgtgtgtgtgcatgtgagtgtgtgagtgtgtgagtgtgtgcatgtgagtgtgtgtgtatg 5990
        tgtgtaagagtgtgtgagtgtggattcagatgcctaaggccctgacacttaggatgcaaagggaagacagttgcacagttacacttgcta 6080
        cctatacatatgtgcacaggtgagtgtttgggtgtgtatatcctggtgtgtataacgtgtcatataaaatcaaacatgtctgtccttacc 6170
        tttatatattcacgaatgcccaaaagagaggcacatatgcactctgagctatatacaccaagaatatgtccagacaagtgacttacttgt 6260
        aggaggatgcgtgcatatatttgaggagctgggacagccccgagccagtccttgtaggctccaggactaacccccgaccacattcctgac 6350
rOAT2   ----------------------TACCCAGGAGGAAGATGTGTAG---------------------------------------- 1666
TI-LTP  acctttcttatggccttgtccagTACCCAGGAGGAAGATGTGTAGgtccgggactgagttggactagcgacagttctccacaggagctgg 6440
TI-LTP  gcacagaaggcagcctcttgtgactgggacatcagactcctccacctaaggatggagctgctcctgatgccctctgcctgtgctctccag 6530
        cagcagaacaacttcccgcagcactgggccgctgggattctggactcccctctcatggccgggggcttctataaataaagacggttgctc 6620
        atgggttggggcagcagtgagattgggggaaaccctcagatggaaagccactgacttgatctgattccagtcttacactgcccatctccc 6710
        aggtggacggcgaaacctcctagtggacaggatgttttgtggtgctcaaattgaacaaggtcatcctaggaatgtcgttaaagcacagtc 6800
        ctgtagtcatttttagtaccgggaggccggtgggtgtactgtctccggtggaagggtagatcagcacaactccggggcaggggaccaata 6890
        gatggttttcttgttgccagggctccctctgaagtagcagactcgtaccctacccctcaaatcactatctgggcttcacacctaaagaaa 6980
        gagcagagtctggggccagcctggcctacagtgagctagcaggtggtaggtagggcacacctttaattccagcactccagaggcagaggc 7070
        aagctagttgcagggctgcacaaagaaacctttctagaaaaaacaaaacagtcataaaacaaaacaaaacaaaaagaaccaaaggtatg 7160
        gggattgacattttattacggaatccagagagctcgacgacctttatgaatacactttatgaaactcaagcattgctgagagaaggactg 7250
hOAT2   -------------------------------TGTGCACAGGACTGTGTCTGTGTACGTGTGA                          1626
TI-LTP  ggagcccaggcaaccaccattctaagcgtgTGTG--------TGTGTGTGTGTGTGTGTGtgtgtgtgtgtgtgtgtgtgtgtgtgcc 7332
TI-LTP  tccagttaggaatggggaaacacagaagtgggagagacagtctagactcaggtctaccacagagcctacacctaggtcccagcccccagg 7422
        atgtcgcctgcttcctccccaaaggactaga                                                          7453
hNLT    TGCCCCAACCAGTCTTCAGGAGGAAGAGATGCCCATGAAGCAGGTCCAGAACTAA                                  1666
```

ACKNOWLEDGEMENTS

I would like to thank the following for people for their support during the course of this study.

Professor Burckhardt, for his advice, support and direction, and excellent organization of the Graduiertenkolleg.

Natascha Wolff, for her support and encouragement, both professional and personal, without which this work would never have been completed.

Professor Dr R Hardeland and Prof Dr K Jungermann, for acting as Referent and Korreferent, respectively.

All my colleagues in the Abteilung Vegetative Physiologie und Pathophysiologie for making my stay in Göttingen unforgettable, especially Erzsébet Beéry, Yohannes Hagos and Jürgen Langer.

My parents, for continued support and encouragement from home.

Most of all I would like to thank my wife, Andrea Fife, for her love and unlimited support, especially during the writing of this thesis.

BIOGRAPHY

Name	Glen Reid
Date of Birth	22. April 1973
Place of Birth	Lower Hutt, New Zealand
Nationality	British/New Zealander
Marital Status	married Andrea Fife on 26th May 1999
1978-1985	Primary and intermediate school, Wellesley College, Eastbourne, New Zealand
1985-1986	High School, Boldon Comprehensive, England
1986-1990	Hutt Valley High School, Lower Hutt, New Zealand Completed 7th Form Bursary (Abitur), 1990.
March 1991-November 1993	Bachelor of Science (major Biochemistry) at the University of Canterbury, Christchurch, New Zealand
March 1994-May1996	Master of Science (hons) in Cellular and Molecular Biology, at the University of Canterbury, Christchurch, New Zealand Thesis title: 'The cell envelope as a barrier to genetic exchange'
June 1997-May2000	Ph D at the Georg-August-Universität, Göttingen Member of the DFG-funded Graduiertenkolleg 335, entitled: 'Clinical, cellular and molecular biology of the internal ogans' Thesis title: 'Characterization of a human renal organic anion transporter'.